2015

Defining the Role of Trps1 in Phosphate Mediated Mineralization

Maria Kuzynski
University of Alabama at Birmingham

DEFINING THE ROLE OF TRPS1 IN PHOSPHATE MEDIATED MINERALIZATION

by

MARIA C. KUZYNSKI

DOBRAWA NAPIERALA, COMMITTEE CHAIR
AMJAD JAVED
MICHAEL MILLER
SELVARANGAN PONNAZHAGAN
ROSA SERRA

A DISSERTATION

Submitted to the graduate faculty of The University of Alabama at Birmingham,
in partial fulfillment of the requirements for the degree of
Doctor of Philosophy

BIRMINGHAM, ALABAMA

2016

DEFINING THE ROLE OF TRPS1 IN PHOSPHATE MEDIATED MINERALIZATION

MARIA C. KUZYNSKI

CELL BIOLOGY

ABSTRACT

Mineralization is a tightly controlled bi-phasic process that occurs when crystals of calcium and phosphate (P_i) are laid down within the extracellular matrix. However, the molecular networks regulating the initiation and progression of this process have not been well characterized. P_i, as one of the components of mineral crystals and a signaling molecule that regulates expression of mineralization-related genes, is essential to the mineralization process. In our studies, we discovered a novel function for P_i in this process: P_i is sufficient to induce secretion of matrix vesicles, which support the initiation of mineralization. Furthermore, we determined that this induction is dependent on P_i-induced ERK1/2-activaiton. In our studies, we discovered that the Trps1 transcription factor is involved in P_i signaling. Trps1 has previously been implicated in the development and homeostasis of mineralizing tissues; however its role in the mineralization process is not well understood. Here, we uncovered a context-dependent function for Trps1 in mineralization. Trps1 is important for the initiation of mineralization as it is involved in the secretion of matrix vesicles and expression of key osteogenic proteins such as TNAP and PHOSPHO1

phosphatases and major osteogenic transcription factors Runx2 and Sp7. During the propagation of mineralization, Trps1 must be downregulated for proper expression of P_i regulating genes: *Phex*, *Vdr*, *Enpp1*, and *Fam20C*. Importantly, we determined that expression of many genes involved in P_i homeostasis and expression of genes regulated by P_i is affected by Trps1, implicating Trps1 in the regulation of P_i and in the P_i signaling pathway. We determined that Trps1 regulates the P_i-induced bi-phasic signaling cascade. Specifically, deficiency of Trps1 caused an absent second activation of ERK1/2 and decreased upregulation of several P_i-responsive genes. In contrast, overexpression of Trps1 resulted in an enhanced and accelerated second activation of ERK1/2 and an increased downregulation of P_i-responsive genes. Furthermore, Trps1 affected expression of the ERK1/2 phosphatase, *Dusp6*, upon stimulation with P_i. This suggests a function for Trps1 in the ERK1/2 negative feedback loop. Altogether, these studies have found a novel function for P_i in mineralizing cells and have further delineated the role of Trps1 in the mineralization process.

KEYWORDS: Trps1, Mineralization, Phosphate, ERK1/2, Gene expression

ACKNOWLEDGEMENTS

This adventure was not a lonely endeavor. There are so many people who helped and supported me along the way. First, I would like to thank my family. Their constant faith and belief that I could do anything fueled the pursuit of my PhD. My family members have always been my biggest fans and though some of them did not live to see me cross the finish-line of this expedition, their pride in my achievements is still felt as warmly as the sun on a hot Alabama July day. Secondly, I need to thank my mentor Dr. Dobrawa Napierala. Without her wisdom and guidance I would likely still be lost and wandering on this journey. I also need to acknowledge my lab mates: Morgan Goss, Callie Mobley, Dr. Sandeep Chaudhary, and Tony Winters. They have made countless contributions to this project and to my life. Without their support, none of this would have been possible. Next, my committee members: Drs. Amjad Javed, Michael Miller, Selvarangan Ponnazhagan, and Rosa Serra helped by shaping this thesis project into the glorious thing it has become and by guiding me every step of the way. Lastly, I need to thank all of my friends. They comforted me and listened to me cry when I thought all was lost. They encouraged me and built me back up when I was ready to listen again. They let me vent and get out every last one of my frustrations about the struggles of graduate school. But most of all, my friends reminded me that there is more to life than graduate school, more to life

than hours of bench-work wasted on failed experiments, more to life than manuscript and thesis edits and revisions, and they helped me live and enjoy all of those moments that are ‘more to life’.

TABLE OF CONTENTS

Page

LIST OF TABLES

Table *Page*

DUAL ROLE OF THE TRPS1 TRANSCRIPTION FACTOR IN DENTIN MINERALIZATION

TRPS1 IS INVOLVED IN PHOSPHATE SIGNALING IN A CELLULAR MODEL OF MINERALIZATION

LIST OF FIGURES

Figures *Page*

DUAL ROLE OF THE TRPS1 TRANSCRIPTION FACTOR IN DENTIN MINERALIZATION

PHOSPHATE INDUCES FORMATION OF MATRIX VESICLES DURING ODONTOBLAST-INITIATED MINERALIZATION IN VITRO

TRPS1 IS INVOLVED IN PHOSPHATE SIGNALING IN A CELLULAR MODEL OF MINERALIZATION

INTRODUCTION

The molecular network, particularly the transcriptional regulation, of mineralization is not fully understood. The transcription factor Trps1 has been suggested to be involved in the mineralization of skeletal and dental tissues, however little is known about its function and molecular interactions [1-8]. In our studies, we discovered that Trps1 has a context-dependent role in mineralization and that its transcriptional network is closely related to phosphate (P_i) regulation [2, 4-7]. Furthermore, we uncovered that Trps1 is required for secretion of matrix vesicles (MV) which support the initiation of mineralization [7]. Further analyses led us to the discovery that P_i is sufficient to induce secretion of MV that contain proteins important for the mineralization process and this production is ERK1/2-dependent [9]. Finally, when we investigated the involvement of Trps1 in the P_i signaling cascade, we uncovered that Trps1 alters P_i signaling and likely has a role in the ERK1/2 negative feedback loop.

Mineralization occurs when crystals of calcium-phosphate are laid down within the extracellular matrix (ECM) [10]. This process is highly regulated and depends upon several factors: the availability of calcium (Ca^{+2}) and P_i (PO_4^{3-}) ions; the presence of mineralization inhibitors, such as osteopontin (Opn), matrix Gla protein (MGP), and inorganic pyrophosphate (PP_i); pH; matrix composition; and proper modifications of matrix proteins [11-15]. Physiologic mineralization

occurs in skeletal and dental tissues (bone, hypertrophic cartilage, dentin, cementum, and enamel). Pathologic mineralization refers to abnormal mineralization and can occur ectopically in soft tissues, such as in joints during the late stages of osteoarthritis or in blood vessels.

MV have been shown to be involved in the initiation of both physiologic and pathologic mineralization [16-20]. MV are a sub-group of extracellular vesicles. Extracellular vesicles are sub-micron size, spherical, membrane-enclosed particles that are released from cells to the extracellular environment. Studies have uncovered that virtually all cell types release vesicles. Vesicle origin and function can be inferred by analyzing which cell surface receptors are expressed and which biologically active proteins, lipids, and nucleic acids are carried. By coming into contact with other cells and/or releasing their intravesicular content, vesicles can modify the function of other cells and/or modify the extracellular environment [21-23]. MV formed by mineralizing cells have been shown to contain proteins critical for supporting the mineralization process [9, 24-28]. For example, these MV are enriched in tissue-nonspecific alkaline phosphatase (TNAP) and PHOSPHO1 phosphatase, that provide P_i [28-30]. While both TNAP and PHOSPHO1 are phosphatases, they have nonredundant functions in supporting mineralization. Specifically, PHOSPHO1 acts upon phospholipids inside MV to initiate deposition of calcium-phosphate crystals, and TNAP is a membrane anchored phosphatase that cleaves the mineralization inhibitor PP_i to P_i, thus regulating mineralization by increasing extracellular P_i availability and decreasing the concentration of a mineralization

inhibitor [15, 24-28]. This influx of P_i and Ca^{+2} inside MV facilitates formation of calcium-phosphate crystals, which are then released to the ECM and promote the progression of mineralization.

Although P_i homeostasis is controlled at the systemic level, many of the proteins involved in this process are highly expressed in cells producing a mineralized matrix. This suggests that they participate in the regulation of local P_i availability at the sites of mineralization [31-34]. In humans, mutations in genes involved in P_i metabolism result in skeletal and dental defects, underscoring the critical role of P_i homeostasis for tissue mineralization. For example, a genetically heterogeneous disorder, hypophosphatemic rickets, manifests as defective mineralization of skeletal and dental tissues due to dysregulated P_i homeostasis [35, 36]. TNAP deficiency (hypophosphatasia) also results in impaired mineralization and is associated with increased levels of mineralization inhibitors [37].

P_i participates in mineralization in a variety of ways. As one of the components of calcium-phosphate crystals, P_i is considered a structural component of the mineralized ECM and thus its availability affects the rate of mineralization. Additionally, P_i moieties can be added and removed from proteins involved in mineralization to regulate their function [38, 39]. Lastly, P_i has been shown to act as a signaling molecule and regulate expression of genes involved in osteogenic differentiation and the mineralization process [33, 34, 40-42]. However, little is known about the P_i-induced signaling cascade as it has not been well studied or characterized.

Previous studies have identified that certain cell types respond to changes of P_i concentrations in their local environment and that this response is independent of systemic P_i levels. Specifically in mineralizing cells, P_i signaling is dependent upon the transport of P_i into the cell via Na/P_i co-transporters, PiT1 or PiT2, and is mediated by ERK1/2, not via p38 or c-jun kinases [32, 43, 44]. However, P_i receptors are unknown. One study suggested that FGF receptors may be involved in transducing the signal and activating ERK1/2 in response to P_i [32]. Another study suggested that PiT1 may be acting as a P_i receptor and that this function is independent of P_i transport [45].

P_i-induced activation of ERK1/2 is bi-phasic. The first activation happens quickly within the first 15-30 minutes of P_i treatment. This is followed by the dephosphorylation of ERK1/2 allowing for a second activation, which typically occurs around 6-8 hours following P_i treatment [31, 32]. This bi-phasic induction results in the regulation of two different sets of genes: early and late response genes [33, 34]. Of particular interest are the late response genes as many of these play a role in mineralization. Also of interest, the promoters of many of these genes are enriched in GATA consensus elements, suggesting that GATA transcription factors are involved in the regulation of gene expression in response to P_i [46]. ERK1/2 activation in response to P_i has been shown to regulate transcription factors in the AP1 family. Interestingly, it was shown that this regulation is not at the transcriptional or translational level, but rather by post-translational modifications which prevent degradation of the protein [41]. The P_i-induced signaling cascade ultimately leads to changes in gene expression.

Studies have identified a number of P_i-responsive genes including: *Spp1*, *MGP*, *Slc20a1*, *Ankh*, *Dmp1*, *Alpl*, and *Ibsp* [32-34, 41, 47]. However, how these genes are regulated by P_i at the transcriptional level currently remains unknown.

Interestingly, many of these mineralization-related, P_i-responsive genes have promoters enriched in GATA binding sites, which suggests that our GATA-type transcription factor of interest, Trps1, may also be involved in the regulation of these genes and thereby, the P_i signaling cascade. Several lines of evidence coming from human and mouse genetic studies, and *in vitro* experiments implicate Trps1 in mineralization. Mutations in the *TRPS1* gene cause tricho-rhino-phalangeal syndrome (TRPS; OMIM#190350) or Ambras syndrome (OMIM#145701) [48, 49]. The entirety of abnormalities observed in these patients is indicative of a role of *TRPS1* in the development of craniofacial elements, endochondral bones, dental tissues, and hair [48-50]. TRPS patients typically have decreased bone mass and *TRPS1* was identified as one of bone mineral density quantitative trait loci, suggesting a role for *TRPS1* in bone formation and/or homeostasis [8, 49, 51, 52]. Little is known about Trps1 and its molecular interactions in mineralizing tissues, but the majority of studies have identified Trps1 as a transcriptional repressor [1, 5-7, 50, 53, 54].

It has been shown that in skeletal and dental tissues, *Trps1* is highly expressed prior to mineralization, and the onset of mineralization coincides with the downregulation of *Trps1* [4, 7, 55]. This expression pattern suggests that Trps1 is involved in the maturation of cells destined to produce a mineralizing matrix or that it prevents premature mineralization. The latter function has been

demonstrated in our previous studies of a mouse model of TRPS (*Trps1*$^{\Delta GT}$ mice, in which the DNA binding domain has been deleted), where we uncovered that Trps1 deficiency leads to premature mineralization of the perichondrium of developing endochondral bones [4]. Due to this phenotype, expression of Runx2, a major osteogenic transcription factor, was analyzed and found to be upregulated in perichondrial cells of *Trps1*$^{\Delta GT}$ mice. Importantly, the expression of Runx2 co-localized with the expression of Trps1 in endochondral bones and teeth implicating an interaction between these transcription factors. Through further analyses, we determined that these two proteins form a complex and that Trps1 represses Runx2-mediated trans-activation [4, 5].

To address the role of *Trps1* upregulation in mineralizing cells *in vivo*, we generated transgenic mice that have sustained high expression of *Trps1* in mature odontoblasts and osteoblasts (*Col1a1-Trps1* mice) [2, 3, 6, 56]. In this study, we discovered that overexpression of *Trps1* resulted in impaired dentin secretion and mineralization. Furthermore, we uncovered decreased expression of the major dentin matrix gene, *Dspp*, in *Col1a1-Trps1* mice in comparison with wild type littermates. Using chromatin immunoprecipitation and reporter analyses, we found that *Trps1* directly regulates *Dspp* expression by binding to GATA elements in its promoter. However, we noticed that the phenotype of *Col1a1-Trps1* mice is more severe than the phenotype of *Dspp* null mice suggesting that the repression of mineralized matrix formation is not solely mediated through *Dspp* downregulation, but that other genes regulated by *Trps1* contribute to this phenotype as well [3]. To address what other genes are

contributing to this defective mineralization, we crossed *Col1a-Trps1* mice with *Col1a1-Dspp* mice to restore *Dspp* expression and uncover *Dspp*-independent consequences of Trps1 upregulation in mature odontoblasts. We determined that restoring *Dspp* only partially rescued the mineralization defects observed in *Col1a1-Trps1* mice. Additionally, we observed downregulation of P_i homeostasis proteins Phex, Vdr, and Fam20C in odontoblasts of both *Col1a1-Trps1* and *Col1a1-Trps1*;*Col1a1-Dspp* mice, which suggests that deficiency of these proteins may be contributing to the defective dentin mineralization of these mice [6].

To uncover the mechanistic roles of Trps1 in phosphate-mediated mineralization, we took an *in vitro* approach and employed an immortalized mouse pre-odontoblastic cell line, 17IIA11 ("17A" cells) [57]. 17A cells are an excellent model for studying mineralization because they express the key transcription factors, enzymes, and ECM proteins required for mineralization. These cells rapidly undergo mineralization (mineralization nodules are visible by day 5/6 of osteogenic differentiation via alizarin red staining) when treated with standard osteogenic medium containing a P_i source (β-glycerophosphate, βGP, or Na-P_i) and ascorbic acid [7, 9, 57, 58]. Furthermore, the Trps1 expression pattern over the course of differentiation is similar to the pattern observed *in vivo*, i.e. Trps1 expression is highest prior to the onset of mineralization (days 0-3) and then is decreased and maintained at a steady level (days 4-9) [4, 7, 59].

DUAL ROLE OF THE TRPS1 TRANSCRIPTION FACTOR IN DENTIN MINERALIZATION

by

MARIA KUZYNSKI, MORGAN GOSS, MASSIMO BOTTINI, MANISHA C. YADAV, CALLIE MOBLEY, TONY WINTERS, ANNE POLIARD, ODILE KELLERMANN, BRENDAN LEE, JOSE LUIS MILLAN, AND DOBRAWA NAPIERALA

Journal of Biological Chemistry 2014 Oct 3;289(40):27481-27493

CHAPTER 1

DUAL ROLE OF THE TRPS1 TRANSCRIPTION FACTOR IN DENTIN MINERALIZATION

Abstract

TRPS1 (tricho-rhino-phalangeal syndrome) is a unique GATA-type transcription factor that acts as a transcriptional repressor. *TRPS1* deficiency and dysregulated *TRPS1* expression result in skeletal and dental abnormalities implicating *TRPS1* in endochondral bone formation and tooth development. Moreover, patients with tricho-rhino-phalangeal syndrome frequently present with low bone mass indicating TRPS1 involvement in bone homeostasis. In addition, our previous data demonstrated accelerated mineralization of the perichondrium in *Trps1* mutant mice and impaired dentin mineralization in *Col1a1-Trps1* transgenic mice, implicating *Trps1* in the mineralization process. To understand the role of *Trps1* in the differentiation and function of cells producing mineralized matrix, we used a preodontoblastic cell line as a model of dentin mineralization. We generated both *Trps1*-deficient and *Trps1*-overexpressing stable cell lines and analyzed the progression of mineralization by alkaline phosphatase and alizarin red staining. As predicted, based on our previous *in vivo* data, delayed and decreased mineralization of *Trps1*-overexpressing odontoblastic cells was

observed when compared with control cells. This was associated with down-regulation of genes regulating phosphate homeostasis. Interestingly, *Trps1*-deficient cells lost the ability to mineralize and demonstrated decreased expression of several genes critical for initiating the mineralization process, including *Alpl* and *Phospho1*. Based on these data, we have concluded that *Trps1* serves two critical and context-dependent functions in odontoblast-regulated mineralization as follows: 1) *Trps1* is required for odontoblast maturation by supporting expression of genes crucial for initiating the mineralization process, and 2) *Trps1* represses the function of mature cells and, consequently, restricts the extent of extracellular matrix mineralization.

Introduction

Mineralization is an orchestrated process in which crystals of calcium phosphate, termed hydroxyapatite (HA),[2] are laid down in precise amounts within the fibrous extracellular matrix (ECM) (1). Physiological mineralization occurs in skeletal tissues (bone and hypertrophic cartilage) and dental tissues (dentin, cementum, and enamel). Dentin, the most abundant component of the tooth, is very similar to bone in its matrix protein composition. However, unlike bone, dentin does not undergo remodeling and does not participate in calcium homeostasis (2). Cells that produce dentin, odontoblasts, differentiate from cranial neural crest-derived mesenchyme in a process that requires sequential

and reciprocal mesenchymal-epithelial interactions. Mature odontoblasts secrete organic and mineral components of the dentin ECM; however, the transcriptional regulation of this process is not well understood (2).

Initiation of mineralization takes place within matrix vesicles (MVs), which bud off from the plasma membrane of cells producing the mineralizing matrix (3–5). The unique protein and lipid composition of MVs supports accumulation of high concentrations of Ca^{2+} and PO_4^{3-} (P_i) ions facilitating initial HA crystal formation (6). In particular, mineralization-competent MVs are enriched in tissue-nonspecific alkaline phosphatase (TNAP) and PHOSPHO1 phosphatase that provide P_i (7, 8). A series of genetic experiments with knock-out and transgenic mice demonstrated that TNAP and PHOSPHO1 have nonredundant functions in supporting mineralization (9, 10). PHOSPHO1 acts inside MVs to initiate deposition of HA in this compartment, whereas TNAP regulates mineralization by modifying the ECM environment (9, 11–13). The release of HA from MVs to the ECM supports further tissue mineralization. The extent of tissue mineralization depends on the composition and modifications of ECM proteins, the availability of Ca^{2+} and P_i, and concentration of mineralization inhibitors, such as osteopontin (Opn), matrix Gla protein (MGP), and inorganic pyrophosphate (PP_i) (14–16). Activity of TNAP and transporters of P_i (PiT1 and PiT2) and PP_i (Ank) establishes a P_i/PP_i ratio that either supports or represses mineralization (11). Although phosphate homeostasis is controlled at the systemic level, many of the proteins involved in this process are highly expressed in cells producing mineralizing matrix, suggesting that they participate in the locally regulated phosphate

availability at the sites of mineralization (17–21). In humans, mutations in genes coding for major matrix proteins as well as in genes involved in phosphate metabolism result in skeletal and dental defects, underscoring the critical role of matrix composition and phosphate homeostasis for tissue mineralization (17, 22–26). For example, a genetically heterogeneous disorder, hypophosphatemic rickets, manifests as defective mineralization of skeletal and dental tissues due to dysregulated phosphate homeostasis (27, 28). TNAP deficiency (hypophosphatasia) also results in impaired mineralization associated with increased levels of mineralization inhibitors (29, 30).

A growing body of evidence implicates the Trps1 transcription factor in mineralization, although its role in this process and the mechanism whereby Trps1 regulates mineralization are not well understood. Trps1 is a unique zinc finger protein that belongs to the GATA family of transcription factors (31). Although a majority of studies have demonstrated that Trps1 is a transcriptional repressor, recently it has been shown that during hair formation Trps1 can activate expression of Wnt pathway genes (32–36). Mutations of the *TRPS1* gene in humans cause the craniofacial and skeletal dysplasia tricho-rhino-phalangeal syndrome (TRPS) and Ambras syndrome (37, 38). Although these two diseases have distinct clinical presentations, abnormalities observed in patients with TRPS and Ambras indicate that *TRPS1* is involved in the development of endochondral bones and teeth. We and others have shown that in perichondrial cells of endochondral bones, as well as in developing odontoblasts, *Trps1* is highly expressed prior to mineralization, and the onset of

mineralization coincides with down-regulation of *Trps1* (32, 39, 40). This expression pattern suggests that *Trps1* is involved in the maturation of cells destined to produce mineralizing matrix or that it prevents premature mineralization. The latter function has been demonstrated in our previous studies of a mouse model of TRPS (*Trps1*$^{\Delta GT}$ mice), where we uncovered that Trps1 deficiency leads to premature mineralization of the perichondrium of developing endochondral bones (32). In those studies, we did not address mineralization of dentin, because this occurs postnatally and *Trps1*$^{\Delta GT/\Delta GT}$ mice die at birth. To determine whether *Trps1* is sufficient to inhibit osteoblast and/or odontoblast-driven mineralization, we generated *Col1a1-Trps1* transgenic mice expressing *Trps1* from a cell type-specific 2.3-kb fragment of the *Col1a1* promoter. Analyses of *Col1a1-Trps1* mice demonstrated that *Trps1* has a strong dominant negative effect on dentin but little effect on bone mineralization. The impairment in dentin formation in *Col1a1-Trps1* mice is associated with repression of the *Dspp* gene, coding for major dentin matrix proteins required for dentin formation (41). Collectively, results of the studies of *Trps1*-deficient mice and mice overexpressing *Trps1* in osteoblasts and odontoblasts suggest a context-dependent function of *Trps1* in the mineralization process. This context may be determined by the type of cell that is driving mineralization or by the cell differentiation stage.

The dental phenotype of TRPS and Ambras patients clearly indicates that *TRPS1* is involved in tooth development. On the molecular level, the dynamic and specific expression pattern of *Trps1* in developing odontoblasts suggests its

role in dentinogenesis. In these studies, we address the role of *Trps1* in odontoblast-driven mineralization. We analyzed the consequences of both *Trps1* deficiency and up-regulation on the mineralization process and the expression of genes involved in it. Results of these studies demonstrate for the first time that *Trps1* regulates mineralization through different mechanisms in preodontoblasts and mature odontoblasts, and thus the role of *Trps1* in the mineralization process depends on the odontoblast differentiation stage.

Experimental Procedures

Cell Culture

Preodontoblastic 17IIA11 cells (42, 43) were maintained in standard DMEM (Invitrogen) with 5% FBS (Thermo Fisher Scientific, Logan, UT) and 100 units/ml penicillin and 100 µg/ml streptomycin (Cellgro, Manassas, VA) at 37 °C and 8% CO_2. For the osteo-odontogenic differentiation experiments, cells were plated at $5x10^5$ cells per well of a 6-well plate. Once cells reached 85–95% confluency, osteo-odontogenic differentiation was induced by osteogenic medium (standard medium supplemented with 7 mM β–glycerophosphate and 50 µg/ml ascorbic acid). Osteogenic medium was changed every 48 h. *Trps1*-deficient, *Trps1*-overexpressing, and control stable cell lines were generated as described previously (41).

RNA Extraction, cDNA Synthesis, and Quantitative RT-PCR (qRT-PCR)

Total RNA was extracted using GenElute Mammalian Total RNA miniprep kit (Sigma). Total RNA (1 μg), after DNase I treatment (Invitrogen), was converted to cDNA with SuperScript III reverse transcriptase kit (Invitrogen). Gene expression analyses were performed using AB Biosystems 7500 fast real time PCR system and Fast SYBR Green reaction mix (Roche Applied Science). Primer sequences are as follows: Gapdh F, GCAAGAGAGGCCCTATCCCAA, and R, CTCCCTAGGCCCCTCCTGTTATT; Actb F, GACGTTGACATCCGTAAAGACC, and R, CAGGAGGAGCAATGATCTTGATC; Trps1 F, ACAACGGCGAGCAGATTATTAG, and R, TAGTCAATGAACCCTGGGCTTCGTA; Phex F, CAGAAAGCCAAAATCCTCTACTCA, and R, TCCAGTCTAAGCACCGACTTCA; Vdr F, GCCTCCAATTCGTGCAGACGTAAGTACA, and R, GAGCCTTCTTCATTCAGATCCATCGTG; Fam20C F, AACCCATGAAGCAGACGAGAG, and R, GGAGGGACTCTGCGGAAATC; Alpl F, CAGTGGGAGTGAGC GCAGCC, and R, GCACTGGGTGTGGCGTGGTT; Phospho1 F, CCTGGGAAACAGCCGCCGATGTG, and R, CCCGGAGGAGCATAGCAAAGCGAAG; Runx2 F, TGGCCGGGAATGATGAGAAC, and R, TGAAACTCTTGCCTCGTCCG; Sp7 F, GGGCGTTCTACCTGCGACTG, and R, ATCGGGGCGGCTGATTG; ATF4 F, GTGGCCAAGCACTTGAAACC, and R, GGAAAAGGCATCCTCCTTGC;MGPF, AAGCCCAAAAGAGAGTCCAGG, and R, AAGTAGCGGTTGTAGGCAGC; Opn F, ATGAGGCTGCAGTTCTCCTGG, and R,

AAAGCTTCTTCTCCTCTGAGCTGCC; Ank F, CACCCTGATAGCCTACAGTGAC, and R, GGAAGGCAGCGAGATACAGG; PiT1 F, AGCACCGTTGCTGGGCTTT, and R, GGCCCAGTGGCACACACTACC; and PiT2 F, CGCGGTTTCCGGAGGGAACG, and R, AGGTTGCTAACTTCGGGAGGCCA. Dspp primer sequences are described in Ref. 44.

Microarray and Data Processing

RNA was isolated as described above, and its purity was assessed by gel electrophoresis (Agilent 2100 Bioanalyzer). Transcriptional profiling was carried out using the Affymetrix Mouse Gene ST 1.0 array at the University of Alabama at Birmingham Heflin Center for Genomic Science using standard methods (Affymetrix GeneChip Expression Technical Manual). The Mouse Gene ST 1.0 chip consists of 24,582 well annotated genes. Briefly, 300 ng of total RNA from each sample was used to generate double strand cDNA by linear amplification using T7-linked random primers and reverse transcriptase. Subsequently, cRNA was generated by standard methods (Affymetrix) followed by single-stranded DNA fragmentation, end label biotinylation, and preparation of hybridization mixture. The arrays were hybridized overnight at 45 °C and then washed, stained, and scanned the next day. Data acquisition software (Affymetrix GeneChip Command Console Software) was used to generate a cell intensity (CEL) file from the stored images containing a single intensity value for each probe cell on the array. The CEL files were imported into GeneSpring GX 11.5.1

(Agilent Technologies, Santa Clara, CA). Using the RMA16 summarization algorithm, GeneSpring GX summarized the CEL data files. Expression values for each mRNA were obtained by the robust multiarray analysis method of *Irizarry et al.* (45). This protocol adjusts for the background on the raw intensity scale, carries out a nonlinear quantile normalization of the perfect match values, log-transforms the background-adjusted perfect match values, and carries out a robust multi-chip analysis of the quantile normalized log-transformed values (45). Each sample underwent baseline transformation to the mean of the control samples. Entities were filtered based on their signal intensity values by satisfying the upper and lower percentile cutoffs 20–100%. Filtered data were further processed in GeneSpring GX by using a one-way analysis of variance and the multiple testing correction method of Benjamini Hochberg. A fold change cutoff of 2 was used to generate downstream datasets (45). To control for the occurrence of false discoveries in the datasets, a corrected p value (q value) ≤ 0.05 was used.

Western Blot

Whole protein extracts were prepared by cell lysis in RIPA buffer supplemented with 1 mM NaF, 2 mM Na_2VO_4, 2 mM leupeptin, 2 mM pepstatin, and 2 mM PMSF. Protein concentration was determined by micro BCA protein assay kit (Thermo Scientific, Rockford, IL). Protein (15 µg) was subjected to electrophoresis on 4–12% precast BisTris gels (Invitrogen) and transferred onto a nitrocellulose membrane. Specific proteins were detected by fluorescence (Li-

Cor Odyssey Infrared Imaging System, LI-COR Biosciences, Lincoln, NE). Primary antibodies against Trps1 (ProteinTech, Chicago) were used at 1:1500 dilution; Vdr (Thermo Scientific, Rockford, IL) and Gapdh (Cell Signaling, Danvers, MA) were used at 1:1000; Runx2 (MBL International, Woburn, MA) was used at 1:250 dilution; Sp7 (Abcam, Cambridge,MA)was used at 1:200; and tubulin (Sigma) was used at 1:10,000. All fluorescent secondary antibodies (LI-COR Biosciences, Lincoln, NE) were used at 1:20,000.

Alizarin Red Staining and Quantification of Mineralization

Cells were fixed in 4% paraformaldehyde and stained with 40 mM alizarin red-S (Sigma) for 10 min. Excess dye was removed by washing with deionized water. To quantify calcium deposits, alizarin red was extracted from stained cells with 10% acetic acid, neutralized with 10% NH_4OH to pH 4.1–4.3, and quantified by colorimetric detection by spectrophotometry at 405 nm.

TNAP Activity Assay

To detect TNAP activity, cells were fixed in 4% paraformaldehyde, and the alkaline phosphatase substrate naphthol AS-MX phosphate (0.1 mg/ml) was added in reaction buffer containing 0.5% N,N-dimethylformamide, 2 mM MgCl2, 0.6 mg/ml Fast blue BB salt, and 0.1 M Tris-HCl, pH 8.5. The reaction was stopped by washing in water, and stained cells were imaged. Densitometry of TNAP activity staining was performed using ImageJ software. Images were formatted to the same size; image background was subtracted, a circular area

was defined to ensure measurements were taken of the same location and size, and the selected area was analyzed for each image. Measurement values were normalized by taking the inverse and multiplying by 50,000 so that the larger numbers correspond to darker staining (46). Statistics were calculated using the raw, untransformed values.

Isolation of Matrix Vesicles

MVs were isolated by collagenase digestion as described previously (13). Briefly, cells were plated at a density of $7x10^5$ cells per 10-cm plate in 10 ml of osteogenic differentiation medium. An equal number of cells was used for each cell line. Plates were incubated at 37 °C with 5% CO_2 for 9 days with media change every 3 days. On day 9, cells were washed and digested for 1.5 h with 2.5 mg/ml collagenase (Worthington). After collagenase digestion, cells were centrifuged at 3000 rpm for 10 min. Supernatant was collected and centrifuged at 19,000 rpm for 10 min. Supernatant was again centrifuged at 42,000 rpm for 45 min to get the MV pellet. The pellet was then resuspended in Tris-buffered saline (20mM Tris, 0.15 mM NaCl).

AFM Images of MVs

Five microliters of MV solution was dropped onto a freshly cleaved mica substrate (Ted Pella, Redding, CA) and allowed to stand for a couple of minutes. Next, 5 µl of glutaraldehyde solution (8% in H_2O) (Sigma) was spotted onto the sample drop and dried at room temperature overnight. Samples were imaged by

noncontact (AAC) mode in air using a 5500 AFM (Agilent Technologies). Silicon-nitride cantilevers with a nominal resonance frequency of 190 kHz (Nanosensors™, Neuchatel, Switzerland) were employed. Tridimensional AFM images were generated by PicoView software (Agilent Technologies).

Calculation of MV Diameter and Number

AFM imaging was used to investigate the morphology (diameter) and number of MVs isolated from cells. MV diameters were calculated as the peak value of the cross-sections of n=100 vesicles for each cell line. Mean and standard deviation values for the diameter distributions were obtained through Gaussian fit. The number of MVs isolated from cells was calculated by counting the globular features in AFM images (scan size 5 x5 μm).

Statistics

All experiments were performed on three control and three Trps1-modified stable cell lines. Data are presented as the mean ±S.D. Probability values were calculated using the Student's t test. $p \leq 0.05$ (*) and 0.005 (**) were considered to be statistically significant and highly significant, respectively.

Results

Trps1 Expression during Osteo-odontogenic Differentiation of 17IIA11 Cells

To gain mechanistic insights into the role of *Trps1* in the physiology and pathology of odontoblast-regulated mineralization, we employed the 17IIA11 cell line (17A cells) derived from mouse odontoblasts (42, 43). 17A cells are a good model to study molecular mechanisms of odontoblast-mediated mineralization, because they express key transcription factors as well as enzymes and matrix proteins required for mineralization (42). Importantly, when induced by osteogenic medium, 17A cells secrete the ECM that rapidly undergoes mineralization (Fig. 1A). Thus, 17A cells maintained in standard cell culture medium represent preodontoblasts, and when cultured in osteogenic medium, they differentiate into odontoblast-like cells (42, 43). However, because in *in vitro* systems odontoblastic cells do not polarize, the ECM produced by these cells lacks the characteristic tubular structure of dentin and resembles osteodentin. To indicate this difference between *in vivo* and *in vitro* odontoblast differentiation, we use the term “osteo-odontogenic differentiation” for the *in vitro* differentiation of 17A cells.

Trps1 expression was compared in 17A cells at the preodontoblastic stage and upon induction of osteo-odontogenic differentiation by analyzing mRNA and protein levels every 24 h starting from day 0 through day 9 of differentiation, when the mineralization of 17A cells plateaus. *Trps1* mRNA and protein were detected in preodontoblastic cells as well as during osteoodontogenic

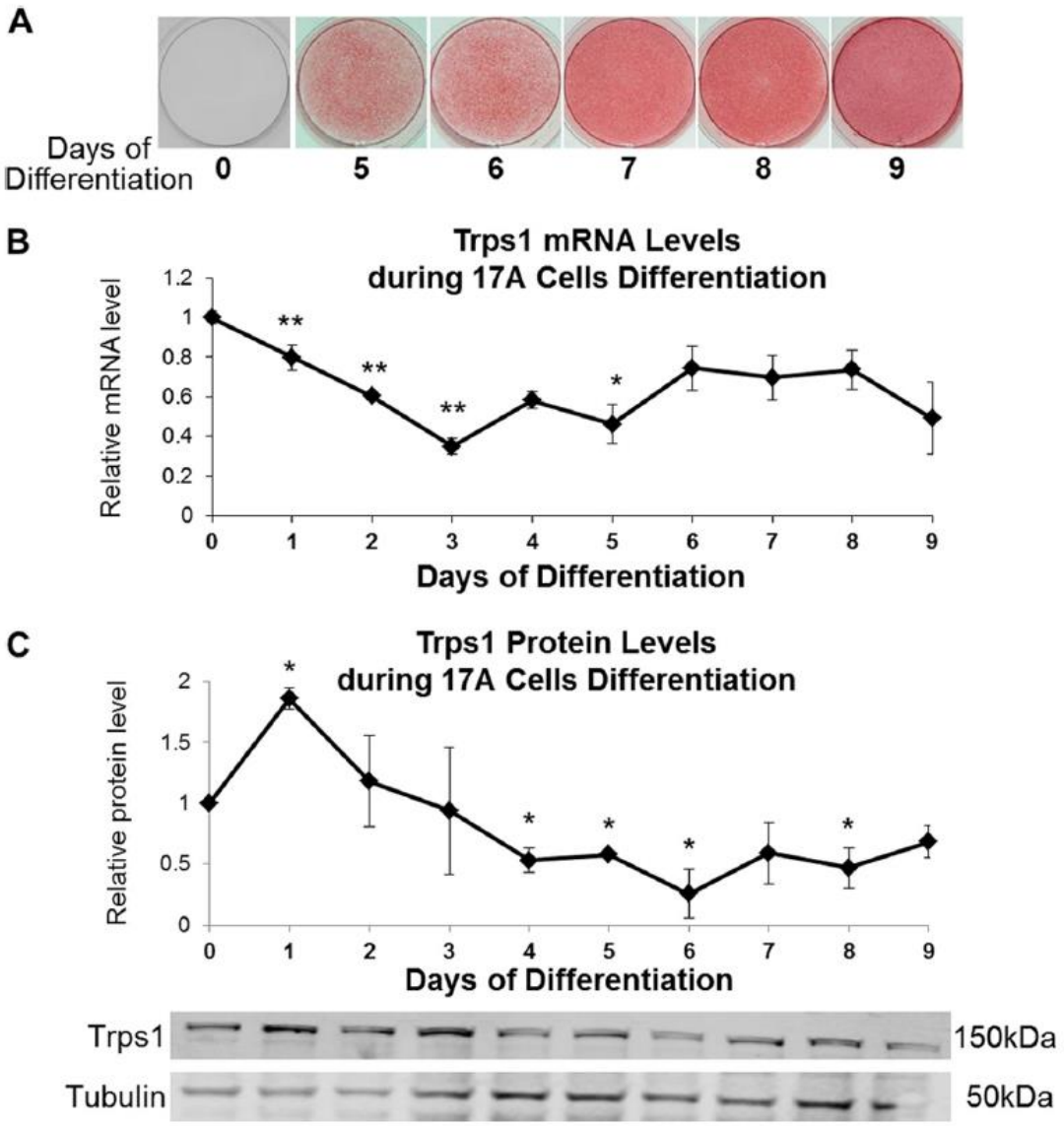

FIGURE 1. **Trps1 expression during osteo-odontogenic differentiation of 17A cells.** *A*, representative images of alizarin red staining showing the progression of 17A-regulated mineralization. *B,* qRT-PCR results demonstrating *Trps1* expression in 17A cells. Data are presented as the mean relative levels of *Trps1* mRNA (normalized to *Gapdh*) ±S.D. from three independent differentiation experiments. *Trps1* levels in undifferentiated 17A cells (day 0 of differentiation) were arbitrarily set at 1 and used as a reference for the remaining time points. *C,* Western blot analyses of Trps1 protein levels. Results of densitometric analyses (*top*) of Western blots (*bottom*) demonstrating relative Trps1 protein levels. Data are represented as the mean relative density of Trps1 normalized to tubulin (a protein loading control)±S.D. from three independent differentiation experiments. Normalized Trps1 levels in undifferentiated 17A cells were arbitrarily set at 1 and used as a reference for the remaining time points. *Asterisks* denote statistically significant differences compared with day 0 of differentiation (*, $p \leq 0.05$; **, $p \leq 0.005$).

differentiation and mineralization of 17A cells. At the mRNA level, the highest *Trps1* expression was observed in 17A preodontoblastic cells (Fig. 1B). Upon induction of differentiation with osteogenic medium, *Trps1* expression transiently decreases, reaching the lowest level prior to formation of mineralization nodules. From days 6 to 9, when differentiated 17A cells support the growth of mineralization nodules, *Trps1* expression is maintained at a steady level. At the protein level, the changes of Trps1 in general follow the mRNA, except from day 1 of differentiation, when transient up-regulation of Trps1 is detected (Fig. 1, B and C). Although the changes of *Trps1* expression during osteo-odontogenic differentiation of 17A cells are not as dramatic as during odontoblast differentiation *in vivo* (39), the overall *Trps1* expression pattern in 17A odontoblastic cells and odontoblasts *in vivo* are similar, with the highest *Trps1* expression in progenitor cells and the lowest expression in newly differentiated cells.

Up-regulation of Trps1 in Differentiated Odontoblastic Cells Impairs Mineralization

We have recently demonstrated that increased *Trps1* expression in mature odontoblasts *in vivo* results in severe impairment in dentin formation and repression of the *Dspp* gene (41). Although there is a significant overlap in dental phenotypes of *Col1a1-Trps1* and *Dspp*$^{-/-}$ mice, the onset of dentin abnormalities and extent of mineralization defects in *Col1a1-Trps1* mice are more severe than the phenotype of *Dspp-/-* mice (41, 47). This suggests that *Trps1*-dependent repression of dentin formation reflects dysregulation of a number of genes

involved in mineralization. 17A cells were used as a model of odontoblast-regulated mineralization to identify additional genes that contribute to impaired mineralization caused by *Trps1* up-regulation in mature odontoblasts.

To generate a cellular model of *Trps1* up-regulation throughout odontoblastic differentiation, a transposon-mediated genomic integration approach was used. We generated three clonal stable cell lines with 3.0-, 3.5-, and 4.5-fold overexpression of V5-tagged Trps1 (Trps1-OE cells) and three control clonal cell lines generated with a “no insert” transposon (Cntr cells). Trps1 overexpression in clonal cell lines was confirmed on both the mRNA and protein level (Fig. 2A). The progress of mineralization in Trps1-OE and Cntr cells was compared using quantification of alizarin red-stained calcium deposits. These analyses demonstrated that mineralization nodules are first detected at day 5 of osteo-odontogenic differentiation of Cntr cells and 2 days later in Trps1-OE cells. Moreover, overexpression of *Trps1* in odontoblastic cells results in decreased mineral formation by Trps1-OE cells in comparison with Cntr (Fig. 2B). All three clonal Trps1-OE cell lines demonstrated delayed and decreased mineralization in comparison with control cell lines. This mineralization defect of Trps1-OE cells is consistent with our previous data from *Col1a1-Trps1* transgenic mice (41), indicating that overexpression of *Trps1* in odontoblasts impairs odontoblast-regulated mineralization *in vitro* and *in vivo*. This impaired mineralization is not caused by TNAP deficiency, because no significant differences in TNAP activity were detected in preodontoblastic and odontoblastic Trps1-OE and control cells (Fig. 2C).

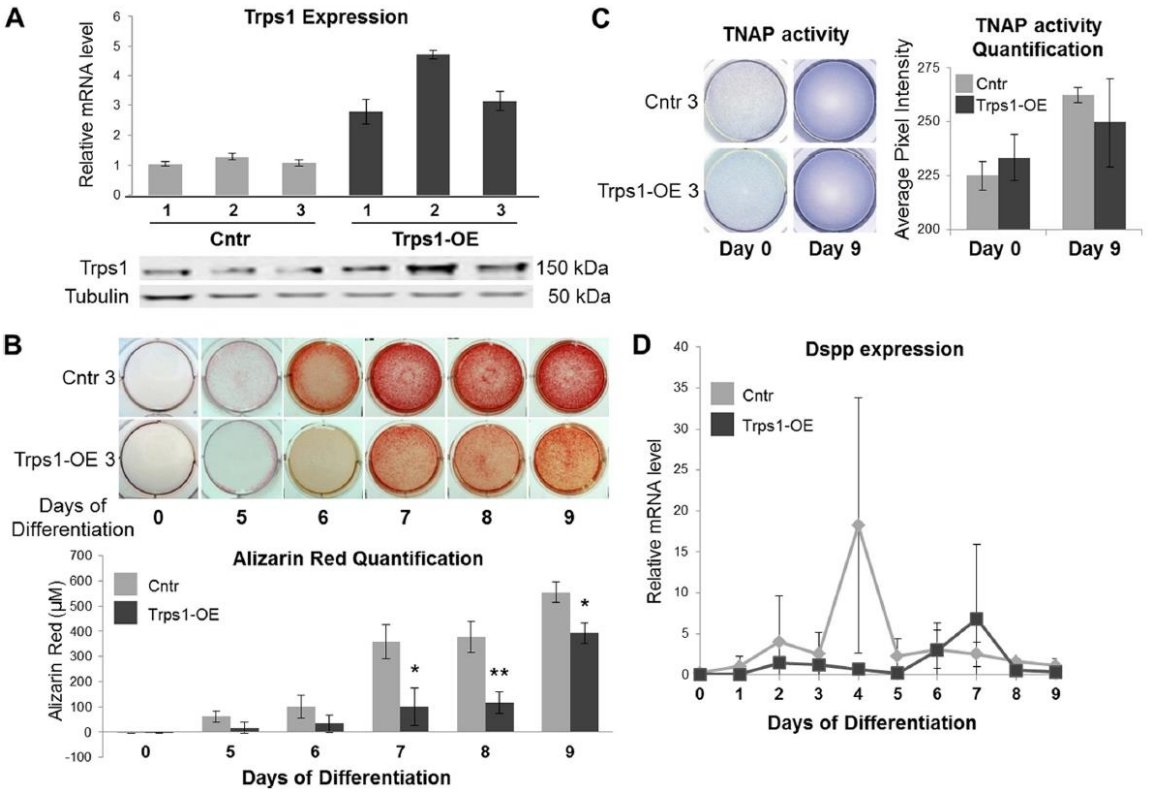

FIGURE 2. **Delayed and decreased mineralization of 17A odontoblastic cells overexpressing *Trps1*.** *A,* qRT-PCR (*top panel*) and Western blot (*bottom panel*) results demonstrating overexpression of *Trps1* in three clonal stable cell lines (Trps1-OE) and controls (Cntr, undifferentiated cells). qRT-PCR data are presented as the mean relative levels of *Trps1* mRNA normalized to *Gapdh*±S.D. from three independent RNA preparations per cell line. Relative *Trps1* levels in one of the Cntr analyses were arbitrarily set at 1 and used as a reference for the remaining control and Trps1-OE cell lines. On the Western blot analyses, tubulin was used as a protein loading control. *B,* representative images of alizarin red staining (*top panel*) and quantification (*bottom panel*) of Trps1-OE and Cntr cell lines during osteo-odontogenic differentiation. Quantification of alizarin red staining is presented as the mean±S.D. from differentiation of three stable cell lines. *Asterisks* denote statistically significant differences (*, $p \leq 0.05$; **, $p \leq 0.005$). *C,* representative images of TNAP activity assay in Trps1-OE and Cntr undifferentiated (day 0) and differentiated (day 9) cells (*left panel*) and results of densitometric quantification of TNAP activity (*right panel*). Data are presented as the mean±S.D. from differentiation of three stable cell lines. No statistically significant difference was detected. *D,* qRT-PCR results demonstrating dynamic *Dspp* expression during osteogenic differentiation of Trps1-OE and Cntr cell lines. Data are presented as the mean relative levels of *Dspp* mRNA (normalized to *Gapdh*)±S.D. from three stable cell lines. *Dspp* expression was not detected in undifferentiated controls; therefore, values for day 1 of Cntr cells were arbitrarily set at 1 and used as a reference for the remaining time points.

In *Col1a1-Trps1* transgenic mice, dentin mineralization defects are associated with repression of the *Dspp* gene; therefore, expression of *Dspp* was compared during the differentiation of Trps1-OE and control cell lines. qRT-PCR analyses did not detect *Dspp* expression in undifferentiated cells. Upon initiation of osteogenic differentiation, *Dspp* is transiently up-regulated shortly before formation of mineralization nodules in control cells. Consistent with the mineralization defects caused by Trps1 overexpression, *Dspp* up-regulation is delayed and less profound in Trps1-OE cells in comparison with controls (Fig. 2D). However, it is important to note that even at the peak of expression in control cell lines, the levels of *Dspp* mRNA are very low. Furthermore, we were unable to detect Dsp protein by Western blot analyses (data not shown). This suggests that other mineralization-related genes are involved in the mineralization defects observed in Trps1-OE cells.

Trps1 Represses Phex and Vdr during Later Stages of Mineralization

After confirming that *Trps1* up-regulation in 17A odontoblastic cells results in similar mineralization defects to those observed in the dentin of *Col1a1-Trps1* mice, we used Trps1-OE cells to identify mineralization-related genes that are dysregulated by *Trps1*-overexpression in mature odontoblasts. The Affymetrix Mouse Gene ST 1.0 array was used to compare global gene expression in Trps1-OE and Cntr cells at day 6 of differentiation. At this time point, mineralization nodules are clearly visible in Cntr but not in Trps1-OE cells, indicating delayed propagation of HA in the ECM. These analyses identified 158

Gene name	Entrez ID	Accession	Log fold change (Trps1-OE *vs.* Cntr)
Il1rl1	17082	NM_001025602	3.91379
Maob	109731	NM_172778	3.13405
Tmem47	192216	NM_138751	2.99411
Cd200	17470	NM_010818	2.46653
Galnt13	271786	NM_173030	2.09059
Tfrc	22042	NM_011638	2.07298
Serpina3g	20715	NM_009251	1.84464
Mpa2l	100702	NM_194336	1.77374
Zcchc5	213436	NM_199468	1.74184
Il18rap	16174	NM_010553	1.69067
Mmp13	17386	NM_008607	−3.59059
Enpp1	18605	NM_008813	−3.58652
Dkk1	13380	NM_010051	−3.16697
Dpep2	319446	NM_176913	−2.76464
Gabra3	14396	NM_008067	−2.68961
Ranbp3l	223332	NM_198024	−2.60713
Phex	18675	NM_011077	−2.35128
Enpp6	320981	NM_177304	−2.34854
Serping1	12258	NM_009776	−2.06617
Vdr	22337	NM_009504	−2.01732

TABLE 1. **Ten most up-regulated and down-regulated genes in 17A odontoblastic cells overexpressing *Trps1* (day 6 of osteogenic differentiation)** Microarray (Affymetrix Mouse Exon 1.0 ST array) was performed with total RNA isolated from Trps1-OE and Cntr clonal cell lines.

genes significantly (over 2-fold) down-regulated and 188 genes significantly up-regulated in Trps1-OE cells in comparison with Cntr. Interestingly, the group of most down-regulated genes in Trps1-OE cells is enriched in mineralization related genes that are associated with hypophosphatemic rickets and mineralization defects in dentin (Table 1). Therefore, the subsequent analyses were focused on determining the changes in *Enpp1*, *Phex*, and *Vdr* expression upon up-regulation of *Trps1*.

Results of qRT-PCR analyses demonstrated that *Phex* and *Vdr* are expressed at low levels in Cntr preodontoblastic cells and during the initiation phase of mineralization (Fig. 3A). *Phex* expression increases shortly before mineralization nodules are detectable by alizarin red staining and reaches the highest level at day 6 of osteo-odontogenic differentiation, when mineralization nodules are clearly visible (Fig. 3A). As in Cntr cells, the highest *Phex* mRNA levels are detected on day 6 of differentiation of Trps1-OE cells; however, the magnitude of *Phex* up-regulation is significantly lower in Trps1-OE cells then in Cntr cells. Western blot analyses of protein extracts isolated on day 8 of

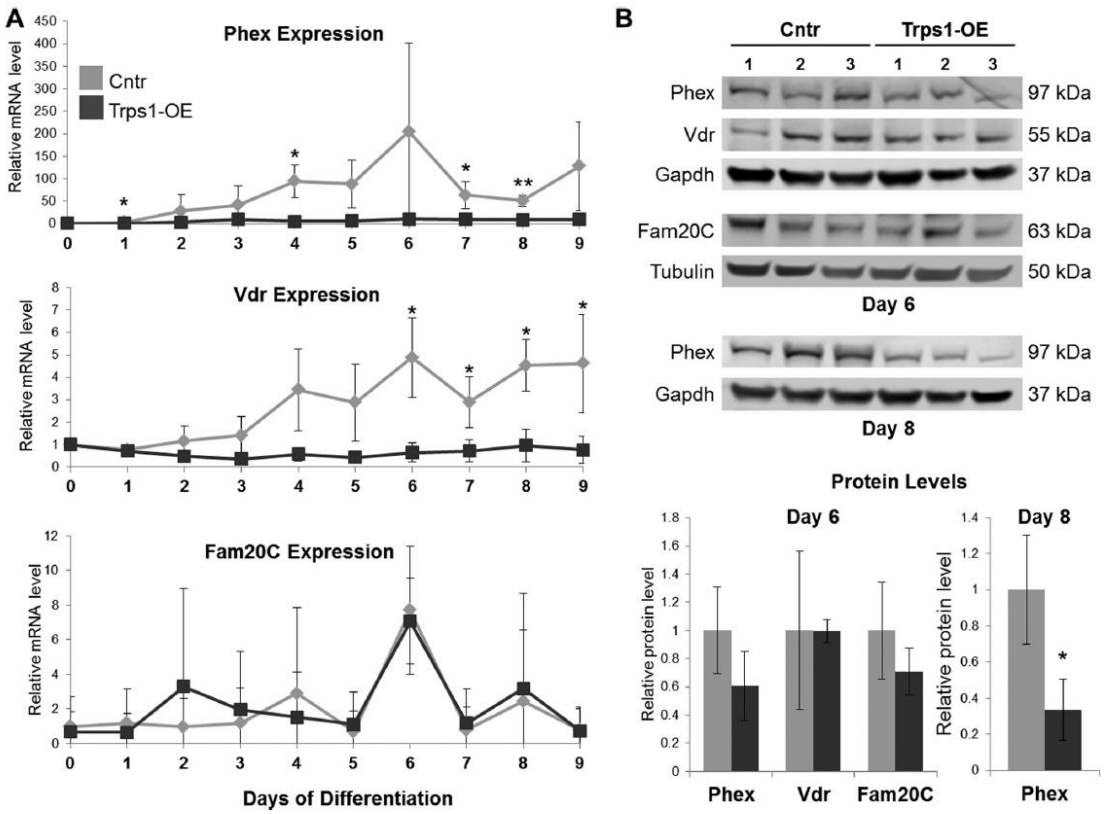

FIGURE 3. **Decreased expression of genes involved in phosphate homeostasis in Trps1-OE cells.** *A,* qRT-PCR graphs depicting *Phex*, *Vdr*, and *Fam20C* mRNA expression during osteo-odontogenic differentiation in Trps1-OE cells in comparison with Cntr cells. Data are presented as the mean relative levels of *Phex*, *Vdr*, and *Fam20C* mRNA (normalized to β-actin)±S.D. from three stable cell lines. Day 0 values for each cell line were arbitrarily set to 1 and used as a reference for remainder of days of differentiation. *B, top panel,* Western blots of Phex, Vdr, and Fam20C expression on day 6 and Phex expression on day 8 of differentiation on protein extracts isolated from Trps1-OE and Cntr cell lines. *Bottom panel,* results of densitometric quantification of the Western blot images. Protein levels were normalized to tubulin or Gapdh as depicted in the *top panel*. *Asterisks* denote statistically significant differences (*, $p \leq 0.05$; **, $p \leq 0.005$).

differentiation confirmed decreased levels of Phex in Trps1-OE cells (Fig. 3B).

The effects of *Trps1* overexpression on *Vdr* were similar to those observed for *Phex*. In Cntr cells, *Vdr* expression increases after day 2 of osteo-odontogenic differentiation and is further up-regulated during the mineralization phase. In contrast to up-regulation of *Vdr* during osteo-odontogenic differentiation of Cntr

cells, Trps1-OE cells express *Vdr* at a steady level. As a result, *Vdr* is down-regulated during the mineralization nodule formation phase in *Trps1*-overexpressing cells (Fig. 3A). Although the differences between expression of *Vdr* in Cntr and Trps1-OE cells were statistically significant on the mRNA level, we did not detect a difference on the protein level by Western blot analyses (Fig. 3B).

During osteo-odontogenic differentiation of Cntr cells, *Enpp1* expression follows the same pattern as *Phex* and *Vdr*; however, *Enpp1* is expressed at very low levels. Overexpression of *Trps1* resulted in a further decrease of *Enpp1* expression, and we were unable to detect *Enpp1* mRNA at any day of osteoodontogenic differentiation in Trps1-OE cells (data not shown).

For comparison, we performed similar expression analyses for the *Fam20C* gene which, like *Phex*, *Vdr*, and *Enpp1*, is associated with hypophosphatemia and abnormal mineralization in humans (48). Microarray analyses did not detect significant differences in *Fam20C* expression between Cntr and Trps1-OE cells (data not shown), and this was confirmed by qRT-PCR and Western blot on day 6 of osteo-odontogenic differentiation (Fig. 3). Interestingly, the pattern of *Fam20C* expression during differentiation and mineralization of Cntr cells is different from the pattern observed for *Phex* and *Vdr* (Fig. 3A). Unlike *Phex* and *Vdr*, which are strongly up-regulated during mineralization nodule formation, expression of *Fam20C* increases only transiently on day 6 of osteo-odontogenic differentiation, suggesting different roles of *Fam20C* versus *Phex* and *Vdr* in the mineralization process. In summary,

overexpression of *Trps1* in odontoblastic cells results in decreased expression of *Phex* and *Vdr* specifically during the later phase of mineralization when the growth of nodules is observed.

Trps1-deficient Odontoblastic Cells Do Not Support Mineralization

As shown, overexpression of *Trps1* results in decreased and delayed mineralization. Therefore, it would be expected that *Trps1*-deficient cells have enhanced and/or accelerated mineralization. To test this hypothesis, we generated stable cell lines deficient for *Trps1* (Trps1-KD) using lentivirus-delivered shRNAs targeting the *Trps1* transcript. Control cell lines were generated using lentivirus-delivered scrambled shRNA (shScr cells). *Trps1* knockdown was confirmed at the mRNA level by qRT-PCR and the protein level by Western blot (Fig. 4A). To characterize the consequences of *Trps1* deficiency on mineralization, we selected three stable cell lines with the most efficient knockdown of *Trps1* as follows: 70, 80, and 85% decreased *Trps1* mRNA levels in comparison with shScr cell lines.

The osteo-odontogenic differentiation of Trps1-KD and shScr cell lines was carried out as before, and progression of mineralization was monitored by alizarin red staining. Surprisingly, even after 9 days of culture in osteogenic medium, there was no evidence of mineralization nodule formation in any of Trps1-KD stable cell lines, whereas in shScr cells abundant mineralization nodules were present already at day 6 of differentiation (Fig. 4B). Considering that 17A cells are already committed to odontoblastic lineage, as demonstrated

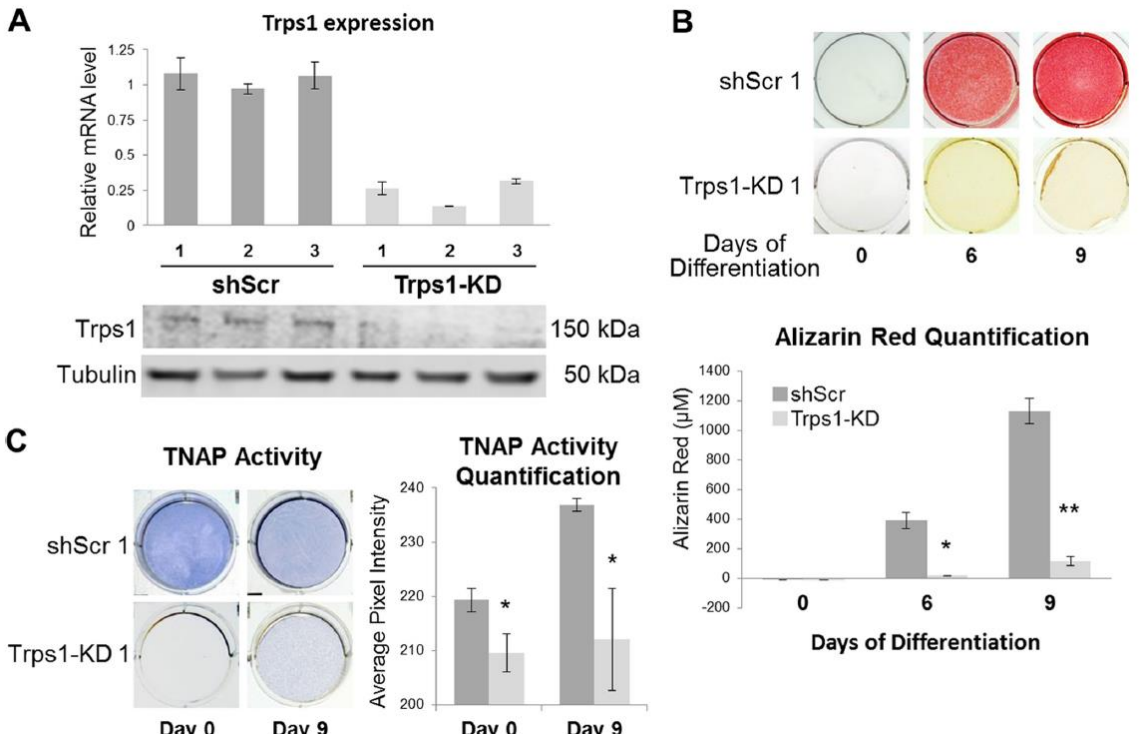

FIGURE 4. **Loss of mineralization potential in *Trps1*-deficient cells.** *A,* qRT-PCR (*top panel*) and Western blot (*bottom panel*) results demonstrating depletion of *Trps1* in 3 clonal stable cell lines (Trps1-KD) in comparison with controls (shScr). qRT-PCR data are presented as the mean relative levels of *Trps1* mRNA normalized to *Gapdh*±S.D. from 3 independent RNA preparations per cell line. Relative *Trps1* levels in one of the shScr analyses was arbitrarily set to 1 and used as a reference for the remaining control and Trps1-KD cell lines. On the Western blot analyses of Trps1 protein, tubulin was used as a protein loading control. *B,* representative images of alizarin red staining (*top panel*) and quantification (*bottom panel*) of undifferentiated (day 0) Trps1-KD and control cells, and on day 6 and 9 of osteo-odontogenic differentiation. Quantification of alizarin red staining is presented as the mean±S.D. from the differentiation experiments of three stable cell lines. *C,* representative images of TNAP activity staining (*left panel*) and quantification of the staining (*right panel*) in Trps1-KD and shScr cells demonstrate decreased TNAP activity in *Trps1*-deficient cells. *Asterisks* denote statistically significant differences (*, $p \leq 0.05$; **, $p \leq 0.005$).

previously by high TNAP activity and expression of osteogenic markers (42, 43), this indicates that *Trps1* deficiency results in loss of the mineralization potential. To identify the underlying cause of this loss, we first analyzed TNAP activity, which is a characteristic feature of mineralizing cells and is required for mineral formation. Comparison of Trps1-KD and shScr cell lines demonstrated that *Trps1*

deficiency in odontoblastic cells results in significant decrease of TNAP activity (Fig. 4C). Furthermore, undifferentiated Trps1-KD cells had dramatically reduced levels of TNAP mRNA (*Alpl*) in comparison with controls as demonstrated by qRT-PCR (Fig. 5A). This indicates that the loss of TNAP activity is due to decreased expression of the *Alpl* gene. Considering that Trps1-KD cells do not form mineralization nodules at all, we also analyzed expression of *Phospho1*, which codes for a phosphatase involved in the initiation of HA crystal formation. It has been demonstrated that expression of this gene is induced in odontoblasts prior to mineralization of the dentin (12, 13, 49). qRT-PCR and Western analyses show that *Phospho1* is also significantly down-regulated in all *Trps1*-deficient odontoblastic cell lines in comparison with shScr control cells (Fig. 5, A and C).

Trps1 Is Required for Expression of Genes Initiating Mineralization

To investigate whether the effects of *Trps1* deficiency are restricted to down-regulation of phosphatases that support HA formation or whether *Trps1* is required for expression of mineralization-related genes in general, we compared global gene expression between preodontoblastic shScr and Trps1-KD cells (day 0 of differentiation). These analyses revealed a total of 204 genes that were significantly (over 2-fold) down-regulated in *Trps1*-deficient preodontoblastic cells in comparison with controls, including *Alpl* and *Phospho1* genes that were among the most down-regulated genes in Trps1-KD cells (Table 2). The group of 10 most down-regulated genes in Trps1-KD cells also included other mineralization-

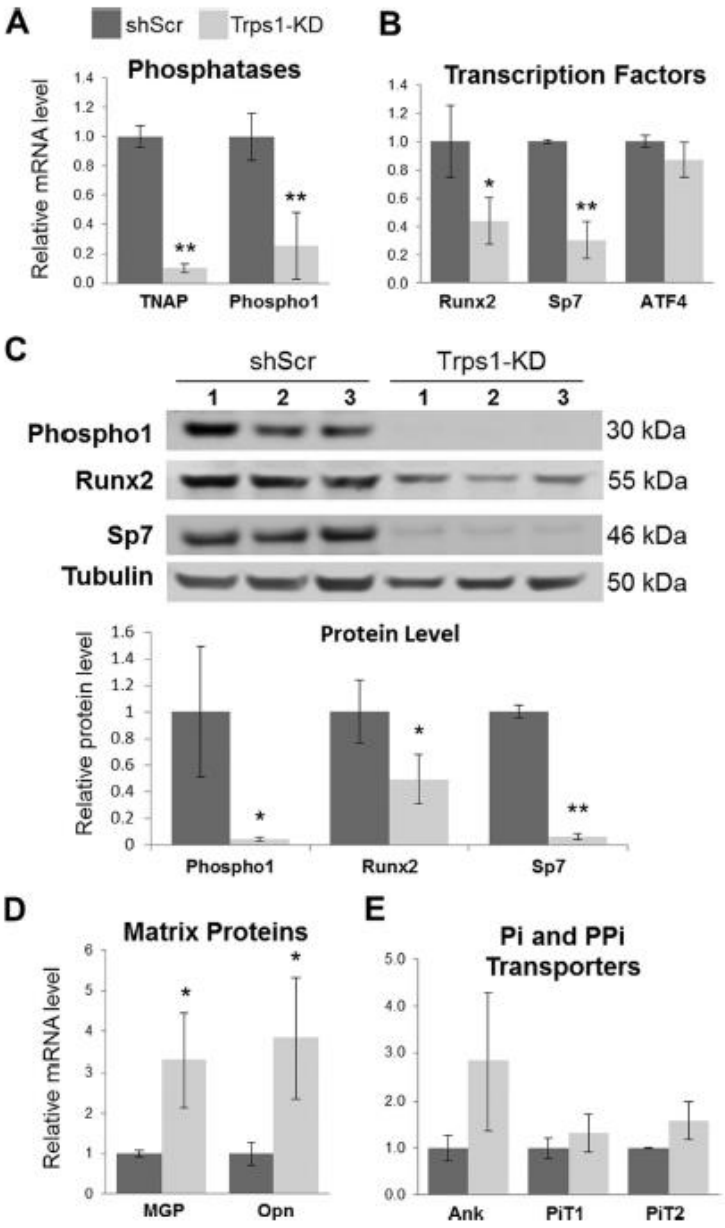

FIGURE 5. **Down-regulation of mineralization-supporting genes in undifferentiated *Trps1*-deficient cells.** *A,* qRT-PCR results for *TNAP* and *Phospho1* (phosphatases).*B,* qRT-PCR results for *Runx2*, *Sp7*, and *ATF4* (osteogenic transcription factors). *C, top panel,* Western blot results confirming down-regulation of Phospho1, Sp7, and Runx2 in Trps1-KD cell lines. Tubulin was used as a protein loading control. *Bottom panel,* results of densitometric analyses of the Western blots. Protein levels were normalized to tubulin. *D,* qRT-PCR results for *MGP* and *Opn* (matrix proteins, mineralization inhibitors). *E,* qRT-PCR results for *Ank*, *PiT1*, and *PiT2* (PPi and Pi transporters, respectively). qRT-PCR data were normalized to *Gapdh* and the average of shScr controls for each gene was arbitrarily set at 1 and used as a reference for all samples. The mean±S.D. is shown for Trps1-KD and shScr. *Asterisks* denote statistically significant differences (*, $p \leq 0.05$; **, $p \leq 0.005$).

Gene name	Entrez ID	Accession	Log fold change (Trps1-KD *vs.* shScr)
Prl2c3	18812	NM_011118	5.05802
Epha7	13841	NM_010141	4.44097
Npr3	18162	NM_001039181	4.09527
Vcam1	22329	NM_011693	3.91533
Igf1	16000	NM_001111275	3.6016
Met	17295	NM_008591	3.55918
Fbn1	14118	NM_007993	3.40414
Atp1b1	11931	NM_009721	3.32497
Sema3e	20349	NM_011348	2.96628
Arhgap29	214137	NM_172525	2.94997
Gpr141	353346	NM_181754	−5.07898
Ibsp	15891	NM_008318	−4.14171
Kcnma1	16531	NM_010610	−3.48697
Smpd3	58994	NM_021491	−3.36718
Alpl	249	NM_007431	−3.32149
Ptprd	19266	NM_001014288	−3.16874
Galnt3	14425	NM_015736	−3.03233
Phospho1	237928	NM_153104	−2.96953
Sema6a	20358	NM_018744	−2.89978
Ramp1	51801	NM_178401	−2.88211

TABLE 2. **Ten most up-regulated and down-regulated genes in undifferentiated 17A preodontoblastic cells deficient for *Trps1.*** Microarray (Affymetrix Mouse Exon 1.0 ST array) was performed with total RNA isolated from Trps1-KD and shScr clonal cell lines.

related genes, such as *Ibsp*, *Smpd3*, and *Galnt3*, suggesting that *Trps1* is required for expression of multiple genes that support mineralization.

It has already been demonstrated that undifferentiated 17A cells are positive for osteogenic transcription factors (42, 43). Runx2 and its downstream target Osx (coded by the *Sp7* gene) are the key transcription factors that control development of cells producing mineralizing matrix and directly regulate expression of osteogenic genes. From the group of osteogenic transcription factors, only expression of the *Sp7* gene was significantly decreased in Trps1-KD cells in the gene array experiment (data not shown). This was confirmed by qRT-PCR on mRNA isolated from three stable Trps1-KD cell lines (Fig. 5B). qRT-PCR analyses also demonstrated significant down-regulation of *Runx2* mRNA in Trps1-KD cell lines (Fig. 5B). Western blot analyses demonstrated a more dramatic decrease of both Sp7 and Runx2 at the protein level (Fig. 5C). There was no significant change in expression of the *Atf4* gene, which codes for a transcription factor that regulates function of more mature osteogenic cells (Fig. 5B). These results suggest that in preodontoblastic cells *Trps1* supports

expression of genes involved in the early stages of osteo-odontogenic differentiation.

To follow up on this hypothesis, we analyzed expression of matrix proteins osteopontin (Opn, coded by the *Spp1* gene) and matrix Gla protein (MGP) that are activated along with TNAP during early osteo-odontogenic differentiation. However, unlike TNAP, Opn and MGP are inhibitors of mineralization. We found that expression of *Opn* and *Mgp* in undifferentiated Trps1-KD cells is higher than in shScr (Fig. 5D). It has been reported that *Opn* is up-regulated upon TNAP deficiency and by increased PP_i levels (14, 50); therefore, we analyzed expression of a PP_i transporter Ank but detected no significant difference in *Ank* expression between Trps1-KD cells and controls (Fig. 5E). Similarly, there were no changes in expression of P_i transporters *PiT1* and *PiT2* (Fig. 5E). In summary, depletion of *Trps1* in preodontoblastic cells results in the loss of the mineralization potential associated with significant down-regulation of phosphatases specifically involved in HA formation, as well as decreased expression of transcription factors essential for the osteogenic program.

Trps1 Deficiency Affects Matrix Vesicles

The inability of *Trps1*-deficient cells to initiate the mineralization process and the significant down-regulation of phosphatases associated with MV function suggest defects in MVs. AFM imaging was employed to investigate the size and number of MVs isolated from Trps1-KD cell lines with respect to control cell lines (Fig. 6). MVs from both Trps1-KD and shScr cells had an average diameter of

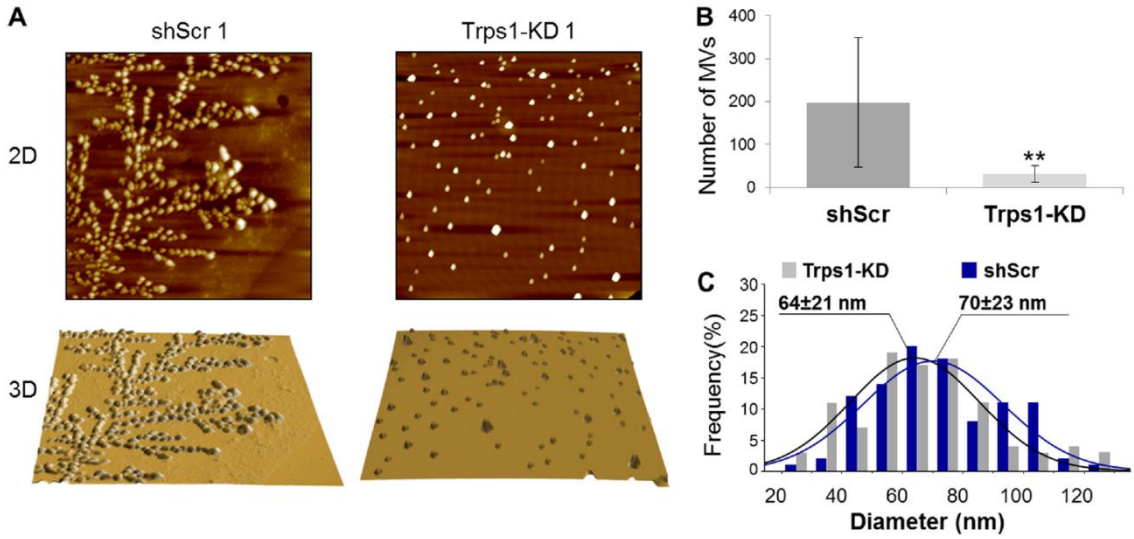

FIGURE 6. ***Trps1* deficiency affects matrix vesicles.** *A,* representative AFM images (scan size 10×10 μm) of MVs isolated from Trps1-KD and shScr cell lines. Topography (*top panel*) and three-dimensional surface rendering (*bottom panel*) are shown. *B,* number of MVs (mean±S.D.) isolated from Trps1-KD and shScr cell lines. *Asterisks* denote statistically significant differences (**, $p \leq 0.005$). *C,* diameter distributions for MVs ($n=100$ for each cell line) isolated from Trps1-KD and shScr cells.

≈70 nm. However, from the same number of cells, ≈10-fold fewer MVs were isolated from Trps1-KD cell lines in comparison with shScr cells, suggesting that fewer MVs are made by Trps1-KD cells. This implicates *Trps1* in MV biogenesis and suggests that *Trps1* is required for MV-dependent initiation of the mineralization process.

Disscussion

Trps1 demonstrates a dynamic and specific expression pattern during odontoblast development. It is highly expressed in preodontoblasts and then is down-regulated upon odontoblast maturation suggesting a *Trps1* role in

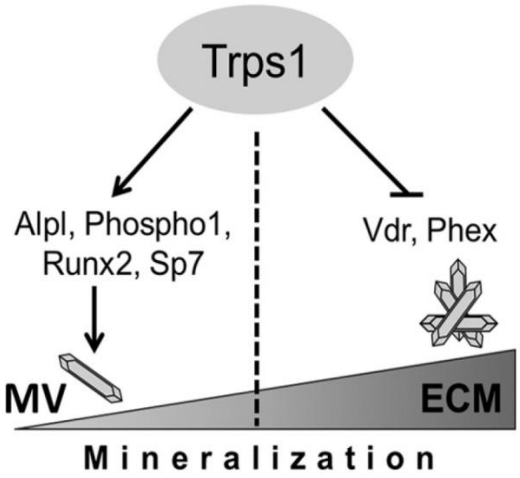

FIGURE 7. **Proposed model of the *Trps1* role in the odontoblast-regulated mineralization process.** The role of *Trps1* in mineralization is context-dependent and differs at the initiation and propagation stages. *Trps1* is required for the MV-dependent initiation of mineralization by supporting expression of major phosphatases and transcription factors required for this process. During the later stages of the mineralization process, *Trps1* acts as a mineralization inhibitor by repressing expression of genes involved in the mineral propagation within the ECM.

odontoblast differentiation (39). *Trps1* expression in secretory odontoblasts is maintained at much lower levels than in progenitors (41). This, in turn, suggests that formation of dentin by mature odontoblasts does not require *Trps1* or that *Trps1* may have a negative effect on their function. We have recently demonstrated that sustained high *Trps1* expression in secretory odontoblasts has deleterious effects on dentin formation (41); however, the role of *Trps1* in odontoblast differentiation and function is unknown. In these studies, using the 17A odontoblastic cell line, we delineated the consequences of *Trps1* deficiency and up-regulation on the odontoblast-regulated mineralization process. Based on our findings, we propose the following model of the *Trps1* role in odontoblasts (Fig. 7). The function of *Trps1* in odontoblasts is context-dependent and is specified by the odontoblast differentiation stage. In preodontoblasts, *Trps1* is required for MV dependent initiation of the mineralization process by supporting expression of major MV-associated phosphatases involved in HA formation and for expression of key osteogenic transcription factors. However, in the mature cells, which actively produce mineralizing matrix, *Trps1* acts as a repressor by

suppressing expression of genes involved in propagating HA within the ECM. We propose that down-regulated expression of the genes involved in the initiation of mineralization is an indirect effect of Trps1 deficiency and may be due to up-regulation of another factor that directly represses these genes. This mechanism incorporates the findings from our *in vitro* studies into the well established molecular function of Trps1 as a transcriptional repressor (31–35). We cannot definitively rule out the possibility that in preodontoblasts Trps1 directly activates a subset of mineralization genes, as it has been demonstrated for Wnt pathway genes in hair follicle progenitor cells (36). However, thus far, there is no evidence that Trps1 can act as a transcriptional activator in cells other than hair follicle progenitors.

In these studies, we determined that in preodontoblastic cells expression of major osteogenic transcription factors Runx2 and Sp7 is decreased upon Trps1 depletion. This contradicts our earlier data from analyses of *Trps1*$^{\Delta GT/\Delta GT}$ endochondral bones where we demonstrated up-regulation of *Runx2* in perichondrium and cartilage of *Trps1* mutant mice (32). This may reflect a combination of cell autonomous and nonautonomous mechanisms regulating mineralization of the perichondrium *versus* effects of only cell autonomous mechanisms in the *in vitro* system. For example, Ihh signaling, which is known to up-regulate *Runx2* in endochondral bones, is increased in the perichondrium of *Trps1*$^{\Delta GT/\Delta GT}$ mice, implicating cell nonautonomous mechanisms in the accelerated perichondrial mineralization in *Trps1*-deficient mice (32). Alternatively, this may indicate that different molecular networks regulate

mineralization of dentin and perichondrium. This possibility is supported by studies, which discovered distinct pools of *Runx2*-dependent genes in bone and dental mesenchyme (51). Similarly, the upstream regulation of *Runx2* may be different in bones and teeth. In developing endochondral bones, the loss of *Trps1* is sufficient to up-regulate *Runx2* (32), although in preodontoblastic cells this effect may be counteracted by simultaneous up-regulation of another repressor of Runx2. The same mechanism involving another repressor may underlie the observed down-regulation of *Alpl* and *Phospho1* in Trps1-KD cells. Therefore, we propose that the observed down-regulation of *Alpl*, *Phospho1*, *Runx2*, and *Sp7* in Trps1-KD cells is an indirect consequence of Trps1 deficiency and results from the released inhibition of a yet unidentified repressor.

Results of our *in vitro* studies, considered together with the *Trps1* expression pattern in odontoblasts, provide first insights into the *Trps1* function in dentinogenesis *in vivo*. We have shown here that *Trps1* depletion from preodontoblastic cells results in the loss of the mineralization potential and downregulation of multiple mineralization-related genes. This supports the hypothesis that *Trps1* is required for odontoblast maturation. Interestingly, the genes most affected by *Trps1* deficiency are those associated with MVs, cellular structures that initiate the mineralization process (Table 2). *In vivo*, a combined deficiency of TNAP and PHOSPHO1 (*Phospho1*$^{-/-}$*; Alpl*$^{+/-}$ mice), two phosphatases that are significantly downregulated in Trps1-KD cells, resulted in a significant decrease of dentin mineralization and was sufficient to almost completely deplete MVs from the mantle dentin (49). Consistent with these data

from animal models, loss of TNAP and PHOSPHO1 in *Trps1*-deficient odontoblastic cells is associated with a decreased number of MVs. Considering that MVs are abundant in mantle dentin, the first dentin layer formed by newly differentiated odontoblasts, but not in the remaining (circumpulpal) dentin formed by mature odontoblasts (2, 52–56), this suggests that *Trps1* is involved in the formation of mantle dentin. The role of *Trps1* in the biogenesis of mineralization-competent MVs remains to be determined.

Mineralization of circumpulpal dentin relies on molecular mechanisms different from those that drive mantle dentin formation (57), as underscored by analyses of human conditions associated with dentin defects. In hypophosphatemia caused by either *PHEX* or *VDR* mutations, formation of circumpulpal dentin is severely disrupted, although mantle dentin is unaffected, demonstrating the crucial role of phosphate homeostasis genes in the later stages of dentin formation (28, 58–62). Consistent with their role in the function of mature odontoblasts, expression of *Phex* and *Vdr* is low in 17A cells prior to mineralization nodule formation and then increases during the propagation of mineralization. This up-regulation of *Phex* and *Vdr* in the later phase of mineralization is hindered by *Trps1* overexpression, whereas *Trps1* has no effect on expression of these genes during the mineralization initiation phase. Our studies demonstrate that Trps1 specifically represses genes that are required for circumpulpal dentin mineralization, and this function is restricted to mature cells that actively support propagation of mineralization in the ECM. This agrees with our recent *in vivo* studies demonstrating that sustained high *Trps1* expression in

secretory odontoblasts results in severely abnormal dentin and direct repression of the *Dspp* gene. However, TNAP levels remain unchanged.

In summary, our studies of an *in vitro* model of odontoblast differentiation and mineralization provide an understanding of the biological significance of the dynamic changes of *Trps1* expression during dentinogenesis. We uncovered that although Trps1 is required for the initiation of odontoblast-regulated mineralization, down-regulation of *Trps1* in secretory odontoblasts is necessary to allow for the formation of circumpulpal dentin.

Acknowledgments

We thank Dr. Rajiv Kumar (Mayo Clinic) for providing Phex antibodies and Dr. Chunlin Qin (Baylor College of Dentistry) for providing Fam20C antibodies. For microarray analyses, we thank the University of Alabama at Birmingham Heflin Center for Genomic Sciences and Brian Dawson (Baylor College of Medicine). We thank Terry Bertin for the assistance with qRT-PCR optimization.

References

1. Gorski, J. P. (2011) Biomineralization of bone: a fresh view of the roles of noncollagenous proteins. Front. Biosci. 16, 2598–2621
2. Goldberg, M., Kulkarni, A. B., Young, M., and Boskey, A. (2011) Dentin: structure, composition and mineralization. Front. Biosci. 3, 711–735

3. Golub, E. E. (2009) Role of matrix vesicles in biomineralization. Biochim. Biophys. Acta 1790, 1592–1598
4. Golub, E. E. (2011) Biomineralization and matrix vesicles in biology and pathology. Semin. Immunopathol. 33, 409–417
5. Anderson, H. C., Garimella, R., and Tague, S. E. (2005) The role of matrix vesicles in growth plate development and biomineralization. Front. Biosci. 10, 822–837
6. Balcerzak, M., Malinowska, A., Thouverey, C., Sekrecka, A., Dadlez, M., Buchet, R., and Pikula, S. (2008) Proteome analysis of matrix vesicles isolated from femurs of chicken embryo. Proteomics 8, 192–205
7. Millán, J. L. (2013) The role of phosphatases in the initiation of skeletal mineralization. Calcif. Tissue Int. 93, 299–306
8. Kirsch, T., Nah, H. D., Shapiro, I. M., and Pacifici, M. (1997) Regulated production of mineralization-competent matrix vesicles in hypertrophic chondrocytes. J. Cell Biol. 137, 1149–1160
9. Yadav, M. C., Simão, A. M., Narisawa, S., Huesa, C., McKee, M. D., Farquharson, C., and Millán, J. L. (2011) Loss of skeletal mineralization by the simultaneous ablation of PHOSPHO1 and alkaline phosphatase function: a unified model of the mechanisms of initiation of skeletal calcification. J. Bone Miner. Res. 26, 286–297
10. McKee, M. D., Yadav, M. C., Foster, B. L., Somerman, M. J., Farquharson, C., and Millán, J. L. (2013) Compounded PHOSPHO1/ALPL deficiencies reduce dentin mineralization. J. Dent. Res. 92, 721–727
11. Harmey, D., Hessle, L., Narisawa, S., Johnson, K. A., Terkeltaub, R., and Millán, J. L. (2004) Concerted regulation of inorganic pyrophosphate and osteopontin by akp2, enpp1, and ank: an integrated model of the pathogenesis of mineralization disorders. Am. J. Pathol. 164, 1199–1209
12. Stewart, A. J., Roberts, S. J., Seawright, E., Davey, M. G., Fleming, R. H., and Farquharson, C. (2006) The presence of PHOSPHO1 in matrix vesicles
and its developmental expression prior to skeletal mineralization. Bone 39, 1000–1007
13. Ciancaglini, P., Yadav, M. C., Simão, A. M., Narisawa, S., Pizauro, J. M., Farquharson, C., Hoylaerts, M. F., and Millán, J. L. (2010) Kinetic analysis of substrate utilization by native and TNAP-, NPP1-, or PHOSPHO1-deficient matrix vesicles. J. Bone Miner. Res. 25, 716–723
14. Addison, W. N., Azari, F., Sørensen, E. S., Kaartinen, M. T., and McKee, M. D. (2007) Pyrophosphate inhibits mineralization of osteoblast cultures by binding to mineral, up-regulating osteopontin, and inhibiting alkaline phosphatase activity. J. Biol. Chem. 282, 15872–15883
15. George, A., and Veis, A. (2008) Phosphorylated proteins and control over apatite nucleation, crystal growth, and inhibition. Chem. Rev. 108, 4670–4693
16. Johnson, K., Goding, J., Van Etten, D., Sali, A., Hu, S. I., Farley, D., Krug, H., Hessle, L., Millán, J. L., and Terkeltaub, R. (2003) Linked deficiencies in extracellular PP(i) and osteopontin mediate pathologic calcification

associated with defective PC-1 and ANK expression. J. Bone Miner. Res. 18, 994–1004
17. van den Bos, T., Handoko, G., Niehof, A., Ryan, L. M., Coburn, S. P., Whyte, M. P., and Beertsen, W. (2005) Cementum and dentin in hypophosphatasia. J. Dent. Res. 84, 1021–1025
18. Suzuki, H., Amizuka, N., Oda, K., Noda, M., Ohshima, H., and Maeda, T. (2008) Involvement of the klotho protein in dentin formation and mineralization. Anat. Rec. 291, 183–190
19. Thompson, D. L., Sabbagh, Y., Tenenhouse, H. S., Roche, P. C., Drezner, M. K., Salisbury, J. L., Grande, J. P., Poeschla, E. M., and Kumar, R. (2002) Ontogeny of Phex/PHEX protein expression in mouse embryo and subcellular localization in osteoblasts. J. Bone Miner. Res. 17, 311–320
20. Ye, L., MacDougall, M., Zhang, S., Xie, Y., Zhang, J., Li, Z., Lu, Y., Mishina, Y., and Feng, J. Q. (2004) Deletion of dentin matrix protein-1 leads to a partial failure of maturation of predentin into dentin, hypomineralization, and expanded cavities of pulp and root canal during postnatal tooth development. J. Biol. Chem. 279, 19141–19148
21. Yoshiko, Y., Wang, H., Minamizaki, T., Ijuin, C., Yamamoto, R., Suemune, S., Kozai, K., Tanne, K., Aubin, J. E., and Maeda, N. (2007) Mineralized tissue cells are a principal source of FGF23. Bone 40, 1565–1573
22. Barron, M. J., McDonnell, S. T., Mackie, I., and Dixon, M. J. (2008) Hereditary dentine disorders: dentinogenesis imperfecta and dentine dysplasia. Orphanet J. Rare Dis. 3, 31
23. Kim, J. W., and Simmer, J. P. (2007) Hereditary dentin defects. J. Dent. Res. 86, 392–399
24. Liu, H., Li, J., Lei, H., Zhu, T., Gan, Y., and Ge, L. (2010) Genetic etiology and dental pulp cell deficiency of hypophosphatasia. J. Dent. Res. 89, 1373–1377
25. MacDougall, M., Dong, J., and Acevedo, A. C. (2006) Molecular basis of human dentin diseases. Am. J. Med. Genet. 140, 2536–2546
26. Souza, M. A., Soares Junior, L. A., Santos, M. A., and Vaisbich, M. H. (2010) Dental abnormalities and oral health in patients with hypophosphatemic rickets. Clinics 65, 1023–1026
27. Bergwitz, C., and Jüppner, H. (2012) FGF23 and syndromes of abnormal renal phosphate handling. Adv. Exp. Med. Biol. 728, 41–64
28. Opsahl Vital, S., Gaucher, C., Bardet, C., Rowe, P. S., George, A., Linglart, A., and Chaussain, C. (2012) Tooth dentin defects reflect genetic disorders affecting bone mineralization. Bone 50, 989–997
29. Hessle, L., Johnson, K. A., Anderson, H. C., Narisawa, S., Sali, A., Goding, J. W., Terkeltaub, R., and Millan, J. L. (2002) Tissue-nonspecific alkaline phosphatase and plasma cell membrane glycoprotein-1 are central antagonistic regulators of bone mineralization. Proc. Natl. Acad. Sci. U.S.A. 99, 9445–9449
30. Foster, B. L., Nagatomo, K. J., Tso, H. W., Tran, A. B., Nociti, F. H., Jr., Narisawa, S., Yadav, M. C., McKee, M. D., Millán, J. I., and Somerman,

M. J. (2013) Tooth root dentin mineralization defects in a mouse model of hypophosphatasia. J. Bone Miner. Res. 28, 271–282
31. Malik, T. H., Shoichet, S. A., Latham, P., Kroll, T. G., Peters, L. L., and Shivdasani, R. A. (2001) Transcriptional repression and developmental functions of the atypical vertebrate GATA protein TRPS1. EMBO J. 20, 1715–1725
32. Napierala, D., Sam, K., Morello, R., Zheng, Q., Munivez, E., Shivdasani, R. A., and Lee, B. (2008) Uncoupling of chondrocyte differentiation and perichondrial mineralization underlies the skeletal dysplasia in trichorhino-phalangeal syndrome. Hum. Mol. Genet. 17, 2244–2254
33. Piscopo, D. M., Johansen, E. B., and Derynck, R. (2009) Identification of theGATAfactor TRPS1 as a repressor of the osteocalcin promoter. J. Biol. Chem. 284, 31690–31703
34. Suemoto, H., Muragaki, Y., Nishioka, K., Sato, M., Ooshima, A., Itoh, S., Hatamura, I., Ozaki, M., Braun, A., Gustafsson, E., and Fässler, R. (2007) Trps1 regulates proliferation and apoptosis of chondrocytes through Stat3 signaling. Dev. Biol. 312, 572–581
35. Wuelling, M., Kaiser, F. J., Buelens, L. A., Braunholz, D., Shivdasani, R. A., Depping, R., and Vortkamp, A. (2009) Trps1, a regulator of chondrocyte proliferation and differentiation, interacts with the activator form of Gli3. Dev. Biol. 328, 40–53
36. Fantauzzo, K. A., and Christiano, A. M. (2012) Trps1 activates a network of secreted Wnt inhibitors and transcription factors crucial to vibrissa follicle morphogenesis. Development 139, 203–214
37. Fantauzzo, K. A., Tadin-Strapps, M., You, Y., Mentzer, S. E., Baumeister, F. A., Cianfarani, S., Van Maldergem, L., Warburton, D., Sundberg, J. P., and Christiano, A. M. (2008)Aposition effect on TRPS1 is associated with Ambras syndrome in humans and the Koala phenotype in mice. Hum. Mol. Genet. 17, 3539–3551
38. Momeni, P., Glöckner, G., Schmidt, O., von Holtum, D., Albrecht, B., Gillessen-Kaesbach, G., Hennekam, R., Meinecke, P., Zabel, B., Rosenthal, A., Horsthemke, B., and Lüdecke, H. J. (2000) Mutations in a new gene, encoding a zinc-finger protein, cause tricho-rhino-phalangeal syndrome type I. Nat. Genet. 24, 71–74
39. Kantaputra, P., Miletich, I., Lüdecke, H. J., Suzuki, E. Y., Praphanphoj, V., Shivdasani, R., Wuelling, M., Vortkamp, A., Napierala, D., and Sharpe, P. T. (2008) Tricho-rhino-phalangeal syndrome with supernumerary teeth. J. Dent. Res. 87, 1027–1031
40. Kunath, M., Lüdecke, H. J., and Vortkamp, A. (2002) Expression of Trps1 during mouse embryonic development. Mech. Dev. 119, S117–S120
41. Napierala, D., Sun, Y., Maciejewska, I., Bertin, T. K., Dawson, B., D'Souza, R., Qin, C., and Lee, B. (2012) Transcriptional repression of the Dspp gene leads to dentinogenesis imperfecta phenotype in Col1a1-Trps1 transgenic mice. J. Bone Miner. Res. 27, 1735–1745
42. Lacerda-Pinheiro, S., Dimitrova-Nakov, S., Harichane, Y., Souyri, M., Petit-Cocault, L., Legrès, L., Marchadier, A., Baudry, A., Ribes, S., Goldberg,

M., Kellermann, O., and Poliard, A. (2012) Concomitant multipotent and unipotent dental pulp progenitors and their respective contribution to mineralised tissue formation. Eur. Cell Mater. 23, 371–386
43. Priam, F., Ronco, V., Locker, M., Bourd, K., Bonnefoix, M., Duchêne, T., Bitard, J., Wurtz, T., Kellermann, O., Goldberg, M., and Poliard, A. (2005) New cellular models for tracking the odontoblast phenotype. Arch. Oral Biol. 50, 271–277
44. Huang, B., Sun, Y., Maciejewska, I., Qin, D., Peng, T., McIntyre, B., Wygant, J., Butler, W. T., and Qin, C. (2008) Distribution of SIBLING proteins in the organic and inorganic phases of rat dentin and bone. Eur. J. Oral Sci. 116, 104–112
45. Irizarry, R. A., Hobbs, B., Collin, F., Beazer-Barclay, Y. D., Antonellis, K. J., Scherf, U., and Speed, T. P. (2003) Exploration, normalization, and summaries of high density oligonucleotide array probe level data. Biostatistics 4, 249–264
46. Street, S. E., Walsh, P. L., Sowa, N. A., Taylor-Blake, B., Guillot, T. S., Vihko, P., Wightman, R. M., and Zylka, M. J. (2011) PAP and NT5E inhibit nociceptive neurotransmission by rapidly hydrolyzing nucleotides to adenosine. Mol. Pain 7, 80
47. Sreenath, T., Thyagarajan, T., Hall, B., Longenecker, G., D'Souza, R., Hong, S., Wright, J. T., MacDougall, M., Sauk, J., and Kulkarni, A. B. (2003) Dentin sialophosphoprotein knockout mouse teeth display widened predentin zone and develop defective dentin mineralization similar to human dentinogenesis imperfecta type III. J. Biol. Chem. 278, 24874–24880
48. Rafaelsen, S. H., Raeder, H., Fagerheim, A. K., Knappskog, P., Carpenter, T. O., Johansson, S., and Bjerknes, R. (2013) Exome sequencing reveals FAM20c mutations associated with fibroblast growth factor 23-related hypophosphatemia, dental anomalies, and ectopic calcification. J. Bone Miner. Res. 28, 1378–1385
49. McKee, M. D., Hoac, B., Addison, W. N., Barros, N. M., Millán, J. L., and Chaussain, C. (2013) Extracellular matrix mineralization in periodontal tissues: noncollagenous matrix proteins, enzymes, and relationship to hypophosphatasia and X-linked hypophosphatemia. Periodontology 2000 63, 102–122
50. Polewski, M. D., Johnson, K. A., Foster, M., Millán, J. L., and Terkeltaub, R. (2010) Inorganic pyrophosphatase induces type I collagen in osteoblasts. Bone 46, 81–90
51. James, M. J., Järvinen, E., Wang, X. P., and Thesleff, I. (2006) Different roles of Runx2 during early neural crest-derived bone and tooth development. J. Bone Miner. Res. 21, 1034–1044
52. Katchburian, E. (1973) Membrane-bound bodies as initiators of mineralization of dentine. J. Anat. 116, 285–302
53. Stratmann, U., Schaarschmidt, K., Wiesmann, H. P., Plate, U., and Höhling, H. J. (1996) Mineralization during matrix-vesicle-mediated mantle dentine

formation in molars of albino rats: a microanalytical and ultrastructural study. Cell Tissue Res. 284, 223–230
54. Massa, L. F., Ramachandran, A., George, A., and Arana-Chavez, V. E. (2005) Developmental appearance of dentin matrix protein 1 during the early dentinogenesis in rat molars as identified by high-resolution immunocytochemistry. Histochem. Cell Biol. 124, 197–205
55. Takano, Y., Sakai, H., Baba, O., and Terashima, T. (2000) Differential involvement of matrix vesicles during the initial and appositional mineralization processes in bone, dentin, and cementum. Bone 26, 333–339
56. Garcés-Ortíz, M., Ledesma-Montes, C., and Reyes-Gasga, J. (2013) Presence of matrix vesicles in the body of odontoblasts and in the inner third of dentinal tissue: a scanning electron microscopy study. Med. Oral Patol. Oral Cir. Bucal. 18, e537–e541
57. Verdelis, K., Lukashova, L., Wright, J. T., Mendelsohn, R., Peterson, M. G., Doty, S., and Boskey, A. L. (2007) Maturational changes in dentin mineral properties. Bone 40, 1399–1407
58. Boukpessi, T., Septier, D., Bagga, S., Garabedian, M., Goldberg, M., and Chaussain-Miller, C. (2006) Dentin alteration of deciduous teeth in human hypophosphatemic rickets. Calcif. Tissue Int. 79, 294–300
59. Goldberg, M., Septier, D., Bourd, K., Hall, R., Jeanny, J. C., Jonet, L., Colin, S., Tager, F., Chaussain-Miller, C., Garabédian, M., George, A., Goldberg, H., and Menashi, S. (2002) The dentino-enamel junction revisited. Connect. Tissue Res. 43, 482–489
60. Chaussain-Miller, C., Sinding, C., Septier, D., Wolikow, M., Goldberg, M., and Garabedian, M. (2007) Dentin structure in familial hypophosphatemic rickets: benefits of vitamin D and phosphate treatment. Oral Dis. 13, 482–489
61. Salmon, B., Bardet, C., Khaddam, M., Naji, J., Coyac, B. R., Baroukh, B., Letourneur, F., Lesieur, J., Decup, F., Le Denmat, D., Nicoletti, A., Poliard, A., Rowe, P. S., Huet, E., Vital, S. O., Linglart, A., McKee, M. D., and Chaussain, C. (2013) MEPE-derived ASARM peptide inhibits odontogenic differentiation of dental pulp stem cells and impairs mineralization in tooth models of X-linked hypophosphatemia. PLoS One 8, e56749
62. Zhang, X., Rahemtulla, F. G., MacDougall, M. J., and Thomas, H. F. (2007) Vitamin D receptor deficiency affects dentin maturation in mice. Arch. Oral Biol. 52, 1172–1179

PHOSPHATE INDUCES FORMATION OF MATRIX VESICLES DURING ODONTOBLAST-INITIATED MIENRALIZAITON IN VITRO

by

SANDEEP C. CHAUDHARY, MARIA KUZYNSKI, MASSIMO BOTTINI, ELIA BENIASH, TERJE DOKLAND, CALLIE G. MOBLEY, MANISHA C. YADAV, ANNE POLIARD, ODILE KELLERMAN, JOSÉ LUIS MILLÁN, AND DOBRAWA NAPIERALA

Matrix Biology 2016 Feb 13

CHAPTER 2

PHOSPHATE INDUCES FORMATION OF MATRIX VESICLES DURING ODONTOBLAST-INITIATED MIENRALIZAITON IN VITRO

Abstract

Mineralization is a process of deposition of calcium phosphate crystals within a fibrous extracellular matrix (ECM). In mineralizing tissues, such as dentin, bone and hypertrophic cartilage, this process is initiated by a specific population of extracellular vesicles (EV), called matrix vesicles (MV). Although it has been proposed that MV are formed by shedding of the plasma membrane, the cellular and molecular mechanisms regulating formation of mineralization-competent MV are not fully elucidated. In these studies, 17IIA11, ST2, and MC3T3-E1 osteogenic cell lines were used to determine how formation of MV is regulated during initiation of the mineralization process. In addition, the molecular composition of MV secreted by 17IIA11 cells and exosomes from blood and B16-F10 melanoma cell line was compared to identify the molecular characteristics distinguishing MV from other EV. Western blot analyses demonstrated that MV released from 17IIA11 cells are characterized by high levels of proteins engaged in calcium and phosphate regulation, but do not express the exosomal markers

CD81 and HSP70. Furthermore, we uncovered that the molecular composition of MV released by 17IIA11 cells changes upon exposure to the classical inducers of osteogenic differentiation, namely ascorbic acid and phosphate. Specifically, lysosomal proteins Lamp1 and Lamp2a were only detected in MV secreted by cells stimulated with osteogenic factors. Quantitative nanoparticle tracking analyses of MV secreted by osteogenic cells determined that standard osteogenic factors stimulate MV secretion and that phosphate is the main driver of their secretion. On the molecular level, phosphate-induced MV secretion is mediated through activation of extracellular signal-regulated kinases Erk1/2 and is accompanied by re-organization of filamentous actin. In summary, we determined that mineralization-competent MV are distinct from exosomes, and we identified a new role of phosphate in the process of ECM mineralization. These data provide novel insights into the mechanisms of MV formation during initiation of the mineralization process.

Introduction

Extracellular vesicles (EV) is a broad term describing sub-micron size, spherical, membrane-enclosed particles released from cells to the extracellular milieu. EV are secreted from cells in various physiological and pathological conditions and can be detected in virtually all biological fluids [1,2]. They express cell surface receptors and carry biologically active proteins, lipids, and nucleic

acids. It has been shown that EV have the capacity to modulate the function of target cells in an autocrine or paracrine manner, therefore they have been recognized as an integral component of the intercellular communication [2,3]. EV are highly heterogeneous and dynamic in nature. Their molecular composition reflects their cell-type of origin, pathophysiological cell state, biogenesis pathway, and biological function [2,3]. Mineralization is a biological process by which crystals of calcium phosphate (hydroxyapatite, HA) are laid down within the fibrous extracellular matrix (ECM). Physiological mineralization occurs in skeletal and dental tissues (bone, terminal hypertrophic cartilage, dentin, cementum, and enamel). Mineralization can also occur ectopically (pathologic mineralization) in soft tissues, for example in the blood vessels (arterial calcification) or in joints during the late stages of osteoarthritis. The progression and extent of both physiologic and pathologic mineralization are regulated locally and systemically. Mineralization depends upon the availability of Ca^{2+} and PO_4^{3-} (P_i), concentration of mineralization inhibitors, and ECM composition [4–13].

P_i participates in the mineralization process in multiple ways. First, P_i is a structural component of the inorganic phase of the mineralized ECM, thus its local availability affects the rate of HA formation. Second, addition or removal of P_i to/from various ECM proteins regulates their function in mineralization [14,15]. Finally, it has been shown that P_i regulates expression of multiple genes involved in osteogenic differentiation and the mineralization process [16–20]. The P_i-induced signaling pathway is not well delineated and its mediators are largely unknown. However, it has been demonstrated that P_i signaling in mineralizing

cells depends on the activity of P_i transporters and is mediated by Erk1/2, but not p38 or c-jun kinases [21–23]. P_i-induced activation of Erk1/2 is bi-phasic with the first activation happening quickly, within 15–30 min of P_i treatment, and the second activation occurring approximately 6–8 h later [23,24].

Initiation of physiologic mineralization of cartilage, mantle dentin, and woven bone is facilitated by a specific population of EV, called matrix vesicles (MV). There is evidence suggesting that ectopic mineralization of arteries is also associated with increased secretion of EV from vascular smooth muscle cells with a presumptive role in supporting pathologic vascular mineralization [25]. Electron microscopy demonstrated that mineralizing cells, such as hypertrophic chondrocytes and newly differentiated odontoblasts and osteoblasts, shed numerous sub-micron size (80–200 nm) vesicles from their plasma membrane [26–30]. Therefore, it has been proposed that MV are formed by budding off the plasma membrane. The plasma membrane origin of MV has been further supported by comparative analyses of lipids and proteins, in which it was demonstrated that there are significant similarities in the molecular composition of MV and the plasma membrane of the cell of origin [31,32]. However, in two more recent studies, vesicles containing electron-dense material composed of calcium and phosphorus were detected in the cytoplasm of mouse calvarial osteoblasts, suggesting that intracellular processes may play a role in initial HA formation [33,34].

MV have a discrete intravesicular environment as well as protein and lipid composition that together support the accumulation of high concentrations of P*i*

and Ca^{2+}, and subsequent HA formation. In particular, MV are enriched in tissue-nonspecific alkaline phosphatase (TNAP) and phosphoethanolamine/phosphocholine phosphatase (PHOSPHO1), whose catalytic activities provide P_i for HA formation, but have non-redundant functions in skeletal mineralization [4,35–39]. Proteomic analyses of vesicles produced by chondrocytes, osteoblast cell lines, and bone marrow stromal cells undergoing osteogenic differentiation consistently detect numerous proteins that are involved in the mineralization process and matrix remodeling. This agrees with the notion that the biological function of MV is to support mineralization [32,40–43]. Of note, MV are also enriched in Ca^{2+} transporters (annexins) which are commonly detected in many different types of EV [26,38,40,43–47].

It is now recognized that cells utilize various cellular mechanisms to secrete EV of diverse biological functions. With the rising interest in using EV as diagnostic markers and therapeutic targets, it is critical to understand the differences between various populations of EV and the mechanisms regulating their secretion. In this study, we use cellular models of mineralization to gain mechanistic insights into the regulation of secretion of a specific group of EV with the biological function to promote mineralization. The goals of our study are to increase our understanding of how the mineralization process is initiated and to delineate characteristic features of mineralization-competent MV.

Results

Stimulation of osteogenic differentiation increases secretion of matrix vesicles in cellular models of mineralization

In studies using cellular models of mineralization, differentiation of progenitor cells and deposition of a mineralizing matrix is most commonly stimulated by treatment of cells with ascorbic acid and phosphate. Under these conditions, the calcium phosphate deposits in ECM are detected around day 21 of culture in most of the mineralizing cells. In our previous studies, we have shown that these standard osteogenic conditions induce rapid (within 6–8 days) mineralization of 17IIA11 cells, which is accompanied by production of MV [48–50]. Therefore, we selected 17IIA11 cells as an *in vitro* model for studies of mineralization-competent MV biogenesis. First, to determine whether 17IIA11 cells are a representative *in vitro* model for MV formation under osteogenic conditions, we compared secretion of vesicles from 17IIA11 cells with other murine osteogenic cell lines derived from cells of different developmental origin. Preodontoblast-derived 17IIA11 cell line, bone marrow stromal cell-derived ST2 cell line, and calvarium osteoblast precursor-derived MC3T3-E1 cell line were grown to confluency. In all experiments, cells were cultured in vesicle-depleted medium to eliminate contamination of MV preparations by vesicles from FBS. Standard osteogenic conditions were used to induce mineralization. To ensure that all secreted vesicles were accounted for in these analyses, both ECM and conditioned media from tested cells were collected for vesicle isolation. Vesicles produced by unstimulated cells at the time of confluency (0 h; base line) were

compared with vesicles produced by cells within 24 h, 48 h, and 72 h of culture in osteogenic conditions (Fig. 1). Nanoparticle tracking analyses (NTA) were used to quantify purified vesicles and determine their size.

NTA revealed that all compared cell lines secrete vesicles when cultured under standard growth conditions. However, the secretion of vesicles significantly increases upon addition of ascorbic acid and P_i (Fig. 1A and C). For 17IIA11 and ST2 cells, a significant increase in the number of secreted vesicles per cell is detected within the first 24 h of growth under osteogenic conditions, while for MC3T3-E1 cells this occurs at 72 h. During the first 24 h of osteogenic differentiation, MV release is the highest in 17IIA11 cells (8 fold) as compared to 3.1 fold in ST2 cells and 1.9 fold in MC3T3-E1 cells (Fig. 1B). In conditioned medium, the number of vesicles increased robustly between 48 h and 72 h for all cell lines. At 24 h, 280.8 ± 68 vesicles/cell were detected in conditioned media of 17IIA11 cells, whereas 26,500 ± 6630 vesicles/cell were detected in ECM. Thus, the ECM vesicle fraction constitutes 98.9% of all vesicles released by 17IIA11 cells. The percentage of vesicles released to media was increased to 11.1% at 72 h of 17IIA11 osteogenic differentiation. The increased contribution of vesicles in media at 72 h was consistent for all analyzed cell lines (Fig. 1D). Thus, for all cell lines, the contribution of vesicles in medium to the total number of vesicles produced per cell increases with time. However, even after 72 h of osteogenic differentiation, ECM vesicles (MV) constitute the vast majority of all EV secreted during the early stage of osteogenic differentiation (Fig. 1D).

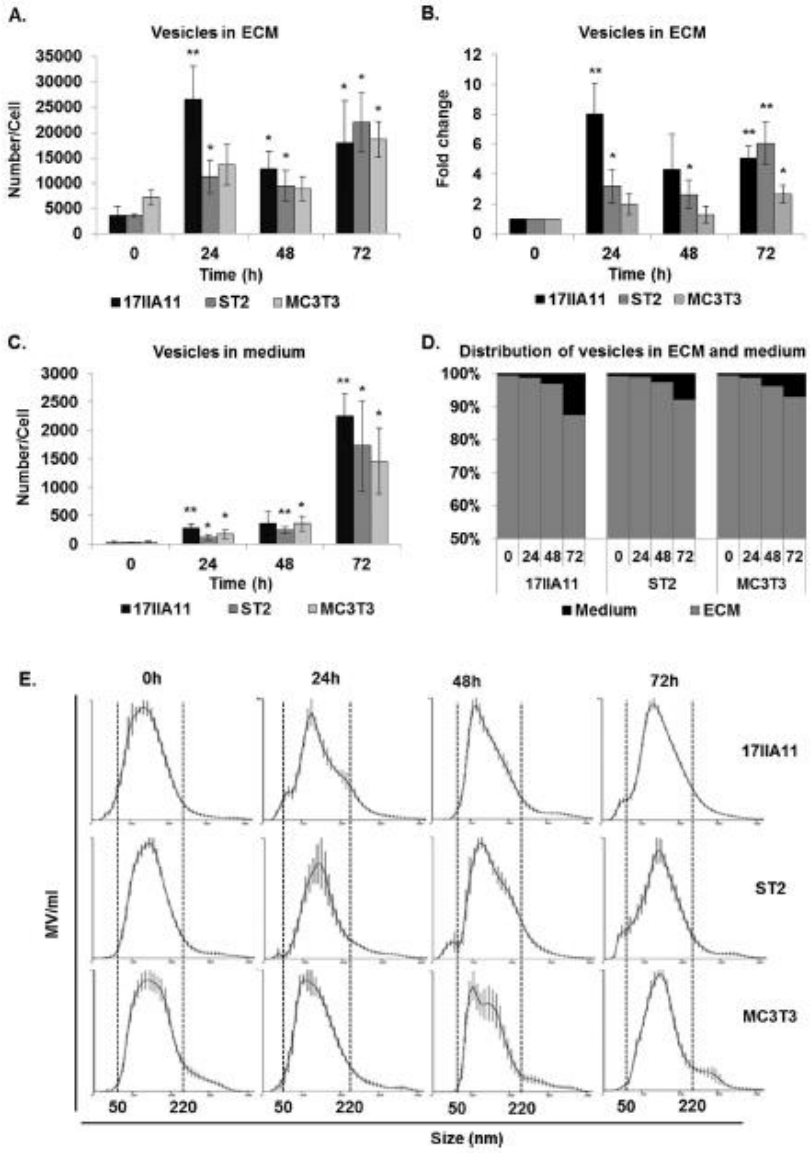

Fig. 1. Osteogenic medium stimulates secretion of EV from mineralizing cell lines. The number of vesicles (A–D) and size distribution (E) were measured using nanoparticle tracking analysis. Secretion of vesicles was stimulated by standard osteogenic conditions (ascorbic acid and P_i) for 24 h, 48 h, or 72 h and compared to unstimulated cells (0 h). Vesicles were collected from the media or extracellular matrix (ECM). (A) Number of vesicles in ECM normalized to the number of cells. Statistical analyses were performed to assess differences between mean values of unstimulated cells and the same cells at different time points of osteogenic treatment. (B) Fold changes in the number of vesicles in ECM compared to 0 h of each cell line. (C) Number of vesicles secreted to medium normalized to the number of cells. (D) Distribution of vesicles between ECM and medium. (E) Size distribution of vesicles in ECM. Dotted lines indicate the size range of vesicles for each cell line. Data are represented as the mean values of three independent experiments ± SD, *$p < 0.05$ and **$p < 0.005$.

The size of MV produced by 17IIA11, ST2, and MC3T3-E1 cells under osteogenic conditions was measured using NTA. These analyses showed that the size distribution of MV does not change during osteogenic differentiation and does not vary between cell lines (Fig. 1E). In all compared cells lines, MV size distribution is in the same range of 50–220 nm, which is consistent with the reported size of MV produced by osteogenic cells [51].

In summary, supplementation of growth medium with standard mineralization-inducing factors (ascorbic acid and P_i) stimulates release of MV from all tested osteogenic cell lines in as early as 24 h. Furthermore, these data show that MV secretion from 17IIA11 cells is comparable to other osteogenic cell lines. Therefore, the 17IIA11 cell line is used in subsequent experiments addressing the regulation of MV formation.

High cell density is required for induction of matrix vesicles secretion in response to mineralization-inducing factors

To determine the key factors regulating secretion of MV at the initiation of the mineralization process, we measured the concentration of vesicles formed by 17IIA11 cells and their size distribution under different culture conditions. First, we compared MV secretion from cells at different cellular confluency states, since cell–cell interactions play a role in the differentiation process [52]. In standard osteogenic differentiation experiments, osteogenic factors are added at high cell density, since the cessation of proliferation is required to enter differentiation pathways. Furthermore, 17IIA11 cells cultured at high density, even without addition of ascorbic acid that stimulates collagen production,

produce ECM containing collagen (Supplemental Fig. 1). Therefore, we sought to determine how cell density affects the secretion of MV. MV release was compared from untreated (control) and stimulated (ascorbic acid and P_i) 17IIA11 cells cultured at high (100% confluent) or low (70% confluent) cell densities. Results of this experiment showed no differences in the concentration of ECM-fraction MV at high or low cell density when cultured for 24 h in standard growth medium (Fig. 2A). As expected, the comparison of MV concentration in ECM of cells grown at high density in standard versus osteogenic conditions shows significantly higher MV secretion under osteogenic conditions. However, there is no difference in the concentration of MV in ECM of stimulated and unstimulated cells grown at low density. Thus, osteogenic factors stimulate MV secretion from confluent cells only. At the same time, there is no difference in the size of MV secreted by cells grown under different cell densities and osteogenic conditions, with the majority of MV in the size range of 50–220 nm in all analyzed groups (Fig. 2B). In summary, high cell density is required for induction of MV secretion by osteogenic factors, but does not affect MV secretion during standard growth.

Osteogenic medium induces secretion of matrix vesicles from 17IIA11 cells

Our comparative analyses of vesicle secretion show that 17IIA11 cells respond to osteogenic stimuli by significantly increasing secretion of vesicles to ECM within 24 h (Fig. 1A). As the next step, we compared the number of MV secreted per cell within 6 h, 12 h, 18 h, and 24 h of treatment with standard osteogenic medium (Fig. 3). These analyses revealed that there is no increase of

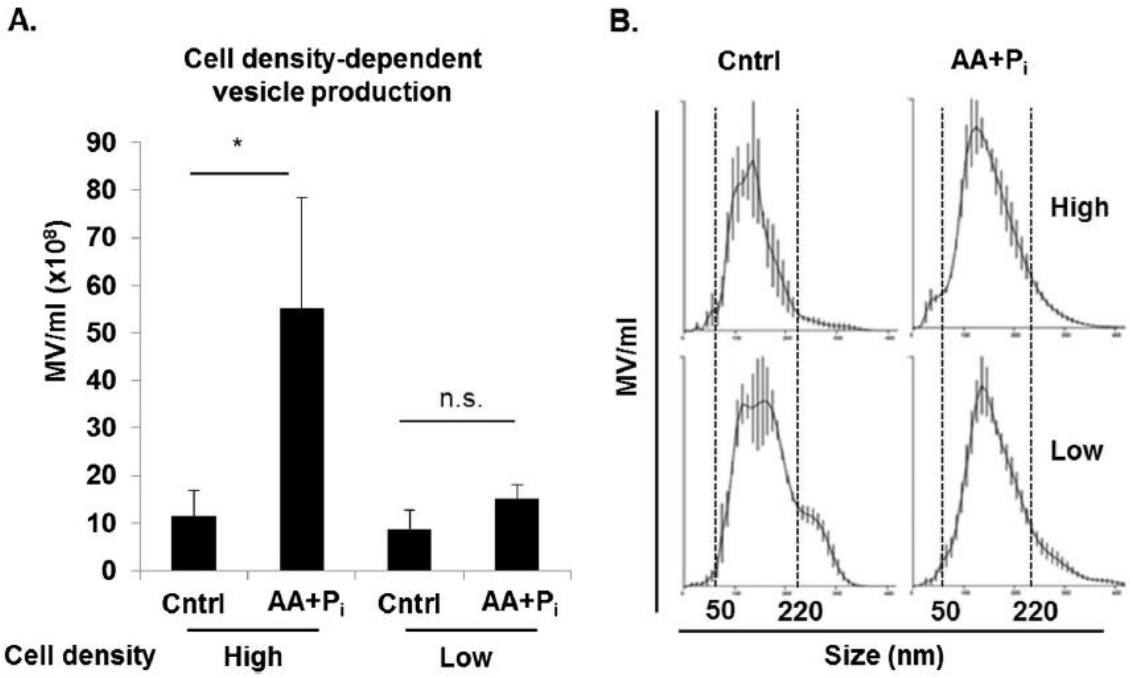

Fig. 2. MV secretion upon induction of osteogenic differentiation depends on cell density. 100% confluent (high) and 70% confluent (low) 17IIA11 cells were treated with standard osteogenic conditions (ascorbic acid and P_i) to stimulate vesicle secretion. Control high and low density cells were grown without osteogenic supplements. After 24 h, vesicles were isolated and the number and size distribution were measured using nanoparticle tracking analysis. (A) Concentration of MV isolated from ECM of 100% confluent (high) and 70% confluent (low) cells treated with ascorbic acid and P_i, and cells cultured in standard growth medium. (B) Graphs showing MV size distribution in all culture conditions. Dotted lines indicate the size range of vesicles for each cell line. Data are represented as the mean values of three independent experiments ± SD, *$p < 0.05$ and **$p < 0.005$.

MV number within the first 6 h of treatment. Then, the number of MV secreted per cell rapidly and significantly increases within 6 h–12 h of osteogenic stimulation. Although MV continue to accumulate in ECM within the next 12 h of osteogenic stimulation, the increase in the MV number per cell at 12–24 h of osteogenic stimulation is lower than the 6–12 h time frame (Fig. 3). These data show that the highest increase in MV secretion by 17IIA11 cells takes place between 6 h and 12 h of treatment, suggesting that MV formation is an early event occurring at the onset of the osteogenic differentiation program.

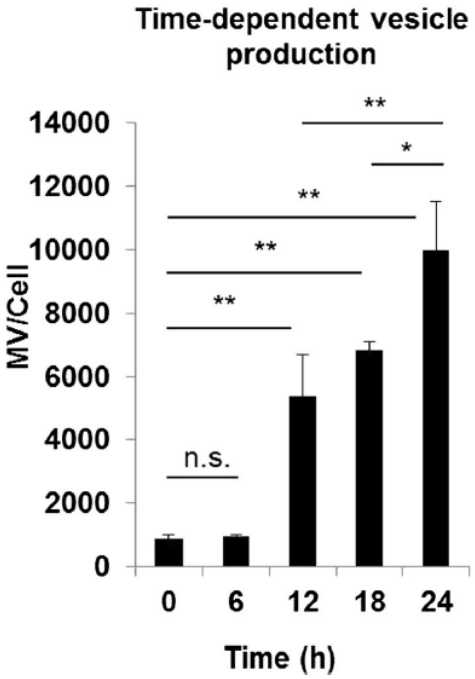

Fig. 3. Osteogenic medium induces rapid secretion of MV from 17IIA11 cells. Comparison of MV concentration in ECM of 17IIA11 cells grown in standard growth conditions (0 h, baseline) and in osteogenic conditions (ascorbic acid and P_i; AA + P_i) for 6 h, 12 h, 18 h, and 24 h. The number of MV secreted per cell was determined using nanoparticle tracking analysis. Data are represented as the mean values of three independent experiments ± SD, *$p < 0.05$ and **$p < 0.005$.

Matrix vesicles are positive for proteins supporting mineralization

To determine if MV secreted by 17IIA11 cells have a role in mineralization and to compare MV with other EV of similar size (specifically exosomes), we analyzed their molecular composition by Western blot. For comparison, we used exosomes isolated from mouse plasma and exosomes produced by melanoma cells (B16-F10). Since there is no common molecular standard for various EV that can be used to confirm equal vesicular protein loading in Western blot analyses, we used silver staining of proteins separated by PAGE to confirm equal protein loading (Fig. 4A). This method also revealed a distinct protein banding pattern of each EV protein extract, suggesting substantial differences in molecular composition of EV from different sources. Interestingly, although the protein banding pattern of MV isolated from 17IIA11 cells cultured in standard growth medium is similar to MV isolated from cells stimulated with osteogenic

factors, clear differences are detected with several bands unique for each group (Fig. 4A).

Western blot analyses demonstrated that two key mineralization supporting phosphatases, TNAP and PHOSPHO1, are detected only in vesicles secreted by 17IIA11 cells and not in plasma or melanoma exosomes (Fig. 4B). Interestingly, in MV from cells stimulated with osteogenic factors, three isoforms of TNAP were detected, while only two TNAP isoforms were detected in MV from unstimulated cells. Similarly, MV from stimulated cells contained an additional isoform of PHOSPHO1, while only one PHOSPHO1 isoform was detected in MV from unstimulated cells. Both PHOSPHO1 isoforms were detected in 17IIA11 cells cultured either in standard growth conditions or with osteogenic factors. MV from both stimulated and unstimulated 17IIA11 cells were highly positive for calcium channel protein annexin V. Consistent with published molecular phenotyping studies, which demonstrated that annexins are commonly detected in different types of EV [44], annexin V was also detected in exosomes from the melanoma cell line. However, unlike melanoma exosomes, MV were negative for exosomal markers HSP70 and CD81. A low but detectable amount of the early endosomal marker Rab5 was present in vesicles from 17IIA11 and melanoma cells. A distinguishing feature of MV from 17IIA11 cells stimulated with osteogenic factors, which contrasts them from MV from unstimulated cells and exosomes, is high expression of lysosomal membrane glycoproteins Lamp1 and Lamp2a. Of note, while MV from stimulated cells are highly positive for Lamp2a, in 17IIA11 cells this protein was barely detectable, which suggests that Lamp2a

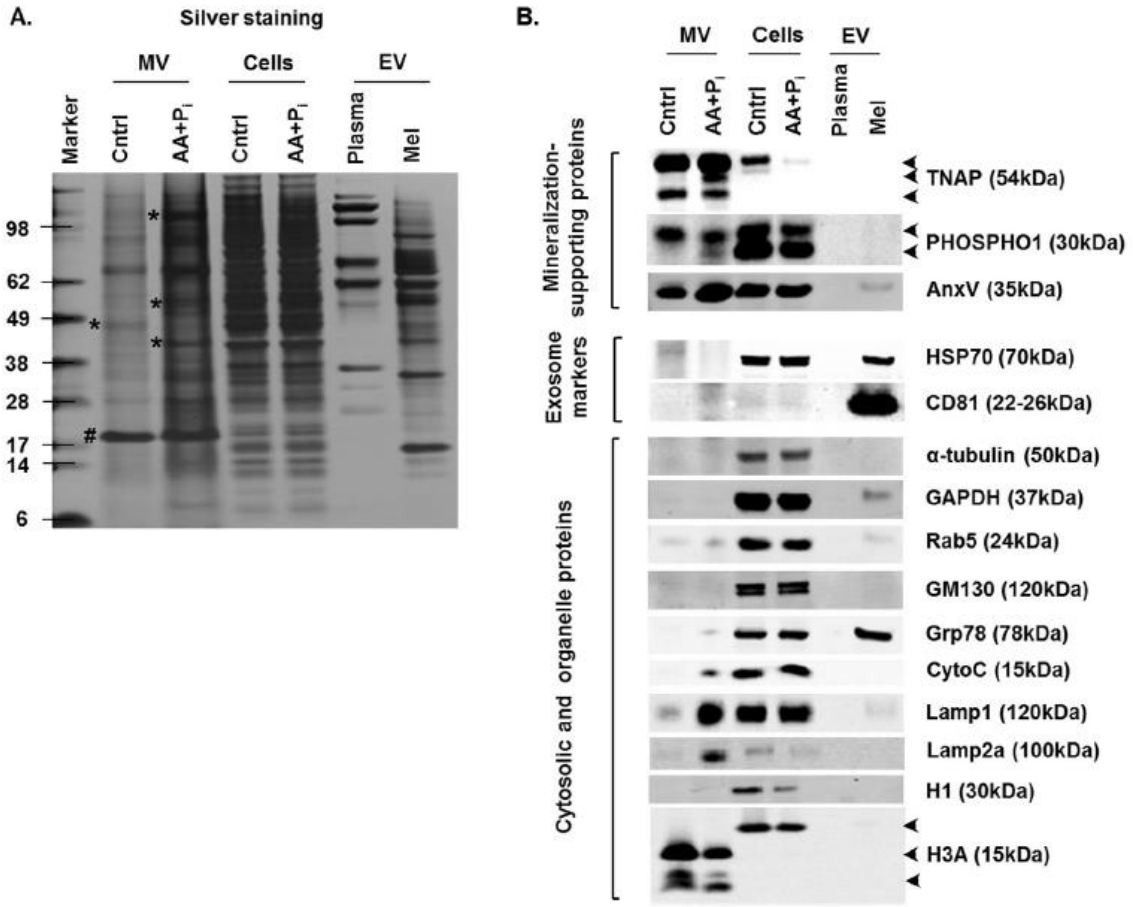

Fig. 4. Osteogenic medium induces formation of mineralization-competent MV. 17IIA11 cells were treated with standard osteogenic conditions (ascorbic acid and P_i; AA + P_i). Proteins from MV and 17IIA11 cells were isolated after 24 h of ascorbic acid and P_i treatment. Proteins from MV and 17IIA11 cells cultured in standard growth medium were used as control (Cntrl). For comparison of molecular composition of MV with other types of EV, EV from murine plasma (Plasma) and B16-F10 melanoma cell line (Mel) were used. (A) Silver stained gel showing protein loading for Western blot analyses and banding pattern of proteins from MV, 17IIA11 cells, and EV from plasma and melanoma cells. Asterisk indicates protein bands that are differentially expressed between MV from treated and untreated cells; pound sign indicates a protein equally expressed in MV from both treated and untreated cells. (B) Western blot analyses of proteins supporting mineralization: TNAP, PHOSPHO1, and annexin V (AnxV); exosomal markers: HSP70 and CD81; cytosolic and cell organelle proteins: α-tubulin, GAPDH, Rab5, GM130, Grp78, cytochrome c (CytoC), Lamp1, Lamp2a, histone 1 (H1), and histone 3a (H3a).

is distributed specifically to MV. Cytochrome c was also detected specifically in MV from stimulated 17IIA11 cells, while Grp78 was detected only in exosomes from melanoma cells. Antibodies against histone 3a detected three smaller-sized proteins, presumptive products of histone 3a proteolysis, in MV but not in exosomes. GAPDH and organelle proteins GM130 and histone 1 were not detected in MV. GAPDH was present only in EV from melanoma cells, which is consistent with previous reports showing GAPDH in exosomes [44].

In summary, comparative analyses of the molecular composition of MV from 17IIA11 cells stimulated with osteogenic factors, MV from unstimulated cells, and exosomes identified a distinct molecular signature of each EV sub-population (Fig. 4). MV from induced cells are specifically enriched in lysosomal proteins. Furthermore, MV from both unstimulated and induced 17IIA11 cells are negative for exosomal markers and positive for proteins providing Ca^{2+} and P_i. This suggests their function in supporting formation of HA, and hence mineralization.

Matrix vesicles from 17IIA11 cells are mineralization-competent

In order to determine, if MV secreted by 17IIA11 cells support formation of hydroxyapatite, we used two different approaches. First, the *in vitro* calcification assay was used [37,53]. MV isolated from 17IIA11 cells grown for 24 h in standard growth medium, osteogenic medium or in standard growth medium supplemented with 10 mM P_i were incubated with varying concentrations of Ca^{2+} and 1 mM ATP as a source of phosphate. Results of this assay demonstrated

that all three groups of MV accumulated Ca^{2+} from the extravesicular environment in a dose-dependent fashion (Fig. 5A). Of note, the Ca^{2+} content in MV incubated with 1 mM Ca^{2+} was under the detection limit.

To further confirm that the MV secreted by 17IIA11 cells are mineralization-competent, we used transmission electron microscopy (TEM) with electron diffraction [54,55] and atomic force microscopy (AFM) phase analyses [56]. In our previous studies we determined that the ECM mineralization of 17IIA11 cells is visible around day 5 of culture under osteogenic conditions [48–50]. Thus, to identify the mineral phase in MV, we compared MV isolated from ECM of 17IIA11 cells cultured either in standard growth medium or in osteogenic medium for 1 day (when there is no detectable ECM mineralization) and 8 days (when ECM mineralization reaches the plateau). TEM with selected area electron diffraction (SAED) detected no crystalline material in day 1 MV (Fig. 5B). Based on the presence of a very weak diffuse ring with d-spacing around 3 Å, it is possible that some amorphous mineral was present in the MV collected from cells grown in osteogenic medium for 1 day (Fig. 5B). In contrast, crystalline material was detected by SAED in MV from both groups on day 8. However, in the sample derived from the cells grown in the standard growth medium only very few particles with very weak diffraction patterns were identified (Fig. 5B). Analysis of the diffraction patterns revealed weak reflections with d-spacings of 3.4 and 2.6 Å, corresponding to (002) and (011) planes of HA reflections, respectively [54,55]. In contrast, particles producing strong reflections with d-

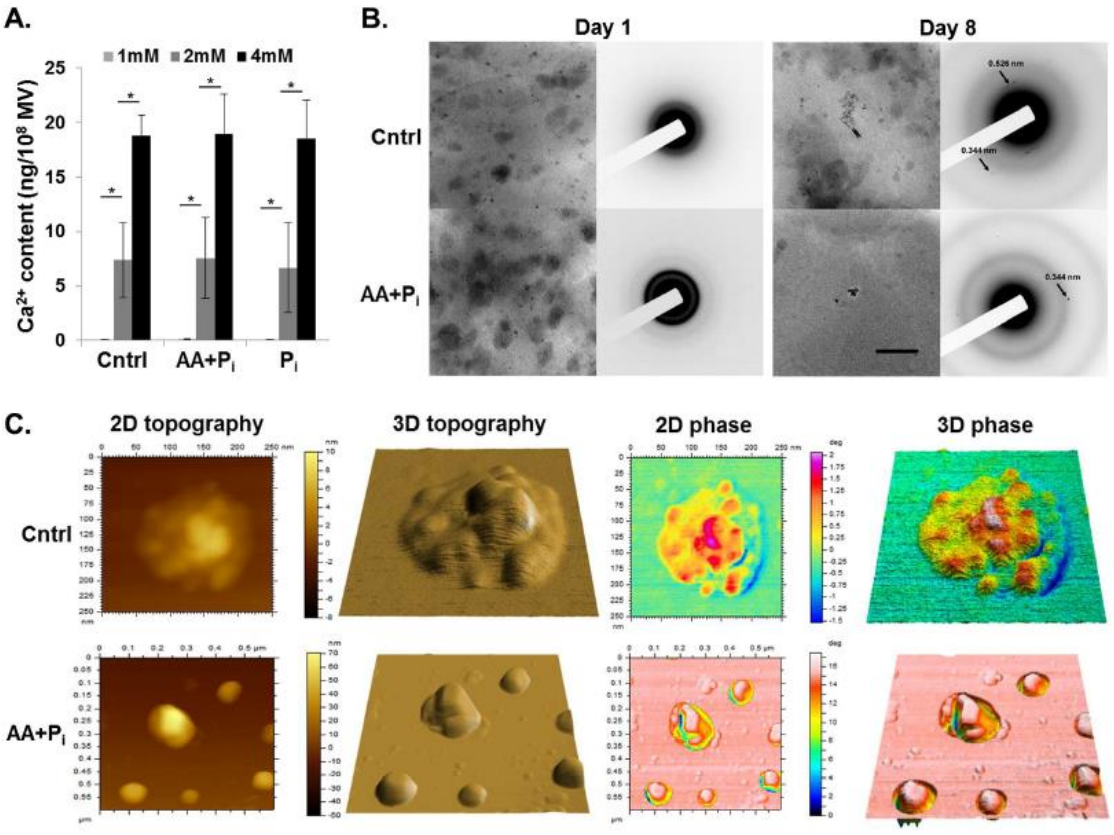

Fig. 5. MV secreted by 17IIA11 cells are able to mineralize. (A) Bar graphs showing Ca^{2+} concentration-dependent accumulation of Ca^{2+} in MV isolated from 17IIA11 cells grown for 24 h in standard growth medium (Cntrl), in osteogenic medium (AA + P_i), or in standard growth medium supplemented with 10 mM P_i (P_i). Under conditions of 1 mM Ca^{2+} in the calcification buffer, there was no detectable Ca^{2+} in MV. (B) Bright field TEM micrographs (left columns) and corresponding electron diffraction patterns (right columns) of MV preparations collected from cells grown either in standard growth medium (Cntrl) or in osteogenic medium (AA + P_i) for 1 day and 8 days. All micrographs were acquired at the same magnification. The scale bar corresponds to 200 nm. (C) AFM images of MV collected from cells grown either in standard growth medium (Cntrl) or in osteogenic medium (AA + P_i) for 8 days. From left to right: 2D topography, 3D topography, 2D phase and 3D phase images. Scan size of the control sample: 600 nm × 600 nm. Scan size of the AA + P_i sample: 250 nm × 250 nm.

spacings of 3.4 Å corresponding to (002) planes of HA were found in the sample prepared from cells grown for 8 days in osteogenic medium (Fig. 5B).

The presence of HA in MV isolated from 17IIA11 cells grown under osteogenic conditions for 8 days was further confirmed by examining MV

dropped onto a mica substrate and imaged by means of AFM, followed by qualitative evaluations of their internal composition by AFM phase analysis [56]. MV AFM phase images showed the presence of internal spots with high phase angle (φ) values surrounded by regions with very low φ values (Fig. 5C). The spots at high φ values were interpreted to be caused by the presence of HA crystals under the MV membrane. HA crystals were surrounded by less crowded media, which made the membrane deformable and able to dampen AFM tip vibrations, which explains the large variations in φ values between the spots and the surrounding regions. Control MV had different topographic and phase properties compared to MV isolated from cells grown under osteogenic conditions. Control MV appeared smaller than MV isolated from cells grown under osteogenic conditions and had either a smooth surface (not shown) or a non-uniform surface with several irregularities that were a few to several Å tall (Fig. 5C). AFM phase images showed that these irregularities corresponded to spots with high phase surrounded by regions with lower phase values. However, the variation in φ values between the spots and the surrounding regions were much smaller for control MV than for MV isolated from cells grown under osteogenic conditions, thus suggesting that control MV were filled with mineral aggregates at an early mineralization stage, i.e. a nucleation core.

In summary, these results together with the Western blot data detecting Ca^{2+} and P_i providing proteins in MV (Fig. 4B), suggest that MV from 17IIA11 cells are competent to support mineralization.

Phosphate is the key inducer of matrix vesicle production by osteogenic cells

Ascorbic acid and phosphate (either in the organic form as β-glycerophosphate or in the inorganic form as Na–P_i buffer) are routinely used to stimulate osteogenic differentiation *in vitro* [24,57]. Ascorbic acid enhances the secretion of type I collagen, a major organic component of the mineralizing ECM [57], while phosphate is a structural component of the inorganic phase of the mineralizing ECM as well as a signaling molecule that regulates expression of multiple genes involved in mineralization [24,57]. Here we determined that treatment of osteogenic cells with ascorbic acid and P_i stimulates secretion of mineralization-competent MV (Figs. 1, 4 and 5). Therefore, we next compared secretion of MV by 17IIA11 cells stimulated with: i) both ascorbic acid and P_i; ii) P_i only; and iii) ascorbic acid only. As a control, MV from untreated 17IIA11 cells were also analyzed. Quantitation of MV secreted by cells within 24 h was done using NTA. These comparative analyses showed that there are no significant differences in the number of MV secreted per cell from cells treated with either both osteogenic factors or P_i only. Furthermore, there is no significant difference in the number of MV secreted per cell from untreated cells and cells treated only with ascorbic acid (Fig. 6A). These results demonstrate that extracellular P_i is the major factor driving MV production from 17IIA11 cells, as ascorbic acid alone is not able to stimulate MV secretion from these cells within 24 h. In all treatment conditions, the size distribution of secreted vesicles was similar (range of 50–220 nm, Fig. 6B).

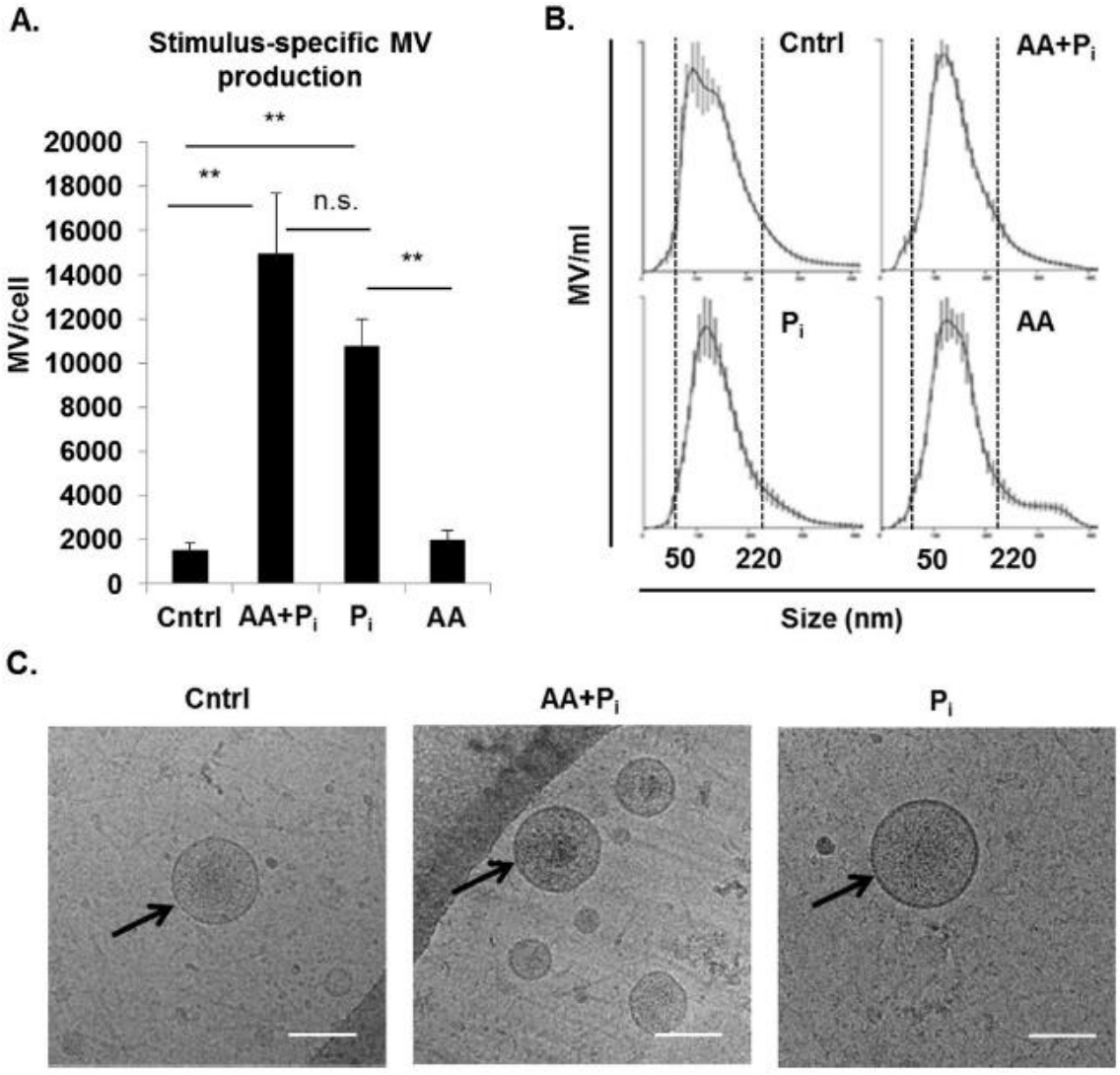

Fig. 6. Inorganic phosphate (P_i) alone is sufficient to induce MV secretion from 17IIA11 cells. (A) Comparison of the number of MV released by cells within 24 h of stimulation with standard osteogenic medium (ascorbic acid and P_i; AA + P_i), 10 mM Na–P_i buffer (P_i), or ascorbic acid (AA), with cells cultured in standard growth medium (Cntrl). Data are represented as the mean values of three independent experiments ± SD, *$p < 0.05$ and **$p < 0.005$. (B) Representative graphs showing MV size distribution in all culture conditions. Dotted lines indicate the size range of vesicles for each cell line. (C) Representative cryo-electron microscopy images of MV secreted by cells cultured for 24 h in standard growth medium (control) or in standard osteogenic medium (AA + P_i), or in the presence of 10 mM Na–Pi buffer (P_i). Scale bar = 100 nm.

We confirmed by cryo-electron microscopy imaging that the nano-particles secreted by 17IIA11 cells were indeed membrane vesicles. MV secreted by cells in all treatment conditions appeared to be translucent with a round shape and clear lipid bilayer (Fig. 6C). These analyses show that MV secreted by untreated 17IIA11 cells, cells treated either with ascorbic acid and P_i, or treated with P_i only have a similar morphology.

Erk1/2 activation is required for matrix vesicle production in response to phosphate

It has been shown that P_i-regulated gene expression in osteogenic cells is mediated through Erk1/2 [24,58,59]. Therefore, the role of Erk1/2 activation in P_i-induced formation of mineralization-competent MV was analyzed. First, to determine the dynamics of Erk1/2 activation in response to P_i in 17IIA11 cells, cells were treated with 2, 5, and 10 mM Na–P_i buffer, and the activation of Erk1/2 was assessed by Western blot at 15 min, 30 min, 45 min, 1 h, 2 h, 4 h, 6 h, and 8 h after addition of P_i (Fig. 7A). Comparison of the levels of phosphorylated (active) Erk1/2 to total Erk1/2 showed that Erk1/2 phosphorylation is highest at the initial 15 min to 1 h after P treatment and is then reduced. We did not detect the second Erk1/2 activation within 8 h of P_i treatment of 17IIA11 cells and this activation pattern was consistent at all three P_i concentrations (Fig. 7A). Next, to address whether Erk1/2 is mediating the release of MV upon P_i treatment, we analyzed MV production when Erk1/2 signaling is inhibited. To do this, 17IIA11 cells were treated with 10 mM Na–P_i for 12 h with or without an Erk1/2 inhibitor (U0126, 10 μM). Because we determined that the most robust MV production

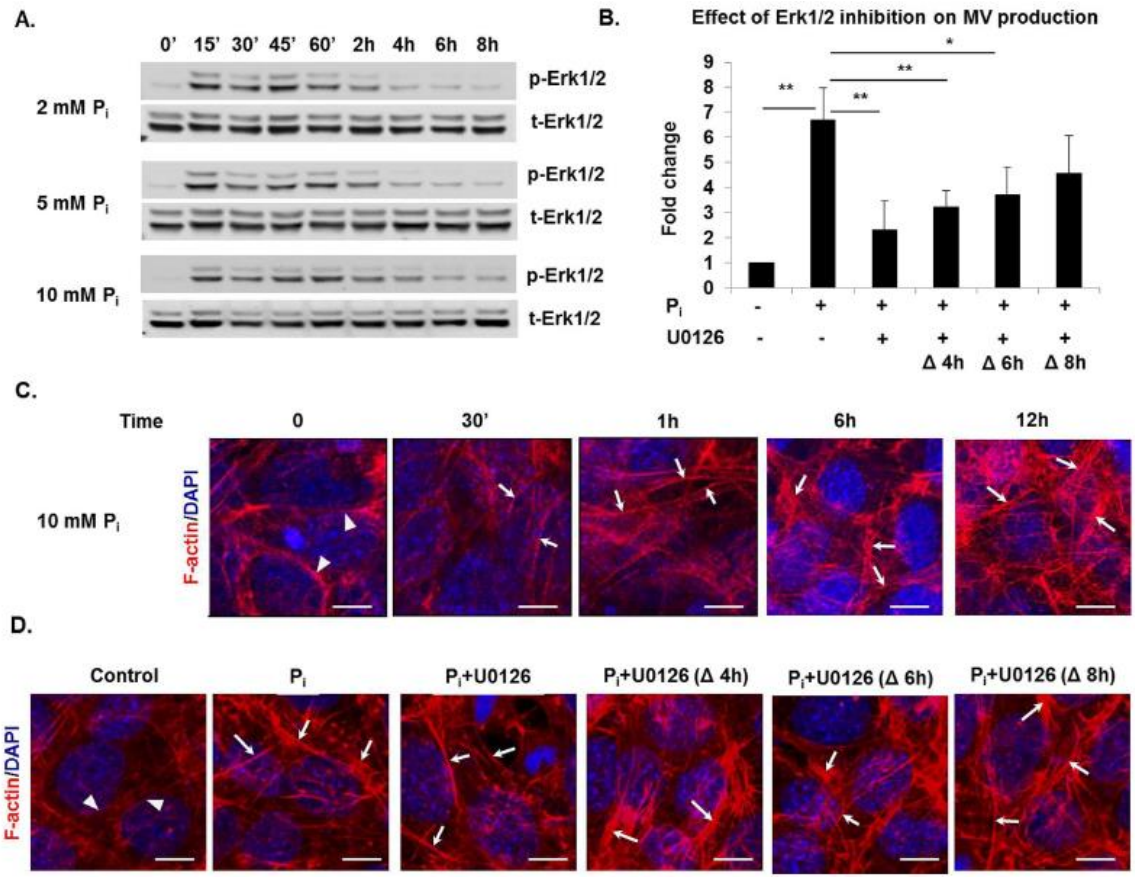

Fig. 7. Phosphate-induced Erk1/2 activation mediates MV secretion from 17IIA11 cells. (A) Western blot analyses of total Erk1/2 (t-Erk1/2) and activated Erk1/2 (p-Erk1/2) in 17IIA11 cells treated with 2, 5, and 10 mM Na–P_i (P_i) for 0 min, 15 min, 30 min, 45 min, 1 h, 2 h, 4 h, 6 h, and 8 h. (B) Comparison of MV secretion from 17IIA11 cells treated with 10 mM Na–P_i in the presence and absence of Erk1/2 inhibitor U0126 (10 μM). U0126 was added to growth medium either together with P_i (0 h) or 4 h, 6 h, or 8 h after Pi. MV were isolated 12 h after P_i treatment and quantified using nanoparticle tracking analysis. Graphs depict fold changes in the number of MV secreted per cell in comparison to untreated cells. Data are represented as the mean values of three independent experiments ± SD, *$p < 0.05$ and **$p < 0.005$. (C) Representative microscopic images of filamentous actin (F-actin; red fluorescent staining) showing changes in F-actin organization induced by the treatment of 17IIA11 cells with 10 mM Na–P_i. F-actin was analyzed at 30 min, 1 h, 6 h, and 12 h after P_i treatment. Blue DAPI staining: nuclei. (D) Representative images showing F-actin organization in 17IIA11 cells treated with 10 mM Na–P_i for 12 h in the presence or absence of Erk1/2 inhibitor U0126 (10 μM). U0126 was added to growth medium either together with P_i (0 h) or 4 h, 6 h, or 8 h after P_i. Arrows indicate elongated and condensed F-actin fibers in 17IIA11 cells treated with P_i, arrowheads indicate perinuclear localization of actin in untreated cells.

occurs within the initial 12 h of osteogenic treatment (Fig. 3), and Erk1/2 activation is highest within the first 4 h of P treatment, we added the Erk1/2 inhibitor either together with P_i or after 4 h, 6 h, or 8 h of P_i treatment. NTA showed that MV production was significantly disrupted by Erk1/2 inhibition at 0 h, 4 h, and 6 h, but not when the Erk1/2 inhibitor was added 8 h after P_i (Fig. 7B). A maximum decrease (65%) in the production of MV was observed when the Erk1/2 inhibitor was added at the same time as P_i. These results demonstrate that MV release in response to P_i is dependent upon Erk1/2 activation.

Recent studies identified mineral-containing vesicles inside osteoblasts, which suggest that MV are formed inside cells [33,34]. Considering this, the involvement of the cytoskeleton in the trafficking of intracellular vesicles and the role of the actin filament assembly in MV secretion [60–62], we analyzed the role of the actin cytoskeleton in the release of MV in response to P_i. First, we analyzed whether P_i influences the organization of the cytoskeleton. To do this, we assessed the filamentous actin (F-actin) cytoskeleton arrangement upon P_i treatment of 17IIA11 cells in a time-dependent manner (Fig. 7C). F-actin fibers were detected using fluorescent phalloidin staining. In untreated cells (0 h), F-actin fibers were oriented randomly and resided close to the nucleus. P treatment resulted in more condensed and elongated F-actin fibers that were distributed throughout the cytoplasm. The changes in F-actin organization were apparent at 30 min of P treatment and became more prominent at 1 h, 3 h, 6 h, and 12 h. To examine if Erk1/2 is involved in the P_i-induced cytoskeleton reorganization, we compared changes in F-actin organization following P_i treatment in the absence

and presence of the Erk1/2 inhibitor. The experimental design was the same as for the MV analyses (Fig. 7B), namely, 17IIA11 cells were treated with P_i for 12 h, and the Erk1/2 inhibitor (U0126, 10 μM) was added either at the same time as P_i (0 h) or 4 h, 6 h, or 8 h after P_i treatment (Fig. 7D). We did not observe any changes in F-actin reorganization in cells treated with the Erk1/2 inhibitor at any time points in comparison with cells treated with P_i without the Erk1/2 inhibitor. This data suggests that while P_i alters the cytoskeletal organization of the cell, this is independent of Erk1/2 activation. However, Erk1/2 is an important mediator of MV secretion by P_i.

Discussion

Initiation of both physiologic and pathologic (ectopic) mineralization is supported by mineralization-competent MV secreted locally by cells with an active osteogenic program. Here, we presented data showing that secretion of MV from osteogenic cells is induced by P_i through Erk1/2-mediated signaling. Furthermore, we determined that molecular characteristics of mineralization-competent MV distinguish this group of EV from exosomes not only by the presence of proteins specific for their biological function, but also intracellular proteins that may be indicative of the biogenesis pathway specific for mineralization-competent MV.

The constitutive and induced secretion of bioactive EV is now recognized as a common biological process of cell–cell communication [63–65]. In this respect, MV are unique among other EV, as they do not transfer their bioactive cargo to other cells, but rather release it to the ECM. Our results show that the vast majority of vesicles produced by osteogenic cells during the early stage of osteogenic differentiation reside in ECM (Fig. 1), which is consistent with the biological function of MV in changing the properties of ECM and is in agreement with studies by Anderson et al. [66]. However, it is not known whether the retention of MV in the ECM is a passive entrapment of vesicles in the ECM or an active process facilitated by molecular interactions between MV and ECM proteins. Although the collagenous network formed by 17IIA11 cells in our experimental conditions is not well developed (Supplemental Fig. 1), the 17IIA11 ECM composition and structure may be sufficient to retain MV. The small percentage of vesicles detected in conditioned medium may simply be MV that escaped from ECM. However, studies by Anderson et al. detected differences in the protein banding pattern of PAGE-separated vesicle proteins isolated from matrix and medium fractions, suggesting a different molecular composition [66]. Thus, a more detailed comparison of the molecular composition and the functional assays of vesicles isolated from ECM and conditioned medium of osteogenic cells is required to determine if these are the same or different populations of EV. Nonetheless, our data from quantitative analyses of vesicles in ECM and medium indicate that measuring vesicles only in medium may

grossly underestimate the magnitude of MV production during osteogenic differentiation.

Out of the variety of available cell lines that undergo mineralization when stimulated with osteogenic factors, we selected three mouse cell lines of different embryonic origins to study secretion of MV. What distinguishes 17IIA11 cells from other osteogenic cell lines is that even under standard growth conditions, 17IIA11 cells express high mRNA levels of multiple genes involved in the mineralization process, including osteogenic transcription factors, ion channels, and ECM proteins [48–50]. Consistent with their commitment to mineralization, 17IIA11 cells respond to stimulation with osteogenic factors with a rapid increase of MV secretion, whereas the secretion of MV from MC3T3-E1 and ST2 cells was delayed (Fig. 1). Furthermore, we showed that both stimulated and unstimulated 17IIA11 cells secrete MV expressing high levels of P_i-providing enzymes, TNAP and PHOSPHO1, and Ca^{2+} channel protein annexin V, which is in agreement with a biological function of supporting HA formation (Fig. 4B) [38,39,67,68]. Consistently, MV produced by 17IIA11 cells, regardless of their growth conditions, are able to accumulate Ca^{2+} from the extravesicular environment (Fig. 5A). The ability of MV to mineralize was further supported by detection of hydroxyapatite in MV isolated from cells grown in the presence of osteogenic factors for 8 days (Fig. 5B and C). Considering that 5 days of culture under osteogenic conditions is required to detect mineral depositions in ECM of 17IIA11 cells [48,49], it is not unexpected that MV isolated at day 1 do not contain crystalline material. While we do not have data on the rate of the HA crystal

formation in MV from 17IIA11 cells, detection of only the amorphous mineral in MV at day 1 suggests that more than 24 h under osteogenic conditions is required to form crystals. This, in turn, suggests that the lifespan of MV is longer than 24 h. Thus, the quantitative analyses of MV at this time point provide reliable assessment of their number, while at the later time points, such quantitative analyses may be inaccurate as they do not capture MV that have already ruptured from the growth of HA crystals. Although we have not analyzed formation of crystals at 48 h and 72 h MV, this may explain the lower number of MV from 17IIA11 cells at 48 h and 72 h in comparison with 24 h (Fig. 1).

Interestingly, MV secreted by 17IIA11 cells stimulated with ascorbic acid and P_i express different isoforms of TNAP and PHOSPHO1 than MV secreted by cells cultured under standard growth conditions. Although the differences in function of these isoforms are unknown, these data indicate that the osteogenic extracellular environment not only stimulates the secretion of MV, but also changes their molecular composition.

The size and morphology of MV are similar to exosomes, which are currently the most studied EV sub-type. These two groups of EV share similarities on the molecular level, therefore it has been suggested that MV are membrane-anchored exosomes [47,69]. In our studies, histone 3a, which has been reported to be present in exosomes [70,71], was also detected in MV (Fig. 4B). However, MV secreted by 17IIA11 cells are negative for CD81 and HSP70 proteins, which are considered typical exosomal markers [44]. Therefore, the results of our studies do not support this concept of MV identity as exosomes, as

their molecular profile is distinct from that of exosomes. Interestingly, we uncovered that MV released upon stimulation with osteogenic factors are enriched in the lysosomal markers Lamp1 and Lamp2a, yet these proteins are not detected in MV from untreated cells or exosomes (Fig. 4B). Of note, there is no difference in Lamp1 and Lamp2a protein levels in unstimulated and stimulated cells, thus osteogenic factors affect only the subcellular distribution of these proteins and not expression. Considering that the EV molecular composition reflects their biological function, this suggests that Lamp1 and Lamp2a are involved in mineralization. Such a role for Lamp1 has already been suggested by studies demonstrating that Lamp1 can localize on the cell surface and bind amelogenin, a major protein of organic dental enamel matrix [72,73]. Alternatively, the presence of these lysosomal markers in MV may be a footprint of their biogenesis pathway. This, in turn, supports the model of the intracellular formation of mineralization-competent MV. However, now, when it is known that multiple cellular mechanisms of vesicle formation exist, it is worth to consider that the biogenesis pathway of EV may be determined by extracellular stimuli or by the pathophysiological state of the cells, and not by the biological function of EV.

In these studies, we found that MV secretion from 17IIA11 cells can be induced by P_i alone (Fig. 5). Thus, we uncovered a new function of P_i in the mineralization process. Similar to P_i-induced expression of mineralization-related genes, this new P_i function is also mediated through Erk1/2. However, in comparison with transcriptional regulation, the secretion of MV in response to P is faster, as it occurs within 6–12 h of treatment, while changes in osteogenic

gene expression have been reported after 24 h [23]. This suggests that induction of MV secretion in response to P_i does not require changes in transcription, or at least not in 17IIA11 cells, in which osteogenic factors are already expressed at high levels [48–50]. This finding is relevant to physiologic mineralization of skeletal and dental tissues and may also provide a better understanding of the mechanisms of pathologic mineralization. For instance, elevated serum phosphate levels are the major factor contributing to vascular calcification, which is a common complication of chronic renal failure [74]. In addition, it has been recently shown that, akin to physiologic mineralization, increased secretion of EV by vascular smooth muscle cells can be detected during pathologic mineralization [25].

We also detected that Pi induces changes in subcellular organization of F-actin. This was an intriguing finding, because secretion of MV has previously been shown to be dependent on reorganization of actin filaments [61,62]. Here, we have shown that similar to Erk1/2 activation, F-actin reorganization in response to P_i occurs rapidly, and the elongation of actin fibers and changes in their intracellular distribution can be detected as early as 30 min after P_i treatment. However, inhibition of Erk1/2 activation had no effect on reorganization of F-actin in response to P_i. This suggests that these are two parallel events that occur in response to P_i independently to regulate MV secretion. Discovering that both MV secretion and reorganization of F-actin are regulated by P_i provides new insights into the molecular mechanisms of MV secretion.

Although these mechanisms still remain poorly deciphered, two recent studies have identified proteins critical for MV formation in odontoblasts: mouse genetic studies uncovered a significantly reduced number of MV in mantle dentin and chondrocytes of *Phospho1*$^{-/-}$;*Alpl*$^{+/-}$ mice [36,56], and our group demonstrated that the Trps1 transcription factor is required for MV secretion from 17IIA11 cells as well as for expression of *Phospho1* and *Alpl* [48]. While the mechanism by which these phosphatases support secretion of MV is unknown, we speculate that PHOSPHO1, which uses phospholipids as substrates [75,76], may affect MV secretion by affecting the fluidity of the plasma membrane. In contrast, TNAP, which is a major enzyme generating P_i and, thus, increasing P_i concentrations in the local cellular microenvironment [77], may support secretion of MV by providing P_i.

It is well recognized that EV present in bodily fluids are a mixed population of vesicles of different origins and functions, both of which are reflected in their molecular composition [44,78]. Therefore, there is a growing interest in using EV as biomarkers, as well as therapeutic targets. The former requires identification of the molecular hallmarks of specific biological functions or pathology, while the latter requires understanding the mechanisms of the formation of EV with specific biological functions or under specific pathophysiological conditions. Results of these studies provide mechanistic insights into the regulation of MV secretion in response to P_i, specifically in the context of osteogenic cells. Furthermore, we determined differences in the molecular composition of MV and exosomes that can be used to distinguish mineralization-competent vesicles from other EV.

Experimental procedures

Cell lines and cell culture conditions

Mouse preodontoblast-derived 17IIA11 cell line was maintained in standard Dulbecco's Modified Eagle's Medium (DMEM, Gibco; Thermo Fisher Scientific, Logan, UT) with 5% FBS (Thermo Fisher Scientific, Logan, UT) and 100 units/ml penicillin and 100 µg/ml streptomycin (Cellgro, Manassas, VA) at 37 °C and 8% CO_2 as described before [48–50]. Mouse melanoma B16-F10 cell line (ATCC; Manassas, VA) was grown in DMEM supplemented with 10% FBS and penicillin/streptomycin at 37 °C and 8% CO_2. Bone marrow stromal cell-derived ST2 cell line (generous gift from Dr. Steven Teitelbaum, Washington University, St. Louis) and calvarium osteoblast precursor-derived MC3T3-E1 cell line (ATCC; Manassas, VA) were maintained in α-MEM (Hyclone, Logan, UT) with 10% FBS, penicillin/streptomycin, and 2 mM L-glutamine. For osteogenic differentiation, cells were plated at 2×10^6 cells per 10 cm dish and grown to confluency. Osteogenic differentiation was induced by supplementing the growth medium with 10 mM Na–P_i buffer (pH 7.4) and 50 µg/ml ascorbic acid (osteogenic medium). For MV analyses, cells were grown in standard medium depleted of exosomes. Exosome-depleted medium was made by centrifuging 20% FBS (diluted in DMEM or α-MEM) at 100,000 ×g for 24 h to remove serum-derived exosomes [79]. To analyze Erk1/2 activation, cells were plated at 5×10^5

cells per well of a 6-well plate. After 24 h, the growth medium was replaced with low-serum (0.5% FBS) medium. Cells were serum-starved overnight, followed by treatment with 2, 5, or 10 mM Na–P_i buffer (pH 7.4).

Isolation and purification of vesicles

Vesicles from ECM and media (MV and EV, respectively) were purified using a differential ultracentrifugation method as previously described [46,48,79]. Briefly, cells were washed twice with PBS. MV were released from ECM by enzymatic digestion with 2.5 mg/ml collagenase IA (Sigma, St. Louis, MO) and 2 mM $CaCl_2$ for 2 h at 37 °C and 8% CO_2. The whole digestion mix containing fragmented ECM, vesicles, and cells was collected and centrifuged at 500 ×g for 5 min to pellet the cells. The supernatant was transferred to a separate tube and centrifuged at 2000 ×g for 10 min to remove dead cells. The supernatant was again centrifuged at 10,000 ×g for 30 min to remove cell debris then at 100,000 ×g for 70 min to obtain the MV pellet. MV pellets were resuspended in PBS and centrifuged at 100,000 ×g for 60 min. Finally, the pellet was resuspended in 100 µl PBS and stored at −80 °C until further use. For isolation of EV from conditioned medium, medium was collected from cells grown under experimental conditions and centrifuged as described above. Cells remaining on a dish were trypsinized at 37 °C for 10 min and combined with the cell pellet collected after the 1st centrifugation. The total number of cells was counted using a hemocytometer (Hausser Scientific, Horsham, PA). EV from conditioned media of B16-F10 melanoma cells were collected after 48 h of culture. EV from blood

plasma and B16-F10 cells were purified using the ultracentrifugation method as described above.

Nanoparticle tracking analyses

Size and concentration of purified vesicles were determined by Nanoparticle Tracking Analysis (NTA) using NanoSight NS300 (Malvern Instruments Ltd., Worcestershire, UK). Data acquisition and analysis was performed using NTA 2.3 Analytical Software. Five video files of 60 s at camera level 10 from each sample were recorded. Detection threshold limit 10 was used to analyze size and concentration of vesicles. Resultant concentration of MV was divided by the total number of cells to calculate the production of MV per cell.

Cryo-electron microscopy

MV suspended in TBS buffer (50 mM Tris–HCl, pH 7.4 and 154 mM NaCl) were applied to holey carbon film (Quantifoil Micro Tools) and vitrified in liquid ethane using an FEI Vitrobot Mark IV. The grids were transferred to a Gatan 626 cryo-sample holder and imaged in an FEI Tecnai F20 electron microscope operated at 200 kV and nominal magnifications ranging from 32,750× to 65,500×. Low-dose images were captured with a Gatan Ultrascan 4000 CCD camera.

Transmission electron microscopy

Suspensions of MV in 70% ethanol were placed on carbon coated Ni grids and air dried. The samples were analyzed using a Joel 2100 TEM (Peabody,

MA) at 200 kV in bright field and selected area electron diffraction (SAED) modes. Images were acquired using a Gatan CCD camera (Warrendale, PA).

Atomic force microscopy

Five microliters of MV solution was dropped onto a freshly cleaved mica substrate (Ted Pella, Redding, CA) and allowed to stand for a couple of minutes. Next, the substrate was rinsed with ddH_2O and dried at room temperature overnight. Samples were imaged by non-contact (AAC) mode in air using a 5500 AFM (Agilent Technologies). Silicon-nitride cantilevers with a nominal resonance frequency of ~190 kHz (Nanosensors™, Neuchatel, Switzerland) were employed. Topography, amplitude and phase images were recorded for each scanned field and three-dimensional AFM images were generated by PicoView software (Agilent Technologies).

In vitro mineralization assay

MV isolated from 17IIA11 cells were assessed *in vitro* for their ability to mineralize as described earlier [37,53]. Briefly, 1 × 1010 MV were incubated with $CaCl_2$ (1 mM, 2 mM, or 4 mM) and 1 mM ATP as a phosphodiester substrate in a calcifying solution (1.6 mM KH_2PO_4, 1mM $MgCl_2$, 85mM NaCl, 15 mM KCl, 10 mM $NaHCO_3$, 50 mM PBS, pH 7.6) at 37 °C for 5.5 h. The reaction was stopped by centrifugation at 8800 ×g for 30 min to pellet MV. The pellet was solubilized by adding 0.6 N HCl for 24 h. The Ca^{2+} content in the MV pellet was determined by

the O-cresolpthalein complexone method (calcium colorimetric assay kit, Sigma-Aldrich, St. Luis, MO).

Western blot analysis

Whole protein extracts from cells and vesicles were prepared in RIPA lysis buffer supplemented with phosphatases and protease inhibitors: 1 mM NaF, 2 mM Na_2VO_4, 2 mM leupeptin, 2 mM pepstatin, 2 mM PMSF, and 10 μM MG132. Protein concentration was determined by a micro BCA protein assay kit (Thermo Scientific, Rockford, IL). Protein (10 μg) was subjected to electrophoresis on 4–12% precast BisTris gels (Invitrogen) and transferred onto a nitrocellulose membrane. Specific proteins were detected by fluorescence (Li-Cor Odyssey Infrared Imaging System, LI-COR Biosciences, Lincoln, NE). Primary antibodies against tissue-nonspecific alkaline phosphatase (1:1000; R&D Systems), PHOSPHO1 (1:500; Abd Serotec), annexin V (1:2000; Abcam), α-tubulin (1:10,000; Sigma), Rab5 (1:1000; Abcam), GM130 (1:1000; Abcam), Grp78 (1:500; Santa Cruz), GAPDH (1:1000; Cell Signaling), Hsp70 (1:1000; System Biosciences), CD81 (1:500; Santa Cruz), Lamp1 (1:1000; Abcam), Lamp2a (1:1000; Abcam), cytochrome c (1:500; Santa Cruz), histone 1 (1:1000; Abcam), histone 3a (1:5000; Abcam), Col1a1 (1:5000; Abcam), phospho-Erk1/2 (1:2000; Cell Signaling), and Erk1/2 (1:1000; Cell Signaling) were used. All fluorescent secondary antibodies (LI-COR Biosciences; Lincoln; NE) were used at 1:20,000 dilution. Proteins separated by gel electrophoresis were visualized using Pierce Silver Stain Kit (Thermo Scientific, MA) according to the manufacturer's protocol.

F-actin staining

Cells (2×10^5/well) were plated on a poly-L-lysine-coated cover slip (Fischer Scientific, MA) in a 24-well plate. After 24 h, cells were treated with 10 mM Na–P_i with or without 10 μM Erk1/2 inhibitor U0126 (Cell signaling, MA). For filamentous actin (F-actin) detection, cells were fixed with 4% paraformaldehyde and stained with phalloidin (1:50, Life Technologies, Carlsbad, CA) for 30 min at room temperature. Finally, cells were mounted with Prolong Gold antifade reagent with DAPI (Life Technologies, Carlsbad, CA). F-actin organization was imaged under a Nikon A1 High Speed Confocal Laser Microscope.

Statistical analysis

All experiments were performed at least three times. Data are presented as the mean ± SD. Probability values were calculated using the Student's t test. $p < 0.05$ (*) and <0.005 (**) were considered to be statistically significant and highly significant, respectively.

Supplementary data to this article can be found online at http://dx.doi.org/10.1016/j.matbio.2016.02.003.

Acknowledgments

We thank Dr. Steven Teitelbaum (Washington University, St. Louis, MO) for providing ST2 cells and Mr. Yang Xu (University of Pittsburgh, PA) for help in the preparation of TEM samples. TEM was carried out at the Nanoscale Fabrication and Characterization Facility at Peterson Institute of Nanoscience and Engineering, University of Pittsburgh. Cryo-electronmicroscopy was carried out at the UAB cryo-EM core facility. We are also thankful to the UAB High Resolution Imaging Facility for assistance with the NTA and fluorescence microscopy. This work was supported by grants R01DE023083 (to D.N.), F31DE024926 (to M.K.), DE12889 and AR53102 (to J.L.M.), and R56 DE016703 (to E.B.).

References

[1] Y. Yuana, A. Sturk, R. Nieuwland, Extracellular vesicles in physiological and pathological conditions, Blood Rev. 27 (2013) 31–39.
[2] M. Yanez-Mo, P.R. Siljander, Z. Andreu, A.B. Zavec, F.E. Borras, E.I. Buzas, et al., Biological properties of extracellular vesicles and their physiological functions, J. Extracell. Vesicles 4 (2015) 27066.
[3] M. Colombo, G. Raposo, C. Thery, Biogenesis, secretion, and intercellular interactions of exosomes and other extracellular vesicles, Annu. Rev. Cell Dev. Biol. 30 (2014) 255–289.
[4] W.N. Addison, F. Azari, E.S. Sorensen, M.T. Kaartinen, M.D. McKee, Pyrophosphate inhibits mineralization of osteoblast cultures by binding to mineral, up-regulating osteopontin, and inhibiting alkaline phosphatase activity, J. Biol. Chem. 282 (2007) 15872–15883.
[5] C.M. Giachelli, M.Y. Speer, X. Li, R.M. Rajachar, H. Yang, Regulation of vascular calcification: roles of phosphate and osteopontin, Circ. Res. 96 (2005) 717–722.

[6] K. Johnson, J. Goding, D. Van Etten, A. Sali, S.I. Hu, D. Farley, et al., Linked deficiencies in extracellular PP(i) and osteopontin mediate pathologic calcification associated with defective PC-1 and ANK expression, J. Bone Miner. Res. 18 (2003) 994–1004.
[7] K.A. Lomashvili, S. Narisawa, J.L. Millan, W.C. O'Neill, Vascular calcification is dependent on plasma levels of pyrophosphate, Kidney Int. 85 (2014) 1351–1356.
[8] G. Luo, P. Ducy, M.D. McKee, G.J. Pinero, E. Loyer, R.R. Behringer, et al., Spontaneous calcification of arteries and cartilage in mice lacking matrix GLA protein, Nature 386 (1997) 78–81.
[9] D.A. Prosdocimo, S.C. Wyler, A.M. Romani, W.C. O'Neill, G.R. Dubyak, Regulation of vascular smooth muscle cell calcification by extracellular pyrophosphate homeostasis: synergistic modulation by cyclic AMP and hyperphosphatemia, Am. J. Physiol. Cell Physiol. 298 (2010) C702–C713.
[10] T. Sallam, H. Cheng, L.L. Demer, Y. Tintut, Regulatory circuits controlling vascular cell calcification, Cell. Mol. Life Sci. 70 (2013) 3187–3197.
[11] L.J. Schurgers, E.C. Cranenburg, C. Vermeer, Matrix Glaprotein: the calcification inhibitor in need of vitamin K, Thromb. Haemost. 100 (2008) 593–603.
[12] Z. Szeberin, M. Fehervari, M. Krepuska, A. Apor, E. Rimely, H. Sarkadi, et al., Serum fetuin-A levels inversely correlate with the severity of arterial calcification in patients with chronic lower extremity atherosclerosis without renal disease, Int. Angiol. 30 (2011) 474-80.
[13] R. Westenfeld, W. Jahnen-Dechent, M. Ketteler, Vascular calcification and fetuin-A deficiency in chronic kidney disease, Trends Cardiovasc. Med. 17 (2007) 124–128.
[14] J. Sodek, B. Ganss, M.D. McKee, Osteopontin, Crit. Rev. Oral Biol. Med. 11 (2000) 279–303.
[15] D.A. McKnight, L.W. Fisher, Molecular evolution of dentin phosphoprotein among toothed and toothless animals, BMC Evol. Biol. 9 (2009) 299.
[16] B.L. Foster, F.H. Nociti Jr., E.C. Swanson, D. Matsa-Dunn, J.E. Berry, C.J. Cupp, et al., Regulation of cementoblast gene expression by inorganic phosphate in vitro, Calcif. Tissue Int. 78 (2006) 103–112.
[17] S. Khoshniat, A. Bourgine, M. Julien, P. Weiss, J. Guicheux, L. Beck, The emergence of phosphate as a specific signaling molecule in bone and other cell types in mammals, Cell. Mol. Life Sci. 68 (2011) 205–218.
[18] R. Kumar, Phosphate sensing, Curr. Opin. Nephrol. Hypertens. 18 (2009) 281–284.
[19] M. Julien, D. Magne, M. Masson, M. Rolli-Derkinderen, O. Chassande, C. Cario-Toumaniantz, et al., Phosphate stimulates matrix Gla protein expression in chondrocytes through the extracellular signal regulated kinase signaling pathway, Endocrinology 148 (2007) 530–537.
[20] M. Julien, S. Khoshniat, A. Lacreusette, M. Gatius, A. Bozec, E.F. Wagner, et al., Phosphate-dependent regulation of MGP in osteoblasts: role of ERK1/2 and Fra-1, J. Bone Miner. Res. 24 (2009) 1856–1868.

[21] M.S. Razzaque, Phosphate and vitamin D in chronic kidney disease, Contrib. Nephrol. 180 (2013) 74–85.
[22] A. von Kriegsheim, D. Baiocchi, M. Birtwistle, D. Sumpton, W. Bienvenut, N. Morrice, et al., Cell fate decisions are specified by the dynamic ERK interactome, Nat. Cell Biol. 11 (2009) 1458–1464.
[23] C.E. Camalier, M. Yi, L.R. Yu, B.L. Hood, K.A. Conrads, Y.J. Lee, et al., An integrated understanding of the physiological response to elevated extracellular phosphate, J. Cell. Physiol. 228 (2013) 1536–1550.
[24] H. Tada, E. Nemoto, B.L. Foster, M.J. Somerman, H. Shimauchi, Phosphate increases bone morphogenetic protein-2 expression through cAMP-dependent protein kinase and ERK1/2 pathways in human dental pulp cells, Bone 48 (2011) 1409–1416.
[25] A.N. Kapustin, M.L. Chatrou, I. Drozdov, Y. Zheng, S.M. Davidson, D. Soong, et al., Vascular smooth muscle cell calcification is mediated by regulated exosome secretion, Circ. Res. 116 (2015) 1312–1323.
[26] H.C. Anderson, D. Harmey, N.P. Camacho, R. Garimella, J.B. Sipe, S. Tague, et al., Sustained osteomalacia of long bones despite major improvement in other hypophosphatasia-related mineral deficits in tissue nonspecific alkaline phosphatase/nucleotide pyrophosphatase phosphodiesterase 1 double-deficient mice, Am. J. Pathol. 166 (2005) 1711–1720.
[27] M. Garces-Ortiz, C. Ledesma-Montes, J. Reyes-Gasga, Presence of matrix vesicles in the body of odontoblasts and in the inner third of dentinal tissue: a scanning electronmicroscopic study, Med. Oral Patol. Oral Cir. Bucal 18 (2013) e537–e541.
[28] E. Katchburian, Membrane-bound bodies as initiators of mineralization of dentine, J. Anat. 116 (1973) 285–302.
[29] D. Magne, G. Bluteau, C. Faucheux, G. Palmer, C. Vignes-Colombeix, P. Pilet, et al., Phosphate is a specific signal for ATDC5 chondrocyte maturation and apoptosis-associated mineralization: possible implication of apoptosis in the regulation of endochondral ossification, J. Bone Miner. Res. 18 (2003) 1430–1442.
[30] K. Rilla, S. Pasonen-Seppanen, A.J. Deen, V.V. Koistinen, S. Wojciechowski, S. Oikari, et al., Hyaluronan production enhances shedding of plasma membrane-derived microvesicles, Exp. Cell Res. 319 (2013) 2006–2018.
[31] D. Abdallah, E. Hamade, R.A. Merhi, B. Bassam, R. Buchet, S. Mebarek, Fatty acid composition in matrix vesicles and in microvilli from femurs of chicken embryos revealed selective recruitment of fatty acids, Biochem. Biophys. Res. Commun. 446 (2014) 1161–1164.
[32] M. Balcerzak, A. Malinowska, C. Thouverey, A. Sekrecka, M. Dadlez, R. Buchet, et al., Proteome analysis of matrix vesicles isolated from femurs of chicken embryo, Proteomics 8 (2008) 192–205.
[33] S. Boonrungsiman, E. Gentleman, R. Carzaniga, N.D. Evans, D.W. McComb, A.E. Porter, et al., The role of intracellular calcium phosphate in

osteoblast-mediated bone apatite formation, Proc. Natl. Acad. Sci. U. S. A. 109 (2012) 14170–14175.
[34] J. Mahamid, A. Sharir, D. Gur, E. Zelzer, L. Addadi, S. Weiner, Bone mineralization proceeds through intracellular calcium phosphate loaded vesicles: a cryo-electron microscopy study, J. Struct. Biol. 174 (2011) 527–535.
[35] M.J. Barron, S.T. McDonnell, I. Mackie, M.J. Dixon, Hereditary dentine disorders: dentinogenesis imperfecta and dentine dysplasia, Orphanet J. Rare Dis. 3 (2008) 31.
[36] M.D. McKee, M.C. Yadav, B.L. Foster, M.J. Somerman, C. Farquharson, J.L. Millan, Compounded PHOSPHO1/ALPL deficiencies reduce dentin mineralization, J. Dent. Res. 92 (2013) 721–727.
[37] S. Roberts, S. Narisawa, D. Harmey, J.L. Millan, C. Farquharson, Functional involvement of PHOSPHO1 in matrix vesicle-mediated skeletal mineralization, J. Bone Miner. Res. 22 (2007) 617–627.
[38] M.C. Yadav, A.M. Simao, S. Narisawa, C. Huesa, M.D. McKee, C. Farquharson, et al., Loss of skeletal mineralization by the simultaneous ablation of PHOSPHO1 and alkaline phosphatase function: a unified model of the mechanisms of initiation of skeletal calcification, J. Bone Miner. Res. 26 (2011) 286–297.
[39] C. Huesa, D. Houston, T. Kiffer-Moreira, M.M. Yadav, J.L. Millan, C. Farquharson, The functional co-operativity of tissue-nonspecific alkaline phosphatase (TNAP) and PHOSPHO1 during initiation of skeletal mineralization, Biochem. Biophys. Rep. 4 (2015) 196–201.
[40] H.S. Kim, D.Y. Choi, S.J. Yun, S.M. Choi, J.W. Kang, J.W. Jung, et al., Proteomic analysis of microvesicles derived from human mesenchymal stem cells, J. Proteome Res. 11 (2012) 839–849.
[41] J. Morhayim, J. van de Peppel, J.A. Demmers, G. Kocer, A.L. Nigg, M. van Driel, et al., Proteomic signatures of extracellular vesicles secreted by nonmineralizing and mineralizing human osteoblasts and stimulation of tumor cell growth, FASEB J. 29 (2015) 274–285.
[42] C. Thouverey, A. Malinowska, M. Balcerzak, A. Strzelecka-Kiliszek, R. Buchet, M. Dadlez, et al., Proteomic characterization of biogenesis and functions of matrix vesicles released from mineralizing human osteoblast-like cells, J. Proteomics 74 (2011) 1123–1134.
[43] Z. Xiao, C.E. Camalier, K. Nagashima, K.C. Chan, D.A. Lucas, M.J. de la Cruz, et al., Analysis of the extracellular matrix vesicle proteome in mineralizing osteoblasts, J. Cell. Physiol. 210 (2007) 325–335.
[44] J. Lotvall, A.F. Hill, F. Hochberg, E.I. Buzas, D. Di Vizio, C. Gardiner, et al., Minimal experimental requirements for definition of extracellular vesicles and their functions: a position statement from the International Society for Extracellular Vesicles, J. Extracell. Vesicles 3 (2014) 26913.
[45] E.E. Golub, Biomineralization and matrix vesicles in biology and pathology, Semin. Immunopathol. 33 (2011) 409–417.

[46] T. Kirsch, H.D. Nah, I.M. Shapiro, M. Pacifici, Regulated production of mineralization-competent matrix vesicles in hypertrophic chondrocytes, J. Cell Biol. 137 (1997) 1149–1160.
[47] I.M. Shapiro, W.J. Landis, M.V. Risbud, Matrix vesicles: are they anchored exosomes? Bone 79 (2015) 29–36.
[48] M. Kuzynski, M. Goss, M. Bottini, M.C. Yadav, C. Mobley, T. Winters, et al., Dual role of the Trps1 transcription factor in dentin mineralization, J. Biol. Chem. 289 (2014) 27481–27493.
[49] S. Lacerda-Pinheiro, S. Dimitrova-Nakov, Y. Harichane, M. Souyri, L. Petit-Cocault, L. Legres, et al., Concomitant multipotent and unipotent dental pulp progenitors and their respective contribution to mineralised tissue formation, Eur. Cells Mater. 23 (2012) 371–386.
[50] F. Priam, V. Ronco, M. Locker, K. Bourd, M. Bonnefoix, T. Duchene, et al., New cellular models for tracking the odontoblast phenotype, Arch. Oral Biol. 50 (2005) 271–277.
[51] H.C. Anderson, Vesicles associated with calcification in the matrix of epiphyseal cartilage, J. Cell Biol. 41 (1969) 59–72.
[52] M. Bitar, R.A. Brown, V. Salih, A.G. Kidane, J.C. Knowles, S.N. Nazhat, Effect of cell density on osteoblastic differentiation and matrix degradation of biomimetic dense collagen scaffolds, Biomacromolecules 9 (2008) 129–135.
[53] R. Garimella, X. Bi, N. Camacho, J.B. Sipe, H.C. Anderson, Primary culture of rat growth plate chondrocytes: an in vitro model of growth plate histotype, matrix vesicle biogenesis and mineralization, Bone 34 (2004) 961–970.
[54] F. Cuisinier, E.F. Bres, J. Hemmerle, J.C. Voegel, R.M. Frank, Transmission electron microscopy of lattice planes in human alveolar bone apatite crystals, Calcif. Tissue Int. 40 (1987) 332–338.
[55] E.I. Suvorova, P.A. Buffat, Electron diffraction from micro- and nanoparticles of hydroxyapatite, J. Microsc. 196 (1999) 46–58.
[56] M.C. Yadav, M. Bottini, E. Cory, K. Bhattacharya, P. Kuss, S. Narisawa, et al., Skeletal mineralization deficits and impaired biogenesis and function of chondrocyte-derived matrix vesicles in Phospho1 and Phospho1/Pit1 double knockout mice, J. Bone Miner. Res. (2016) (ahead of print).
[57] F. Langenbach, J. Handschel, Effects of dexamethasone, ascorbic acid and beta-glycerophosphate on the osteogenic differentiation of stem cells in vitro, Stem Cell Res. Ther. 4 (2013) 117.
[58] T. Matsushita, Y.Y. Chan, A. Kawanami, G. Balmes, G.E. Landreth, S. Murakami, Extracellular signal-regulated kinase 1 (ERK1) and ERK2 play essential roles in osteoblast differentiation and in supporting osteoclastogenesis, Mol. Cell. Biol. 29 (2009) 5843–5857.
[59] J.H. Kang, R. Toita, D. Asai, T. Yamaoka, M. Murata, Reduction of inorganic phosphate-induced human smooth muscle cells calcification by inhibition of protein kinase A and p38 mitogen-activated protein kinase, Heart Vessel. 29 (2014) 718–722.

[60] H. Cai, K. Reinisch, S. Ferro-Novick, Coats, tethers,Rabs, and SNAREs work together tomediate the intracellular destination of a transport vesicle, Dev. Cell 12 (2007) 671–682.
[61] J.E. Hale, R.E. Wuthier, The mechanism of matrix vesicle formation. Studies on the composition of chondrocyte microvilli and on the effects of microfilament-perturbing agents on cellular vesiculation, J. Biol. Chem. 262 (1987) 1916–1925.
[62] C. Thouverey, A. Strzelecka-Kiliszek, M. Balcerzak, R. Buchet, S. Pikula, Matrix vesicles originate from apical membrane microvilli of mineralizing osteoblast-like Saos-2 cells, J. Cell. Biochem. 106 (2009) 127–138.
[63] H. Kalra, R.J. Simpson, H. Ji, E. Aikawa, P. Altevogt, P. Askenase, et al., Vesiclepedia: a compendium for extracellular vesicles with continuous community annotation, PLoS Biol. 10 (2012) e1001450.
[64] C. Thery, Exosomes: secreted vesicles and intercellular communications, F1000 Biol. Rep. 3 (2011) 15.
[65] M. Simons, G. Raposo, Exosomes—vesicular carriers for intercellular communication, Curr. Opin. Cell Biol. 21 (2009) 575–581.
[66] H.C. Anderson, D.J. Stechschulte Jr., D.E. Collins, D.H. Jacobs, D.C. Morris, H.H. Hsu, et al., Matrix vesicle biogenesis in vitro by rachitic and normal rat chondrocytes, Am. J. Pathol. 136 (1990) 391–398.
[67] T. Kirsch, G. Harrison, E.E. Golub, H.D. Nah, The roles of annexins and types II and X collagen in matrix vesicle mediated mineralization of growth plate cartilage, J. Biol. Chem. 275 (2000) 35577–35583.
[68] P. Ciancaglini, M.C. Yadav, A.M. Simao, S. Narisawa, J.M. Pizauro, C. Farquharson, et al., Kinetic analysis of substrate utilization by native and TNAP-, NPP1-, or PHOSPHO1-deficient matrix vesicles, J. Bone Miner. Res. 25 (2010) 716–723.
[69] A.K. Rosenthal, C.M. Gohr, J. Ninomiya, B.T. Wakim, Proteomic analysis of articular cartilage vesicles from normal and osteoarthritic cartilage, Arthritis Rheum. 63 (2011) 401–411.
[70] G. Nangami, R. Koumangoye, J. Shawn Goodwin, A.M. Sakwe, D. Marshall, J. Higginbotham, et al., Fetuin-A associates with histones intracellularly and shuttles them to exosomes to promote focal adhesion assembly resulting in rapid adhesion and spreading in breast carcinoma cells, Exp. Cell Res. 328 (2014) 388–400.
[71] U. Muthukrishnan, B. Natarajan, S. Rome, H.J. Johansson, J.Z. Nordin, O. Wiklander, et al., Stress-induced changes in exosomal histone secretion in The Fourth International Meeting of ISEV, ISEV2015, J. Extracell. Vesicles 4 (2015) 27783.
[72] K. Tompkins, A. George, A. Veis, Characterization of a mouse amelogenin [A-4]/M59 cell surface receptor, Bone 38 (2006) 172–180.
[73] H. Zhang, K. Tompkins, J. Garrigues, M.L. Snead, C.W. Gibson, M.J. Somerman, Full length amelogenin binds to cell surface LAMP-1 on tooth root/periodontium associated cells, Arch. Oral Biol. 55 (2010) 417–425.
[74] G.M. London, A.P. Guerin, S.J. Marchais, F. Metivier, B. Pannier, H. Adda, Arterial media calcification in end-stage renal disease: impact on all-cause

and cardiovascular mortality, Nephrol. Dial. Transplant. 18 (2003) 1731–1740.
[75] S.J. Roberts, A.J. Stewart, P.J. Sadler, C. Farquharson, Human PHOSPHO1 exhibits high specific phosphoethanolamine and phosphocholine phosphatase activities, Biochem. J. 382 (2004) 59–65.
[76] S.J. Roberts, A.J. Stewart, R. Schmid, C.A. Blindauer, S.R. Bond, P.J. Sadler, et al., Probing the substrate specificities of human PHOSPHO1 and PHOSPHO2, Biochim. Biophys. Acta 2005 (1752) 73–82.
[77] J.L. Millan, The role of phosphatases in the initiation of skeletal mineralization, Calcif. Tissue Int. 93 (2013) 299–306.
[78] A. Bobrie, M. Colombo, S. Krumeich, G. Raposo, C. Thery, Diverse subpopulations of vesicles secreted by different intracellular mechanisms are present in exosome preparations obtained by differential ultracentrifugation, J. Extracell. Vesicles 1 (2012) 18397.
[79] C. Thery, S. Amigorena, G. Raposo, A. Clayton, Isolation and characterization of exosomes from cell culture supernatants and biological fluids, Curr. Protoc. Cell Biol. (2006) (Chapter 3:Unit 3.22.1-9).

TRPS1 IS INVOLVED IN PHOSPHATE SIGNALING IN A CELLULAR MODEL OF MINERALIZATION

by

MARIA KUZYNSKI, SANDEEP C. CHAUDHARY, CALLIE G. MOBLEY, ANNE POLIARD, ODILE KELLERMAN, DOBRAWA NAPIERALA

In preparation for Journal of Bone and Mineral Research

Format adapted for dissertation

CHAPTER 3

TRPS1 IS INVOLVED IN PHOSPHATE SIGNALING IN A CELLULAR MODEL OF MINERALIZATION

Abstract

The process of mineralization is highly controlled and depends upon several factors, including the availability of phosphate (P_i). P_i has several roles in the mineralization process, including the induction of a P_i signaling cascade which results in bi-phasic activation of ERK1/2 and changes in expression of mineralization-related genes. The transcription factor, Trps1, has also been implicated in the mineralization process. Previously, we identified a context-dependent role for Trps1 in mineralization, where loss of Trps1 results in decreased expression of phosphatases *Alpl* and *Phospho1* and upregulation of Trps1 causes impaired upregulation of P_i regulating genes *Phex*, *Vdr*, *Enpp1*, and *Fam20C*. The involvement of Trps1 in the expression of P_i regulating proteins caused us to analyze whether Trps1 plays a role in P_i signaling. Using a cellular model of mineralization, the odontoblastic 17IIA11 cell line, we uncovered several novel P_i-responsive genes: *Phex*, *Bglap2*, *Phospho1*, *ATF4*, *Sp7*, *Runx2*, *Vdr*, and *Dusp6*. Furthermore, in cells modified to either overexpress Trps1 or be deficient for Trps1, we discovered Trps1 affects the second activation of ERK1/2 and expression of P_i-responsive genes: *Spp1*, *Dmp1*, *Phex*, *Alpl*, *Sp7*, and

Dusp6. Furthermore the dysregulation of *Dusp6*, an ERK1/2 phosphatase involved in the ERK1/2 negative feedback loop, in Trps1-modified cell lines suggests a role for Trps1 in the ERK1/2 negative feedback loop.

Introduction

Mineralization is a tightly regulated process in which crystals of calcium-phosphate, called hydroxyapatite (HA), are laid down within the extracellular matrix (ECM) [1]. The rate of mineralization depends upon: pH, the presence of mineralization inhibitors, matrix composition, proper modifications of matrix proteins, and the availability of calcium (Ca^{+2}) and P_i (PO_4^{3-}) ions [2-5]. Both systemic and local P_i levels are critical for proper mineralization, as demonstrated by impaired bone and dentin mineralization in patients with hypophosphatemic rickets or hypophosphatasia [6-8].

P_i participates in mineralization in a variety of ways. As one of the components of HA, P_i is considered a structural component of the mineralized ECM. Furthermore, addition or removal of P_i moieties regulates the function of several proteins involved in mineralization [9, 10]. Lastly, P_i has been shown to act as a signaling molecule that affects expression of genes involved in osteogenic differentiation and the mineralization process [11-15]. Recently, we have shown that P_i signaling induces formation of matrix vesicles (MV), containing TNAP, Phospho1, and AnxV; which initiate and support mineralization

[16]. However, little is known about the P_i-induced signaling cascade as it has not been well studied or characterized. Previous studies have identified that certain cell types respond to changes of P_i concentrations in their local environment and that this response is independent of systemic P_i regulation. In mineralizing cells, P_i signaling is dependent upon the activity of P_i transporters and is mediated by ERK1/2, not p38 or c-jun kinases [17-19]. P_i-induced activation of ERK1/2 is bi-phasic. This bi-phasic induction results in the regulation of two different sets of genes: early and late response genes [14, 15]. Of particular interest are the late response genes as many of these, such as *Spp1*, *MGP*, *Slc20a1*, *Ankh*, *Dmp1*, *Alpl*, and *Ibsp*, play a role in mineralization. Also of interest, the promoters of many of these genes are enriched in GATA consensus elements, suggesting that GATA transcription factors are involved in the regulation of gene expression in response to P_i [19].

Trps1 is a GATA-type transcription factor. Mutations in the *TRPS1* gene cause tricho-rhino-phalangeal syndrome (TRPS; OMIM#190350) or Ambras syndrome (OMIM#145701) [20, 21]. The abnormalities observed in these patients indicate a role for *TRPS1* in the development of craniofacial elements, endochondral bones, dental tissues, and hair [20-22]. TRPS patients typically have decreased bone mass and TRPS1 was identified as one of bone mineral density quantitative trait loci, suggesting a role for TRPS1 in bone formation and/or homeostasis [21, 23-25]. Trps1 has primarily been described as a transcriptional repressor, however one study found Trps1 to act as a transcriptional activator in hair follicles [22, 26-31].

In our previous *in vivo* studies using *Trps1*$^{\Delta GT}$ mutant mice (functional knock out allele) and mice that overexpress Trps1 in osteoblasts and odontoblasts (*Col1a1-Trps1* transgenic mice), as well as in *in vitro* studies using cells lines that are either deficient for or overexpress Trps1, we identified a number of mineralization-related genes that are regulated by Trps1 [27-29, 32, 33]. Interestingly, the majority of genes that are affected by Trps1 are involved in P_i homeostasis, suggesting a role for Trps1 in P_i regulation. Furthermore, we have determined that P_i signaling induces secretion of mineralization competent MV, and in Trps1-deficient cells secretion of MV is significantly impaired [16, 29]. Based on these findings, we hypothesized that Trps1 is involved in the cellular response to P_i during the mineralization process.

Experimental Procedures

Cell Culture

Preodontoblastic 17IIA11 (17A) cells [16, 29, 34, 35] were maintained in standard DMEM (Life Technologies, Grand Island, NY, USA) with 5% FBS (Thermo Fisher Scientific, Waltham, MA, USA) and 100 units/ml penicillin and 100 µg/ml streptomycin (Cellgro, Manassas, VA, USA) at 37°C and 8% CO_2. *Trps1*-deficient, *Trps1*-overexpressing, and control stable cell lines were generated as previously described [29, 32].To analyze P_i signaling, cells were plated at $5x10^5$ cells per well of a 6-well plate. After 24 hours, cells were serum

starved (0.5%FBS) overnight and then treated with P_i (7 mM βGP or 5 mM Na-P_i buffer).

Protein Isolation and Western blot

Whole protein extracts were prepared by cell lysis in RIPA buffer supplemented with 1 mM NaF, 2 mM Na_2VO_4, 2 mM leupeptin, 2 mM pepstatin, and 2 mM PMSF. Protein concentration was determined by Micro BCA Protein Assay Kit (Thermo Scientific, Rockford, IL, USA). Protein (15 µg) was subjected to electrophoresis on 4-12% precast Bis-Tris gels (Life Technologies Grand Island, NY, USA) and transferred on a nitrocellulose membrane. Specific proteins were detected by fluorescence (Li-Cor Odyssey Infrared Imaging System, LI-COR Biosciences, Lincoln, NE, USA). Primary antibodies against Phospho-ERK1/2 (Cell Signaling, Danvers, MA, USA) were used at 1:2000 dilution, Total-ERK1/2 (Cell Signaling) were used at 1:1000 dilution, Dusp6 (Abcam, Cambridge, UK) were used at 1:500 dilution. All fluorescent secondary antibodies (LI-COR Biosciences, Lincoln, NE, USA) were used at 1:20,000.

RNA Isolation and qRT-PCR

Total RNA was extracted using GenElute Mammalian Total RNA Miniprep Kit (Sigma Aldrich, St. Louis, MO, USA). Total RNA (1 µg), after DNase I treatment (Life Technologies, Grand Island, NY, USA), was converted to cDNA with SuperScript III Reverse Transcriptase kit (Life Technologies, Grand Island, NY, USA). Gene expression analyses were performed using AB Biosystems

7500 Fast Real-Time PCR System and Fast SYBR Green reaction mix (Roche, Indianapolis, IN, USA). Primer sequences are: Dmp1 F:GCTGGGTCACCACCACCACC and R: GGAGGGTCCTCCCCACTGTCC, Ibsp F: ACGAACAAACAGGCAACGAAT and R: GGGCTTCACTGATGGTAGTAATAA, Bglap2 F: GCACACCTAGCAGACACCAT and R: GCTTGGACATGAAGGCTTTGT, Dusp6 F: ACGAGAATAGCAGCGACTGG and R: TTACTGAAGCCACCTTCCAGG. Gapdh, Spp1, Ankh, Slc20a1, Phex, Alpl, Phospho1, Sp7, Runx2, ATF4, Vdr, MGP, Slc20a2 primer sequences were described in [29]. For RNA-seq experiment, cells were treated with 10mM Na-P_i and RNA was isolated with Trizol (Thermo Fisher Scientific) according to the manufacturer's protocol. RNA sequencing and statistical analyses of the data was carried out at the Genomics Core Laboratories at the University of Alabama at Birmingham Heflin Center for Genomic Science.

Statistical analyses

All experiments were performed on three control and three Trps1-modified stable cell lines. Data are presented as the mean ±S.D. Probability values were calculated using the Student's t test. $p \leq 0.05$ (*) and 0.005 (**) were considered to be statistically significant and highly significant, respectively.

Results

Delineating the P_i signaling cascade in 17A cells.

Previous studies have shown that P_i signaling is dependent upon Na/P_i co-transporters PiT1 and PiT2, is mediated via ERK1/2, and causes changes in gene expression [11-15, 36]. To elucidate the role of Trps1 in the P_i signaling cascade, we first analyzed P_i signaling in the 17A cell line. To do this, we assessed ERK1/2 activation in response to P_i. Cells were serum starved overnight and then treated with 7 mM βGP for 15min, 30min, 45min, 1h, 2h, 4h, and 6h. As reported in other cell lines, 17A cells have a biphasic induction of ERK1/2 activation, with the initial activation happening quickly, within 15 minutes of treatment, and the second activation occurring around 4-6 hours [19, 37]. Furthermore, this activation appeared to be specific to ERK1/2 as we were unable to detect activation of the p38 and Akt pathways (Fig 1A). To identify P_i-responsive genes, 17A cells were treated with 10 mM Na-P_i for 24h and RNA-seq was performed. We uncovered 20 genes that are significantly altered upon treatment with P_i (Table 1). Interestingly, 2 of the top 10 genes most upregulated are involved in ERK1/2 activation/deactivation: Dusp6 and Sema7a. To confirm changes in gene expression discovered by RNA-seq as well as analyze expression of other mineralization-related genes of interest, we treated cells with 5 mM Na-P_i and isolated RNA 12h and 48h later. Results from qRT-PCR analyses found that classic P_i-responsive genes *Spp1*, *Dmp1*, and *Ankh* were significantly upregulated at 12h and further upregulated at 48h (Fig 1B) [14, 15].

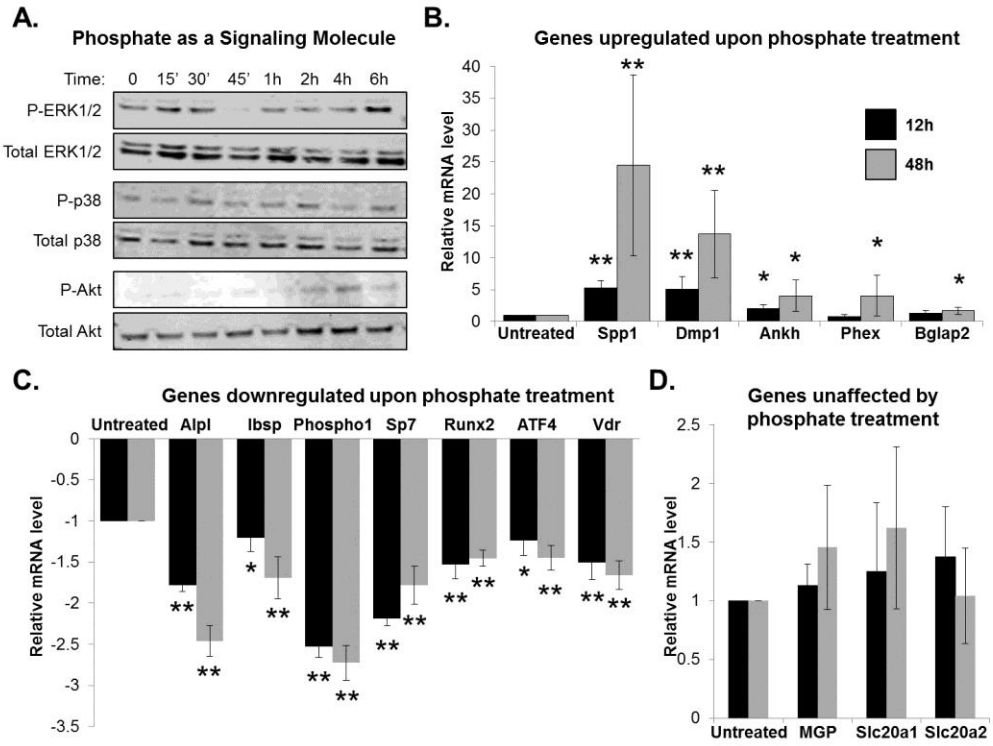

Figure 1. Characterization of the 17A cell response to phosphate. A. Biphasic ERK1/2-activation. Following overnight serum starvation, 17A cells were treated with 7 mM βGP for 15min, 30min, 45min, 1h, 2h, 4h, and 6h. Activation of ERK1/2, p38, and Akt proteins was assessed by Western blot. Total ERK1/2, total p38, and total Akt were used as loading controls. **B-D.** Effect of P_i on gene expression. 17A cells were treated with 5mM Na-P_i buffer and changes in gene expression at 12h and 48h were analyzed by qRT-PCR. **B.** *Spp1*, *Dmp1*, and *Ankh* were found to be significantly upregulated 12h and 48h after P_i treatment. *Phex* and *Bglap2* were upregulated at 48h following P_i treatment. **C.** *Alpl*, *Ibsp*, *Phospho1*, *Sp7*, *Runx2*, *ATF4*, and *Vdr* were significantly downregulated 12h and 48h after treatment with P_i. **D.** No significant changes in *MGP*, *Slc20a1*, or *Slc20a2* expression were observed at 12h or 48h after P_i treatment. Relative expression was calculated by comparing each time point to its untreated control (12h P_i treatment versus 12h untreated). Data are represented as the mean values of three experiments ± SD, *p≤0.05 and **p≤0.005.

Additionally, *Phex* and *Bglap2* were significantly upregulated at 48h following P_i treatment, which has not been previously described (Fig 1B). *Alpl* and *Ibsp* are P_i-responsive genes, but these genes have been shown to be downregulated upon P_i treatment [14, 15]. Our findings were in agreement with previous studies

Gene Name	Entrez ID	Accession Number	Log2 Fold Change
Txk	7294	NM_013698	∞
F2rl3	9002	NM_007975	∞
Dmp1	1758	NM_016779	7.68619
Spp1	6696	NM_001204202	6.98307
Serpinb2	5055	NM_011111	6.97641
Hmga2	8091	NM_010441	4.84733
Dusp6	1848	NM_026268	4.81334
Wnt7b	7477	NM_001163634	4.71776
Sema7a	8482	NM_011352	4.38508
Egr3	1960	NM_001289925	4.30555
Gadd45g	10912	NM_011817	-2.49743
Pth1r	5745	NM_001083936	-2.55382
Car3	761	NM_007606	-2.66524
Fam180a	389558	NM_173375	-2.67809
Cdsn	1041	NM_001008424	-2.83891
Trib3	57761	NM_175093	-2.9425
Megf6	1953	NM_001162977	-3.10359
Slc13a5	284111	NM_001004148	-3.91959
Nr1i3	9970	NM_009803	-∞
Akr1b7	57016	NM_009731	-∞

Table 1. Top 10 genes most up/downregulated upon P_i treatment in 17A cells. RNA-seq was performed with total RNA isolated from 17A cells treated with 10 mM Na-P_i for 24h.

and we also identified *Phospho1*, *Sp7*, *Runx2*, *ATF4*, and *Vdr* as additional genes that are downregulated upon P_i treatment (Fig 1C). Lastly, we found no changes in *MGP*, *Slc20a1*, or *Slc20a2* expression following P_i treatment (Fig 1D).

Trps1 affects the second activation of ERK1/2 in response to P_i.

Now that we have assessed the P_i signaling cascade in 17A cells, we wanted in investigate how Trps1 affects the 17A cell response to P_i. We used Trps1-deficient (Trps1-KD) and Trps1-overexpressing (Trps1-OE) cell lines. These cell lines were previously generated and described [29, 32]. Briefly, clonal Trps1-deficient (70-85% of Trps1 knocked-down) cell lines were generated using lentivirus-delivered short hairpin RNA-expression vectors (shRNAs). Control cell lines (shScr or Cntr) were generated in the same fashion using scrambled shRNA. To generate Trps1-overexpressing cell lines, we used a transposon-mediated genomic integration approach. We generated 3 clonal, stable cell lines with 2.5-4.5 fold overexpression of Trps1. Control cell lines (Cntr) were

generated in the same way using a “no insert” transposon. To analyze changes caused by Trps1 in the P_i signaling cascade, Trps1-deficient and Trps1-overexpressing cells were treated with P_i (βGP or Na-P_i) and ERK1/2 activation was assessed by Western blot. As predicted, bi-phasic ERK1/2 activation was observed in control cell lines (shScr and Cntr; Fig. 2A-B) [19, 37]. In contrast, Trps1-deficient cells failed to have a second activation of ERK1/2 in response to P_i (Fig. 3A), whereas Trps1-overexpressing cells displayed an accelerated second activation of ERK1/2 (Fig. 2B). These data support involvement of Trps1 in the P_i signaling cascade.

Trps1 affects expression of P_i-responsive genes.

To determine how Trps1 affects the transcriptional program of P_i siganling, we analyzed changes in expression of P_i-responsive genes. Trps1-deficient cells had a decreased ability to upregulate *Spp1*, *Phex*, and *Dmp1* in response to P_i (Fig 3A) whereas Trps1-overexpressing cells displayed enhanced downregulation of *Alpl* and *Sp7* (Fig 3B).

To summarize, Trps1-deficient cells had a delayed and decreased second activation of ERK1/2 which was accompanied with a decreased upregulation of P_i-responsive genes, while Trps1-overexpressing cells had an enhanced and accelerated second activation of ERK1/2 and increased downregulation of P_i-responsive genes.

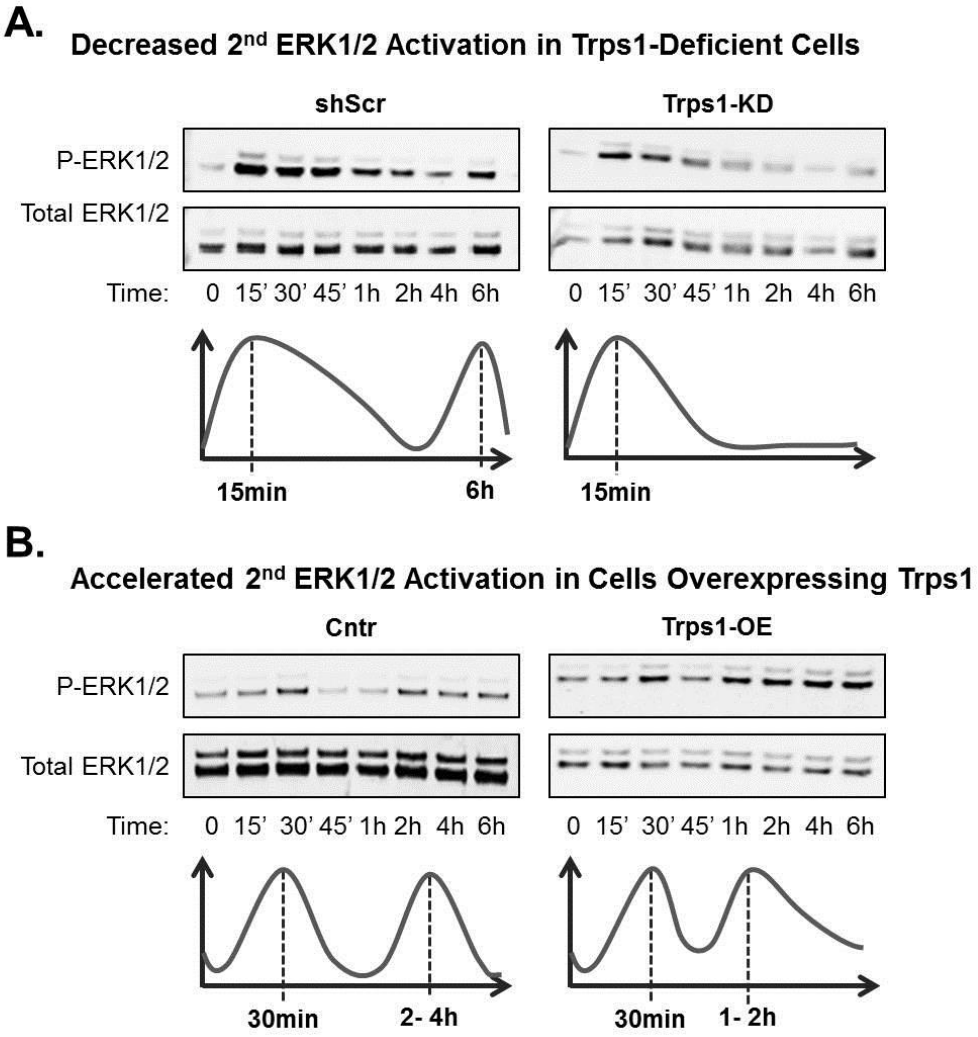

Figure 2. ERK1/2 activation upon phosphate treatment is altered in Trps1-deficient and Trps1-overexpressing cells. ERK1/2 activation was assessed from 0 to 6 hours after P_i treatment in shScr vs. Trps1-deficient (Trps1-KD) cells and Cntr vs. Trps1-overexpressing (Trps1-OE) cells. **A.** Upon treatment with 2 mM Na-P_i, shScr cells have an initial ERK1/2 activation at 15' and a second activation at 6h. Trps1-KD cells have an initial ERK1/2 activation at time 15' comparable to shScr, but the second ERK1/2 activation at 6h is undetectable in Trps1-KD cells. **B.** Treatment with 7 mM βGP results in an initial ERK1/2 activation in Cntr cells around 30' and a second activation at 4h. Trps1-OE cells have an initial activation of ERK1/2 30' after treatment, similar to control cell lines. However, the second ERK1/2 activation occurs more rapidly, around 1h, in Trps1-OE cells.

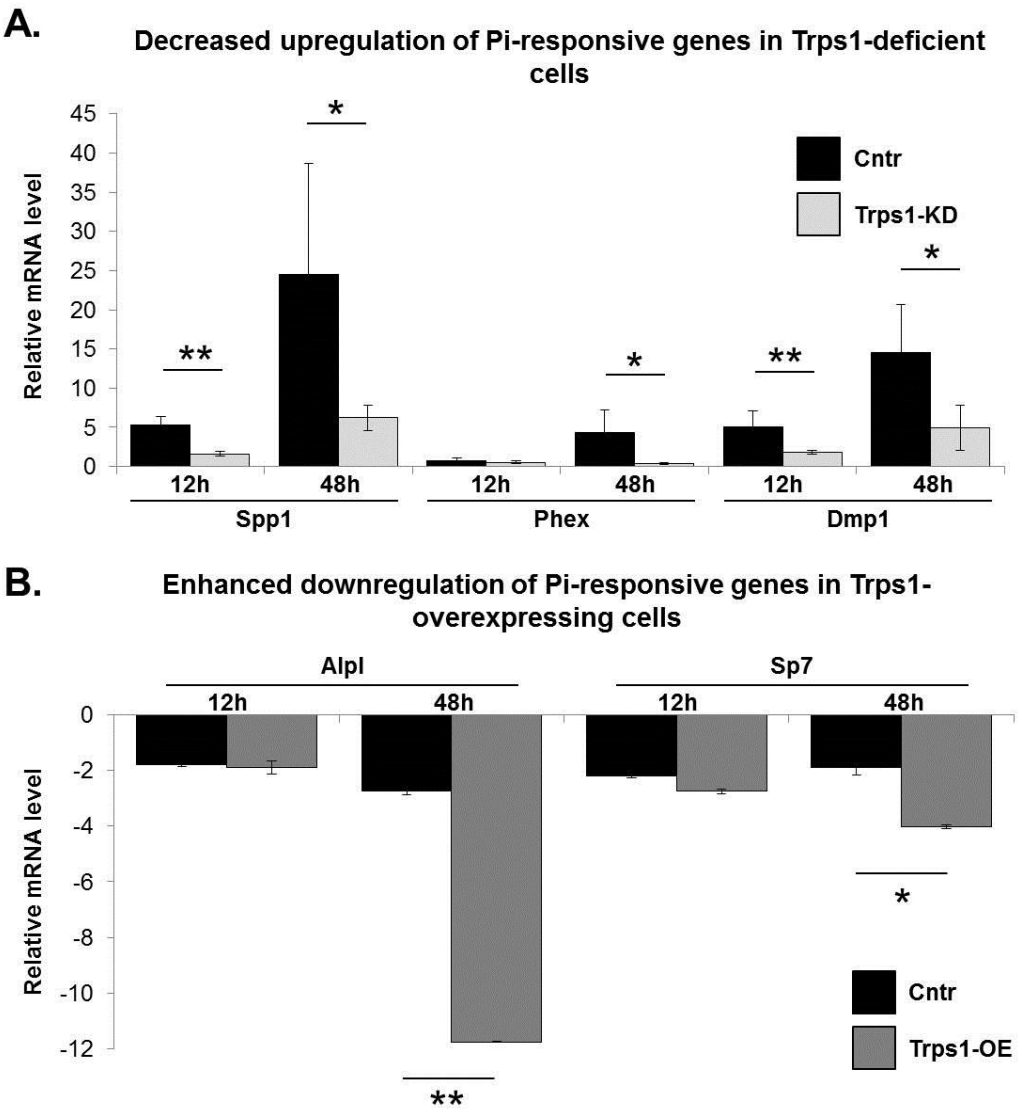

Figure 3. Trps1 affects the expression of phosphate responsive genes. qRT-PCR was performed to identify the effect of Trps1 deficiency and upregulation on P_i-responsive gene expression. **A.** Trps1-deficient cells (Trps1-KD) had a decreased ability to upregulate *Spp1* and *Dmp1* at 12h and 48h and *Phex* at 48h after P_i treatment. **B.** Trps1-overexpressing (Trps1-OE) cells had an enhanced downregulation of *Alpl* and *Sp7* 48h following treatment with P_i. Relative expression was calculated by comparing each time-point to its respective untreated control for each cell line (Trps1-KD1 12h untreated versus Trps1-KD1 12h P_i treatment). Statistical differences were calculated by comparing changes in control cell lines upon P_i treatment to changes in Trps1-KD and Trps1-OE cell lines upon P_i treatment for each time-point. Data are represented as the mean values of experiments performed in three clonal cell lines ± SD, *p≤0.05 and **p≤0.005.

Trps1 may be involved in the ERK1/2 negative feedback loop.

Taking these data into consideration, it appears that Trps1 is involved in the P_i signaling cascade. To determine how this regulation is occurring, we analyzed RNA-seq data on control cells treated with P_i for 24h and found that one of the genes most upregulated is dual specificity phosphatase 6 (Dusp6), an ERK1/2 specific phosphatase that is involved in the negative feedback loop. We compared *Dusp6* expression in Trps1-deficient and Trps1-overexpressing cells with controls. Cells grown in standard growth medium (without additional P_i) express *Dusp6* at a low level, and there are no significant differences in *Dusp6* expression in Trps1-deficient, Trps1-overexpressing, and control cells (Fig 4A). Upon treatment with P_i, *Dusp6* is significantly upregulated in control cells 12h and 48h after treatment. However, Trps1-deficient cells were unable to upregulate *Dusp6* at 12h or 48h and Trps1-overexpressing cells had a decreased ability to upregulate *Dusp6* at 48h in response to P_i (Fig 4B). This effect was confirmed at the protein level in Trps1-deficient cells (Fig 4C). Altogether, this data suggests that Trps1 is involved in P_i signaling by altering the second activation of ERK1/2 and modifying expression of P_i-responsive genes, including expression of the ERK1/2 phosphatase, *Dusp6*.

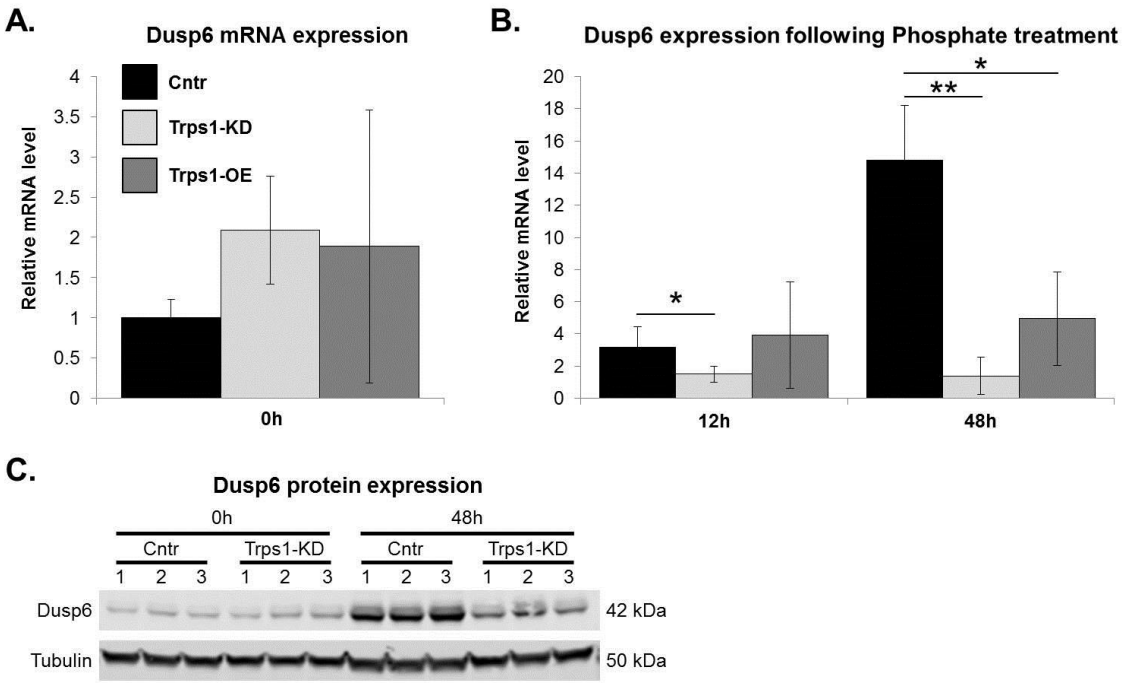

Figure 4. Trps1 affects Dusp6 expression in response to phosphate. A. Trps1-deficient (Trps1-KD) and Trps1-overexpressing (Trps1-OE) cells have comparable *Dusp6* expression to controls at 0h. **B.** *Dusp6* expression does not increase upon P_i treatment in Trps1-KD cells. Trps1-OE cells displayed decreased upregulation of *Dusp6* at 48h compared to controls **C.** Western blot of Dusp6. Dusp6 protein level increases after 48h of P_i treatment in control cells. There is no change in Dusp6 protein level in Trps1-KD cells upon P_i treatment. Relative expression was calculated by comparing each time-point to its respective untreated control for each cell line (ex: Trps1-KD1 12h untreated versus Trps1-KD1 12h P_i treatment). Statistical differences were calculated by comparing changes in control cell lines upon P_i treatment to changes in Trps1-KD and Trps1-OE cell lines at the same time-point. Data are represented as the mean values of experiments performed in three clonal cell lines ± SD, *p≤0.05 and **p≤0.005.

Discussion

These studies uncovered several novelties about P_i signaling. First, we discovered additional P_i-responsive genes that have not been previously

described (*Phex*, *Bglap2*, *Phospho1*, *Sp7*, *Runx2*, *ATF4*, *Vdr*, and *Dusp6*). Overall, 17A cells responded as expected/predicted upon P_i signaling, i.e. the upregulation of *Spp1*, *Dmp1*, and *Ankh* and downregulation of *Alpl* and *Ibsp*. On the other hand, the 17A cell line did display some differences in the P_i signaling cascade in comparison with results of other in vitro models of osteogenic differentiation. Specifically, expression of *MGP* and *Slc20a1* was not changed in response to P_i in 17A cells, whereas a 2.5-3 fold increase in *Slc20a1* expression 24h after 10mM Na-P_i treatment was reported previously [19]. We did detect significant changes in *Slc20a1* expression (2.36 fold increase, $p<0.005$) at 24h by RNA-seq, but we only observed a non-significant upregulation at 48h by qRT-PCR (1.6 fold increase, $p=0.052$). This may be the result of stimulation with a higher concentration of P_i (10mM Na-P_i for RNA-seq and 5 mM Na-P_i for qRT-PCR). Alternatively, this may indicate a transient upregulation of *Slc20a1* at 24h, but not 12h or 48h. These differences stress the importance of validating and confirming signaling pathways in different cellular models.

The downregulation of phosphatases (*Alpl* and *Phospho1*) upon P_i treatment is likely part of a feedback mechanism in the regulation of P_i availability and mineralization; as the P_i levels increase in the extracellular environment, phosphatases, which provide P_i and remove mineralization inhibitor PP_i (TNAP), are decreased. The downregulation of osteogenic transcription factors *Runx2* and *Sp7* was a surprising finding. We have previously shown that P_i increases MV secretion which support the initiation of mineralization; therefore we would expect the expression of transcription factors, which are critical for osteogenic

differentiation, to be upregulated [16]. However, it is possible that these transcription factors may be regulated at the post-transcriptional level. This becomes an even greater possibility for Runx2, as it is post-translationally modified (phosphorylated) via ERK1/2, which is activated upon P_i treatment [38]. Alternatively, there may be other transcription factors mediating this response.

Additionally, we identified that the transcription factor Trps1 is involved in the P_i signaling cascade. Either upregulation or deficiency of Trps1 affects the dynamics of Erk1/2 activation by P_i and the expression of P_i-responsive genes, including *Dusp6*, which is an ERK1/2-specific phosphatase. This suggests that Trps1 is one of the transcription factors regulating gene expression in response to P_i. In addition, Trps1 may indirectly affect the dynamics of ERK1/2 activation through regulation of *Dusp6* expression.

In our studies, we used two different sources of P_i to activate P_i signaling. βGP is commonly used as a P_i source in osteogenic differentiation studies. However, in our analyses on the consequences of Trps1-deficiency *in vitro*, we discovered that decreased Trps1 levels resulted in a significant decrease in TNAP activity, which is required for cleaving the P_i moiety from the βGP molecule. Therefore, we used Na-P_i, as P_i in this form does not require TNAP activity to be taken up by cells. Importantly, use of either P_i source (Na-P_i or βGP) results in bi-phasic ERK1/2 activation.

Lastly, there still remain several questions about the P_i signaling cascade. Currently, the receptors for this pathway are unknown. One study has suggested that FGF receptors (FGFR) may be mediating the signal, as FGFR activate

ERK1/2 and have been implicated in this process by a previous study [19]. A different study suggested that the Na/P_i co-transporter PiT1 may act as a P_i receptor and that this function is independent of P_i transport [36]. Furthermore, while the identification of P_i-responsive genes has been fairly well studied, the transcriptional factors regulating expression of these genes in response to Pi still remain unknown. It is possible that Trps1 is one the transcription factors involved in this regulation, as promoters of these genes are enriched in GATA consensus elements [39]. Furthermore, Trps1 has been shown to repress *Runx2* and suggested to repress *Vdr* (both of which are downregulated upon P_i treatment) [29, 33]. However, further studies would need to be performed to validate this idea.

References

1. Gorski, J., *Biomineralization of bone: a fresh view of the roles of noncollagenous proteins.* Front Biosci, 2011. **16**: p. 2598-2621.
2. Addison, W.N., et al., *Pyrophosphate inhibits mineralization of osteoblast cultures by binding to mineral, up-regulating osteopontin, and inhibiting alkaline phosphatase activity.* J Biol Chem, 2007. **282**(21): p. 15872-83.
3. Harmey, D., et al., *Concerted regulation of inorganic pyrophosphate and osteopontin by akp2, enpp1, and ank: an integrated model of the pathogenesis of mineralization disorders.* Am J Pathol, 2004. **164**(4): p. 1199-209.
4. Johnson, K., et al., *Linked deficiencies in extracellular PP(i) and osteopontin mediate pathologic calcification associated with defective PC-1 and ANK expression.* J Bone Miner Res, 2003. **18**(6): p. 994-1004.
5. George, A. and A. Veis, *Phosphorylated proteins and control over apatite nucleation, crystal growth, and inhibition.* Chem Rev, 2008. **108**(11): p. 4670-93.

6. Alizadeh Naderi, A.S. and R.F. Reilly, *Hereditary disorders of renal phosphate wasting.* Nat Rev Nephrol, 2010. **6**(11): p. 657-65.
7. Bergwitz, C. and H. Juppner, *Regulation of phosphate homeostasis by PTH, vitamin D, and FGF23.* Annu Rev Med, 2010. **61**: p. 91-104.
8. Davideau, J.L., et al., *In situ investigation of vitamin D receptor, alkaline phosphatase, and osteocalcin gene expression in oro-facial mineralized tissues.* Endocrinology, 1996. **137**(8): p. 3577-85.
9. Sodek, J., B. Ganss, and M.D. McKee, *Osteopontin.* Crit Rev Oral Biol Med, 2000. **11**(3): p. 279-303.
10. McKnight, D.A. and L.W. Fisher, *Molecular evolution of dentin phosphoprotein among toothed and toothless animals.* BMC Evol Biol, 2009. **9**: p. 299.
11. Foster, B.L., et al., *Regulation of cementoblast gene expression by inorganic phosphate in vitro.* Calcif Tissue Int, 2006. **78**: p. 103-12.
12. Khoshniat, S., et al., *The emergence of phosphate as a specific signaling molecule in bone and other cell types in mammals.* Cellular and Molecular Life Sciences, 2011. **68**: p. 205-18.
13. Kumar, R., *Phosphate sensing.* Curr Opin Nephrol Hypertens, 2009. **18**: p. 281-4.
14. Julien, M., et al., *Phosphate stimulates matrix Gla protein expression in chondrocytes through the extracellular signal regulated kinase signaling pathway.* Endocrinology, 2007. **148**: p. 530-7.
15. Julien, M., et al., *Phosphate-dependent regulation of MGP in osteoblasts: role of ERK1/2 and Fra-1.* J Bone Miner Res, 2009. **24**: p. 1856-68.
16. Chaudhary, S.C., et al., *Phosphate induces formation of matrix vesicles during odontoblast-initiated mineralization in vitro.* Matrix Biol, 2016.
17. Razzaque, M.S., *Phosphate and Vitamin D in Chronic Kidney Disease.* Contributions to Nephrology, 2013. **180**: p. 74-85.
18. von Kriegsheim, A., et al., *Cell fate decisions are specified by the dynamic ERK interactome.* Nat Cell Biol, 2009. **11**(12): p. 1458-64.
19. Camalier, C.E., et al., *An integrated understanding of the physiological response to elevated extracellular phosphate.* J Cell Physiol, 2013. **228**(7): p. 1536-50.
20. Ishimori, N.S., I.;Korstanje, R.; Marion, M.; Li, R.; Donahue, L.; Rosen, C.; Beamer, W.; Paigen, B.; Churchill, G., *Quantitative trait loci for BMD in an SM/J by NZB/BlNJ intercross population and identification of Trps1 as a probable candidate gene.* J Bone Miner Res, 2008. **23**(9): p. 1529-1537.
21. Bennett, C.G., C.J. Hill, and J.L. Frias, *Facial and oral findings in trichorhinophalangeal syndrome type 1 (characteristics of TRPS 1).* Pediatr Dent, 1981. **3**: p. 348-352.
22. Malik, T.H., et al., *Transcriptional repression and developmental functions of the atypical vertebrate GATA protein TRPS1.* EMBO J, 2001. **20**(7): p. 1715-25.
23. Ishimori, N., et al., *Quantitative trait loci for BMD in an SM/J by NZB/BlNJ intercross population and identification of Trps1 as a probable candidate gene.* Journal of Bone and Mineral Research, 2008. **23**(9): p. 1529-1537.

24. Ackert-Bicknell, C.D., S.; Tsaih, S.; Beamer, W.; Cupples, L.; Paigen, B.; Hsu, Y.; Kiel, D.; Karasik, D., *Genetic variation in TRPS1 may regulate hip geometry as well as bone mineral density.* Bone, 2012. **50**(5): p. 1188-1195.
25. Wang, L.L., W.; Zhang, L.; Huang, Y.; Scheib, R.; Liu, X.; Myers, L.; Lu, L.; Farber, C.; Liu, G.; Wang, C.; Deng, H.; Williams, R.; Wang, Y.; Gu, W.; Jiao, Y., *Trps1 differentially modulates the bone mineral density between male and female mice and its polymorphism associates with BMD differently between women and men.* PLoS One, 2014. **9**(1).
26. Piscopo, D.M.J., E.B.; Derynck R., *Identification of the GATA factor TRPS1 as a repressor of the osteocalcin promoter.* J Biol Chem, 2009. **284**(46): p. 31690-31703.
27. Napierala, D., et al., *Mutations and promoter SNPs in RUNX2, a transcriptional regulator of bone formation.* Mol Genet Metab, 2005. **86**(1-2): p. 257-68.
28. Mobley, C.G., et al., *Dspp-independent Effects of Transgenic Trps1 Overexpression on Dentin Formation.* J Dent Res, 2015. **94**(8): p. 1128-34.
29. Kuzynski, M., et al., *Dual role of the Trps1 transcription factor in dentin mineralization.* J Biol Chem, 2014. **289**(40): p. 27481-93.
30. Fantauzzo, K.A. and A.M. Christiano, *Trps1 activates a network of secreted Wnt inhibitors and transcription factors crucial to vibrissa follicle morphogenesis.* Development, 2012. **139**(1): p. 203-14.
31. Bach, A.S., et al., *Nuclear cathepsin D enhances TRPS1 transcriptional repressor function to regulate cell cycle progression and transformation in human breast cancer cells.* Oncotarget, 2015. **6**(29): p. 28084-103.
32. Napierala, D., et al., *Transcriptional repression of the Dspp gene leads to dentinogenesis imperfecta phenotype in Col1a1-Trps1 transgenic mice.* J Bone Miner Res, 2012. **27**(8): p. 1735-45.
33. Napierala, D., et al., *Uncoupling of chondrocyte differentiation and perichondrial mineralization underlies the skeletal dysplasia in tricho-rhino-phalangeal syndrome.* Hum Mol Genet, 2008. **17**(14): p. 2244-54.
34. Lacerda-Pinheiro, S., et al., *Concomitant multipotent and unipotent dental pulp progenitors and their respective contribution to mineralised tissue formation.* Eur Cell Mater, 2012. **23**: p. 371-86.
35. Priam, F., et al., *New cellular models for tracking the odontoblast phenotype.* Arch Oral Biol, 2005. **50**(2): p. 271-7.
36. Chavkin, N.W., et al., *Phosphate uptake-independent signaling functions of the type III sodium-dependent phosphate transporter, PiT-1, in vascular smooth muscle cells.* Exp Cell Res, 2015. **333**(1): p. 39-48.
37. Tada, H., et al., *Phosphate increases bone morphogenetic protein-2 expression through cAMP-dependent protein kinase and ERK1/2 pathways in human dental pulp cells.* Bone, 2011. **48**: p. 1409-16.
38. Ge, C., et al., *Identification and functional characterization of ERK/MAPK phosphorylation sites in the Runx2 transcription factor.* J Biol Chem, 2009. **284**(47): p. 32533-43.

39. Camalier, C.E., et al., *An integrated understanding of the physiological response to elevated extracellular phosphate.* J Cell Physiol, 2012.

DISCUSSION

The transcriptional regulation of mineralization has not been well studied. Mineralization is a tightly regulated process, and various disorders result from insufficient, disorganized, or increased mineralization as well as ectopic mineralization in non-mineralizing tissues. P_i has been shown to be important in mineralization in a variety of ways, including regulation of expression of mineralization-related genes [32-34, 41, 47]. Disturbances in systemic and local P_i homeostasis result in defective mineralization [31-37] . In these studies, we identified the role of the transcription factor Trps1 in the mineralization process and discovered its involvement in P_i signaling [7]. Furthermore, we identified a novel function of P_i in mineralization: stimulation of secretion of MV that support initiation of the mineralization process [9].

Altogether, our data suggest that Trps1 has a context dependent function in the bi-phasic process of mineralization. Trps1 is required to initiate mineralization and must then be downregulated for proper propagation of mineralization in the ECM. During the initiation of mineralization, Trps1 is important for the expression of phosphatases (TNAP and PHOSPHO1) and major osteogenic transcription factors (Runx2 and Sp7), as well as the production of MV. Thereafter, during propagation of mineralization in the ECM, Trps1 must be downregulated to allow for the expression of P_i regulating proteins

(Phex, Vdr, Enpp1, and Fam20C) [4-7]. Furthermore, we determined that Trps1 is involved in the P_i signaling cascade. Specifically, Trps1 affects the second activation of ERK1/2 and expression of P_i-responsive genes (*Spp1*, *Phex*, *Dmp1*, *Alpl*, and *Sp7*). In addition, the dysregulation of Dusp6, which is part of the ERK1/2 negative feedback loop, in Trps1-modified cell lines suggests that the function of Trps1 in the P_i signaling cascade is by its involvement in the activation/deactivation of ERK1/2.

The majority of studies have identified Trps1 as a transcriptional repressor [1, 2, 4-7, 50, 54, 60]. Therefore we predict that the downregulation of genes (*Alpl*, *Phospho1*, *Runx2*, and *Sp7*) in Trps1-deficient cells is mediated by the released inhibition of another repressor, and thus these genes are not direct targets of Trps1. Currently, little is known about the direct interactions of Trps1 in mineralizing cells. Our group has previously identified that Trps1 can inhibit *Dspp* and *Runx2* transcription, as well as interact with Runx2 to block Runx2-mediated trans-activation [2, 4, 5]. Another group discovered Trps1 regulates *Bglap2* transcription [1]. To further identify genes which are transcriptionally regulated by Trps1, we plan to perform chromatin immunoprecipitation-sequencing analyses. This will be the next step in deciphering the molecular network of Trps1 in mineralizing cells.

Our results from Trps1-deficient odontoblast-derived cell lines in comparison with *in vivo* studies of endochondral bones suggest a context-dependent function for Trps1, i.e. Trps1 has a different role in the developing skeleton than in the developing tooth. In preodontoblastic cells deficient for

Trps1, we found reduced expression of osteogenic transcription factors Runx2 and Sp7. In the endochondral bones of *Trps1*$^{\Delta GT/\Delta GT}$ mice, we observed upregulation of *Runx2* in the perichondrium and cartilage [4, 5, 7]. We predict this difference may be the effect of cell autonomous and non-autonomous mechanisms within the perichondrium, such as Ihh signaling, versus cell autonomous effects in a cellular model of mineralization. However, this may also be the result of different molecular networks that regulate the mineralization of perichondrium and dentin, as has been described by various studies. For instance, one study identified distinct sets of genes regulated by Runx2 in bone and dental mesenchyme [61]. This is further supported by a recent study on the Runx2 function in these tissues which uncovered different roles of this key osteogenic transcription factor in bone and tooth. In these experiments, mice deficient for Runx2 (2.3kb *Col1a1-Cre;Runx2*$^{\Delta 8/\Delta 8}$) displayed skeletal defects with no apparent dental abnormalities [62-64].

It is important to note that while both Trps1-deficient and Trps1-overexpressing cells demonstrate impaired mineralization, the changes in gene expression and the role of the affected genes in the mineralization process suggest different underling molecular mechanisms and an additional context-dependent function of Trps1. Trps1-deficient cells displayed a complete loss of mineralization potential that was associated with a lack of MV production and decreased expression of osteogenic transcription factors and phosphatases. This suggests Trps1 is required to initiate mineralization [7]. In contrast, sustained upregulation of Trps1 in mature cells has deleterious effects on dentin

mineralization *in vivo* as well as in odontoblastic-mediated mineralization *in vitro*. Trps1 overexpression results in an inability to upregulate genes involved in P_i regulation in the propagation phase of mineralization (Phex, Vdr, Enpp1, and Fam20C), which suggests that Trps1 has a negative effect on the function of differentiated cells [2, 6, 7]. This correlates well with the dynamic Trps1 expression pattern observed both *in vivo* in developing endochondral bones and teeth as well as in *in vitro* cellular models of mineralization: Trps1 is highly expressed in progenitor cells and is downregulated upon maturation [4, 7, 55, 59]. Based on these results, we propose that Trps1 is involved in the maturation of cells destined to produce a mineralizing matrix.

The initiation of mineralization is supported by MV which accumulate Ca^{+2} and P_i ions to facilitate formation of hydroxyapatite crystals, which are then released to the ECM to promote mineralization [28-30]. In our studies, we found that P_i alone induces secretion of MV and this secretion is dependent upon P_i-induced ERK1/2 activation. Of note, 17A cells secrete MV containing TNAP, PHOSPHO1, and AnxV even without osteogenic stimulation [9]. This indicates that these cells are already primed to secrete a mineralized matrix, which is in agreement with the high expression of osteogenic genes (*Col1a1*, *Runx2*, *Sp7*, *Alpl*, *Phospho1*, *Bglap2*, *Ibsp*) under standard growth conditions [58, 65]. Interestingly, 17A cells stimulated with ascorbic acid and P_i produce MV containing different isoforms of TNAP and PHOSHPO1 than MV secreted by unstimulated cells. This indicates that stimulating cells with osteogenic factors not only induces secretion of MV, but also affects the MV molecular composition

[9]. Also of note, no MV were detected in mice deficient for TNAP and PHOSPHO1 [25, 26, 66]. This suggests that decreased expression of TNAP and PHOSPHO1 in Trps1-deficient cells is an underlying cause of impaired MV secretion [7]. While it is still unclear how these phosphatases contribute to MV formation, based on their function and our results demonstrating that P_i is sufficient to induce MV secretion, we predict that TNAP may support MV formation by increasing concentrations of available P_i in the local environment and that PHOSPHO1 activity on the phospholipid bilayer may modulate the fluidity of the cell membrane.

The biogenesis of MV is yet unclear. The current proposed model of MV formation is that they are formed by budding off of the plasma membrane. This model is supported by studies which have identified similar lipid and protein composition of MV to the cell membrane of origin; however, the mechanisms regulating MV formation are not known [16, 67, 68]. Intracellular processes have previously been identified in the biogenesis of extracellular vesicles, such as the endocytic pathway in the production of exosomes. Interestingly, recent studies have found vesicles in the cytoplasm of mineralizing cells that contain calcium-phosphate crystals, suggesting intracellular processes are involved in MV biogenesis [69, 70]. We discovered that MV produced by cells stimulated with osteogenic factors are enriched in lysosomal proteins, Lamp1 and Lamp2a [9]. This suggests that that these proteins may be involved in the mineralization process or may be a footprint of the biogenesis pathway of MV. A role for Lamp1 in mineralization has already been proposed by a previous study which detected

Lamp1 localizing to the cell surface and binding a major enamel matrix protein, amelogenin [71-74]. Lamp1 may have a similar function in dentin mineralization by binding and/or recruiting dentin matrix proteins to the ECM. Alternatively, as it has been proposed by other studies, intracellular processes may be involved in the generation of MV [69, 70]. In such case, our results suggest lysosomes may be playing a role in this process. However, more experiments need to be performed to definitively say lysosomes are involved in MV biogenesis.

P_i is essential in the mineralization process. In these studies, we discovered a novel function of P_i: P_i can induce secretion of MV, and we determined that this secretion is dependent upon P_i-induced ERK1/2 activation [9]. Following P_i treatment, ERK1/2 is activated and results in secretion of MV and changes in expression of P_i-responsive genes [32-34, 41, 47]. Interestingly, the release of MV happens quickly, within 6-12h. This suggests the production of MV is not dependent on the activation of the transcriptional program, or at least not in 17A cells which are already primed/committed to mineralization [7, 58, 65]. For instance, high expression of TNAP and PHOSPHO1 are required for MV production *in vivo* and may explain why 17A cells secrete MV more rapidly than other mineralizing cell lines, such as MC3T3-E1 and ST2 [9, 25].

Through our experiments comparing gene expression in cells treated with P_i and untreated cells, we identified new genes that are P_i-responsive (*Phex*, *Bglap2*, *Phospho1*, *Sp7*, *Runx2*, *ATF4*, and *Vdr*). Also worth noting, the 17A cell line displayed some differences in expression of previously identified P_i-responsive genes. For example, *MGP* and *Slc20a1* have been characterized as

P_i-responsive genes [32-34, 41, 47]. However, we did not detect significant differences in the expression of either of these genes upon P_i treatment in 17A cells. Previous studies have reported a 2.5-3 upregulation of *Slc20a1* after 24h of treatment with 10mM Na-P_i [32]. We observed a slight upregulation at 48h upon treatment with 5mM Na-Pi (fold increase=1.6, p-value=0.052) by qRT-PCR and a significant upregulation (2.36 fold increase, $p<0.005$) at 24h after treatment with 10mM Na-Pi by RNA-seq. This variance in gene regulation and transcriptional output indicates a cell type specific response to P_i, and stresses the importance of analyzing pathways of interest in new models prior to use.

Furthermore, we identified Trps1 is involved in P_i signaling. Trps1 affected the dynamics of ERK1/2 activation in response to P_i and the expression of P_i-responsive genes. More specifically, Trps1-deficient cells displayed an absent second activation of ERK1/2, decreased upregulation of *Spp1*, *Phex*, and *Dmp1*, and an inability to upregulate *Dusp6* in response to P_i. Trps1-overexpressing cells had an enhanced and accelerated second activation of ERK1/2, increased downregulation of *Alpl* and *Sp7*, and a decreased upregulation of *Dusp6* in response to P_i. The precise role of Trps1 in P_i signaling is still unknown, but we predict Trps1 is one of the transcription factors that regulates gene expression in response to P_i. However, which of the P_i-responsive genes are directly regulated by Trps1 remains to be determined.

It is still unknown how the P_i signal is transduced. Na/P_i co-transporters has been shown to be critical for initiating P_i signaling, but P_i receptors and the transcriptional regulators of P_i-responsive genes remain unknown [41]. Two

mechanisms of P_i sensing have been proposed. The first one implicates FGF receptors (FGFR) in this response, as FGF signaling also results in ERK1/2 activation and one study has reported FGFR involvement in P_i signaling [32]. The second one is that the Na/P_i co-transporter PiT1 is acting as a P_i receptor and that this function is independent of P_i transport [45]. However, additional studies need to be performed to determine if either of these is involved in mediating P_i signaling in 17A cells. Several studies, including this one, have identified several P_i-regulated genes, but how this regulation is occurring remains unknown [32, 41]. Trps1 may be a transcriptional regulator of some of the genes that are downregulated; other potential candidates are those involved in mineralization, such as mineralization-related transcription factors: *Runx2*, *Sp7*, and *ATF4*. These genes are downregulated upon P_i signaling, so they may be acting as part of the negative feedback loop or their expression may be regulated at the translational or post-translational level. This is a more-likely possibility for Runx2, as its activity is modulated upon phosphorylation by ERK1/2 [75]. However, the role of these transcription factors in regulating P_i-responsive genes has yet to be addressed.

In conclusion, our studies determined that Trps1 is necessary for the initiation of mineralization by supporting expression of osteogenic transcription factors (Runx2 and Sp7) and phosphatases (TNAP and PHOSPHO1), as well as the production of MV [4, 5, 7]. The secretion of MV, which support the initiation of mineralization, is induced by P_i signaling and is dependent upon P_i-induced ERK1/2 activation [9]. In mature mineralizing cells, Trps1 must be downregulated

to allow for the upregulation of P_i regulating proteins (Phex, Vdr, and Fam20C) and proper propagation of mineralization in the ECM [2, 6, 7]. Lastly, Trps1 is involved in P_i signaling by affecting the second activation of ERK1/2 and the expression of P_i-responsive genes (*Spp1*, *Phex*, *Dmp1*, *Alpl*, and *Sp7*), as well as expression of the ERK1/2 phosphatase, *Dusp6*, which is involved in the ERK1/2 negative feedback loop and thus suggests a role for Trps1 in this regulatory loop.

Additional future directions include deciphering whether FGFR are involved in the P_i signaling pathway. This can be addressed by analyzing how inhibition of FGFR affects cellular response to P_i. Additionally, ERK1/2 has been described to act as a transcription factor for several mineralization-related genes [76]. We will test whether P_i signaling modifies ERK1/2 occupancy of these promoters as well as how that is affected by Trps1 deficiency and overexpression. We will also analyze whether Trps1 directly regulates expression of P_i-responsive genes. Lastly, we plan to determine how Trps1 is involved in the ERK1/2 negative feedback loop. To assess this, we will focus on *Dusp6* as a P_i-responsive gene whose expression is affected by Trps1.

GENERAL LIST OF REFERNCES

1. Piscopo, D.M.J., E.B.; Derynck R., *Identification of the GATA factor TRPS1 as a repressor of the osteocalcin promoter.* J Biol Chem, 2009. **284**(46): p. 31690-31703.
2. Napierala, D., et al., *Transcriptional repression of the Dspp gene leads to dentinogenesis imperfecta phenotype in Col1a1-Trps1 transgenic mice.* J Bone Miner Res, 2012. **27**(8): p. 1735-45.
3. Napierala, D., et al., *Transcriptional repression of the Dspp gene leads to dentinogenesis imperfecta phenotype in Col1a1-Trps1 transgenic mice.* J Bone Miner Res, 2012. **27**: p. 1735-45.
4. Napierala, D., et al., *Uncoupling of chondrocyte differentiation and perichondrial mineralization underlies the skeletal dysplasia in tricho-rhino-phalangeal syndrome.* Hum Mol Genet, 2008. **17**(14): p. 2244-54.
5. Napierala, D., et al., *Mutations and promoter SNPs in RUNX2, a transcriptional regulator of bone formation.* Mol Genet Metab, 2005. **86**(1-2): p. 257-68.
6. Mobley, C.G., et al., *Dspp-independent Effects of Transgenic Trps1 Overexpression on Dentin Formation.* J Dent Res, 2015. **94**(8): p. 1128-34.
7. Kuzynski, M., et al., *Dual role of the Trps1 transcription factor in dentin mineralization.* J Biol Chem, 2014. **289**(40): p. 27481-93.
8. Ishimori, N., et al., *Quantitative trait loci for BMD in an SM/J by NZB/BlNJ intercross population and identification of Trps1 as a probable candidate gene.* Journal of Bone and Mineral Research, 2008. **23**(9): p. 1529-1537.
9. Chaudhary, S.C., et al., *Phosphate induces formation of matrix vesicles during odontoblast-initiated mineralization in vitro.* Matrix Biol, 2016.
10. Gorski, J., *Biomineralization of bone: a fresh view of the roles of noncollagenous proteins.* Front Biosci, 2011. **16**: p. 2598-2621.
11. Arana-Chavez, V.E. and L.F. Massa, *Odontoblasts: the cells forming and maintaining dentine.* Int J Biochem Cell Biol, 2004. **36**: p. 1367-1373.
12. Butler, W.T., J.C. Brunn, and C. Qin, *Dentin extracellular matrix (ECM) proteins: comparison to bone ECM and contribution to dynamics of dentinogenesis.* Connect Tissue Res, 2003. **44 Suppl 1**: p. 171-178.
13. Linde, A. and M. Goldberg, *Dentinogenesis.* Crit Rev Oral Biol Med, 1993. **4**: p. 679-728.
14. Zhang, B., et al., *Expression and distribution of SIBLING proteins in the predentin/dentin and mandible of hyp mice.* Oral Dis, 2010. **16**: p. 453-464.

15. Addison, W.N., et al., *Pyrophosphate inhibits mineralization of osteoblast cultures by binding to mineral, up-regulating osteopontin, and inhibiting alkaline phosphatase activity.* J Biol Chem, 2007. **282**(21): p. 15872-83.
16. Balcerzak, M., et al., *Proteome analysis of matrix vesicles isolated from femurs of chicken embryo.* Proteomics, 2008. **8**(1): p. 192-205.
17. Kim, H.S., et al., *Proteomic analysis of microvesicles derived from human mesenchymal stem cells.* J Proteome Res, 2012. **11**(2): p. 839-49.
18. Morhayim, J., et al., *Proteomic signatures of extracellular vesicles secreted by nonmineralizing and mineralizing human osteoblasts and stimulation of tumor cell growth.* FASEB J, 2015. **29**(1): p. 274-85.
19. Thouverey, C., et al., *Proteomic characterization of biogenesis and functions of matrix vesicles released from mineralizing human osteoblast-like cells.* J Proteomics, 2011. **74**(7): p. 1123-34.
20. Xiao, Z., et al., *Analysis of the extracellular matrix vesicle proteome in mineralizing osteoblasts.* J Cell Physiol, 2007. **210**(2): p. 325-35.
21. Yanez-Mo, M., et al., *Biological properties of extracellular vesicles and their physiological functions.* J Extracell Vesicles, 2015. **4**: p. 27066.
22. Yuana, Y., A. Sturk, and R. Nieuwland, *Extracellular vesicles in physiological and pathological conditions.* Blood Rev, 2013. **27**(1): p. 31-9.
23. Colombo, M., G. Raposo, and C. Thery, *Biogenesis, secretion, and intercellular interactions of exosomes and other extracellular vesicles.* Annu Rev Cell Dev Biol, 2014. **30**: p. 255-89.
24. Barron, M.J., et al., *Hereditary dentine disorders: dentinogenesis imperfecta and dentine dysplasia.* Orphanet J Rare Dis, 2008. **3**: p. 31.
25. McKee, M.D., et al., *Compounded PHOSPHO1/ALPL deficiencies reduce dentin mineralization.* J Dent Res, 2013. **92**(8): p. 721-7.
26. Roberts, S., et al., *Functional involvement of PHOSPHO1 in matrix vesicle-mediated skeletal mineralization.* J Bone Miner Res, 2007. **22**(4): p. 617-27.
27. Yadav, M.C., et al., *Loss of skeletal mineralization by the simultaneous ablation of PHOSPHO1 and alkaline phosphatase function: a unified model of the mechanisms of initiation of skeletal calcification.* J Bone Miner Res, 2011. **26**(2): p. 286-97.
28. Huesa, C., et al., *The Functional co-operativity of Tissue-Nonspecific Alkaline Phosphatase (TNAP) and PHOSPHO1 during initiation of Skeletal Mineralization.* Biochem Biophys Rep, 2015. **4**: p. 196-201.
29. Millan, J.L., *The role of phosphatases in the initiation of skeletal mineralization.* Calcif Tissue Int, 2013. **93**(4): p. 299-306.
30. Bobryshev, Y.V., et al., *Role of bone-type tissue-nonspecific alkaline phosphatase and PHOSPO1 in vascular calcification.* Curr Pharm Des, 2014. **20**(37): p. 5821-8.
31. Tada, H., et al., *Phosphate increases bone morphogenetic protein-2 expression through cAMP-dependent protein kinase and ERK1/2 pathways in human dental pulp cells.* Bone, 2011. **48**: p. 1409-16.

32. Camalier, C.E., et al., *An integrated understanding of the physiological response to elevated extracellular phosphate.* J Cell Physiol, 2013. **228**(7): p. 1536-50.
33. Julien, M., et al., *Phosphate stimulates matrix Gla protein expression in chondrocytes through the extracellular signal regulated kinase signaling pathway.* Endocrinology, 2007. **148**: p. 530-7.
34. Julien, M., et al., *Phosphate-dependent regulation of MGP in osteoblasts: role of ERK1/2 and Fra-1.* J Bone Miner Res, 2009. **24**: p. 1856-68.
35. Alizadeh Naderi, A.S. and R.F. Reilly, *Hereditary disorders of renal phosphate wasting.* Nat Rev Nephrol, 2010. **6**(11): p. 657-65.
36. Bergwitz, C. and H. Juppner, *Regulation of phosphate homeostasis by PTH, vitamin D, and FGF23.* Annu Rev Med, 2010. **61**: p. 91-104.
37. Davideau, J.L., et al., *In situ investigation of vitamin D receptor, alkaline phosphatase, and osteocalcin gene expression in oro-facial mineralized tissues.* Endocrinology, 1996. **137**(8): p. 3577-85.
38. Sodek, J., B. Ganss, and M.D. McKee, *Osteopontin.* Crit Rev Oral Biol Med, 2000. **11**(3): p. 279-303.
39. McKnight, D.A. and L.W. Fisher, *Molecular evolution of dentin phosphoprotein among toothed and toothless animals.* BMC Evol Biol, 2009. **9**: p. 299.
40. Foster, B.L., et al., *Regulation of cementoblast gene expression by inorganic phosphate in vitro.* Calcif Tissue Int, 2006. **78**: p. 103-12.
41. Khoshniat, S., et al., *The emergence of phosphate as a specific signaling molecule in bone and other cell types in mammals.* Cellular and Molecular Life Sciences, 2011. **68**: p. 205-18.
42. Kumar, R., *Phosphate sensing.* Curr Opin Nephrol Hypertens, 2009. **18**: p. 281-4.
43. Razzaque, M.S., *Phosphate and Vitamin D in Chronic Kidney Disease.* Contributions to Nephrology, 2013. **180**: p. 74-85.
44. von Kriegsheim, A., et al., *Cell fate decisions are specified by the dynamic ERK interactome.* Nat Cell Biol, 2009. **11**(12): p. 1458-64.
45. Chavkin, N.W., et al., *Phosphate uptake-independent signaling functions of the type III sodium-dependent phosphate transporter, PiT-1, in vascular smooth muscle cells.* Exp Cell Res, 2015. **333**(1): p. 39-48.
46. Camalier, C.E., et al., *An integrated understanding of the physiological response to elevated extracellular phosphate.* J Cell Physiol, 2012.
47. Rendenbach, C., et al., *Effects of extracellular phosphate on gene expression in murine osteoblasts.* Calcif Tissue Int, 2014. **94**(5): p. 474-83.
48. Ishimori, N.S., I.;Korstanje, R.; Marion, M.; Li, R.; Donahue, L.; Rosen, C.; Beamer, W.; Paigen, B.; Churchill, G., *Quantitative trait loci for BMD in an SM/J by NZB/BlNJ intercross population and identification of Trps1 as a probable candidate gene.* J Bone Miner Res, 2008. **23**(9): p. 1529-1537.
49. Bennett, C.G., C.J. Hill, and J.L. Frias, *Facial and oral findings in trichorhinophalangeal syndrome type 1 (characteristics of TRPS 1).* Pediatr Dent, 1981. **3**: p. 348-352.

50. Malik, T.H., et al., *Transcriptional repression and developmental functions of the atypical vertebrate GATA protein TRPS1.* EMBO J, 2001. **20**(7): p. 1715-25.
51. Ackert-Bicknell, C.D., S.; Tsaih, S.; Beamer, W.; Cupples, L.; Paigen, B.; Hsu, Y.; Kiel, D.; Karasik, D., *Genetic variation in TRPS1 may regulate hip geometry as well as bone mineral density.* Bone, 2012. **50**(5): p. 1188-1195.
52. Wang, L.L., W.; Zhang, L.; Huang, Y.; Scheib, R.; Liu, X.; Myers, L.; Lu, L.; Farber, C.; Liu, G.; Wang, C.; Deng, H.; Williams, R.; Wang, Y.; Gu, W.; Jiao, Y., *Trps1 differentially modulates the bone mineral density between male and female mice and its polymorphism associates with BMD differently between women and men.* PLoS One, 2014. **9**(1).
53. Fantauzzo, K.A. and A.M. Christiano, *Trps1 activates a network of secreted Wnt inhibitors and transcription factors crucial to vibrissa follicle morphogenesis.* Development, 2012. **139**(1): p. 203-14.
54. Bach, A.S., et al., *Nuclear cathepsin D enhances TRPS1 transcriptional repressor function to regulate cell cycle progression and transformation in human breast cancer cells.* Oncotarget, 2015. **6**(29): p. 28084-103.
55. Fantauzzo, K.A., et al., *Dynamic expression of the zinc-finger transcription factor Trps1 during hair follicle morphogenesis and cycling.* Gene Expr Patterns, 2008. **8**(2): p. 51-7.
56. Slavkin, H.C., et al., *Enamel gene products during murine amelogenesis in vivo and in vitro.* J Dent Res, 1982. **Spec No**: p. 1467-1471.
57. Lacerda-Pinheiro S, D.-N.S., Harichane Y, Souyri M, Petit-Cocault L, Legrès L, Marchadier A, Baudry A, Ribes S, Goldberg M, Kellermann O, Poliard A., *Concomitant multipotent and unipotent dental pulp progenitors and their respective contribution to mineralised tissue formation.* Eur Cell Mater, 2012. **23**: p. 371-86.
58. Priam, F., et al., *New cellular models for tracking the odontoblast phenotype.* Arch Oral Biol, 2005. **50**(2): p. 271-7.
59. Kantaputra, P., et al., *Tricho-rhino-phalangeal syndrome with supernumerary teeth.* J Dent Res, 2008. **87**(11): p. 1027-31.
60. Kaiser, *SUMOylation modulates transcriptional repression by TRPS1.* Biol Chem, 2007. **388**(4): p. 381-90.
61. James, M.J., et al., *Different roles of Runx2 during early neural crest-derived bone and tooth development.* J Bone Miner Res, 2006. **21**(7): p. 1034-44.
62. Adhami, M.R., R.; Chen, H.; Javed, A., *Runx2 activity in committed osteoblasts is not essential for embryonic skeletogenesis.* Connect Tissue Res, 2014. **55**: p. 102-106.
63. Adhami, M.K., K.; Clarke, J.; Rashid, R.; Chen, H.; Hassan, M.; Javed, A., *Runx2 Gene Deletion in Odonoblast Does Not Imparin Dentin Formation.* 2016 AADR abstract. 2016.
64. Adhami, M.D., et al., *Loss of Runx2 in committed osteoblasts impairs postnatal skeletogenesis.* J Bone Miner Res, 2015. **30**(1): p. 71-82.

65. Lacerda-Pinheiro, S., et al., *Concomitant multipotent and unipotent dental pulp progenitors and their respective contribution to mineralised tissue formation.* Eur Cell Mater, 2012. **23**: p. 371-86.
66. Yadav, M.C., et al., *Skeletal Mineralization Deficits and Impaired Biogenesis and Function of Chondrocyte-Derived Matrix Vesicles in Phospho1 and Phospho1/Pit1 Double Knockout Mice.* J Bone Miner Res, 2016.
67. Abdallah, D., et al., *Fatty acid composition in matrix vesicles and in microvilli from femurs of chicken embryos revealed selective recruitment of fatty acids.* Biochem Biophys Res Commun, 2014. **446**(4): p. 1161-4.
68. Rilla, K., et al., *Hyaluronan production enhances shedding of plasma membrane-derived microvesicles.* Exp Cell Res, 2013. **319**(13): p. 2006-18.
69. Boonrungsiman, S., et al., *The role of intracellular calcium phosphate in osteoblast-mediated bone apatite formation.* Proc Natl Acad Sci U S A, 2012. **109**(35): p. 14170-5.
70. Mahamid, J., et al., *Bone mineralization proceeds through intracellular calcium phosphate loaded vesicles: a cryo-electron microscopy study.* J Struct Biol, 2011. **174**(3): p. 527-35.
71. Zou, Y., et al., *Determination of protein regions responsible for interactions of amelogenin with CD63 and LAMP1.* Biochem J, 2007. **408**(3): p. 347-54.
72. Xu, L., H. Harada, and A. Taniguchi, *The effects of LAMP1 and LAMP3 on M180 amelogenin uptake, localization and amelogenin mRNA induction by amelogenin protein.* J Biochem, 2008. **144**(4): p. 531-7.
73. Shapiro, J.L., et al., *Cellular uptake of amelogenin, and its localization to CD63, and Lamp1-positive vesicles.* Cell Mol Life Sci, 2007. **64**(2): p. 244-56.
74. Zhang, H., et al., *Full length amelogenin binds to cell surface LAMP-1 on tooth root/periodontium associated cells.* Arch Oral Biol, 2010. **55**(6): p. 417-25.
75. Ge, C., et al., *Identification and functional characterization of ERK/MAPK phosphorylation sites in the Runx2 transcription factor.* J Biol Chem, 2009. **284**(47): p. 32533-43.
76. Greenblatt, M.B., J.H. Shim, and L.H. Glimcher, *Mitogen-activated protein kinase pathways in osteoblasts.* Annu Rev Cell Dev Biol, 2013. **29**: p. 63-79.